UNIVERSITÀ DEGLI STUDI DI PADOVA

DIPARTIMENTO DI INGEGNERIA INDUSTRIALE
Corso di Laurea Magistrale in Ingegneria Meccanica

Tesi di Laurea Magistrale in Ingegneria Meccanica

Design and construction of a multichannel bench test for running specific prostheses

Relatore: **Prof. Nicola Petrone**

Laureando: **Gianfabio Costa**
Matricola: **1130966**

Anno accademico: 2017-2018

SUMMARY

Running specific prostheses (RSPs) are designed to enable athletes with lower-limb amputations to run. RSPs are passive-elastic prostheses, inspired by the spring-like nature of running, mimic the mechanical energy storage and return of tendons during ground contact. RSPs are J-shaped or C-shaped carbon leaf springs attached to the sockets that encompass the residual limbs. Amputation can be transtibial if under the knee, transfemoral if it is above, unilateral or bilateral depending on whether it involves only one or both lower limbs.

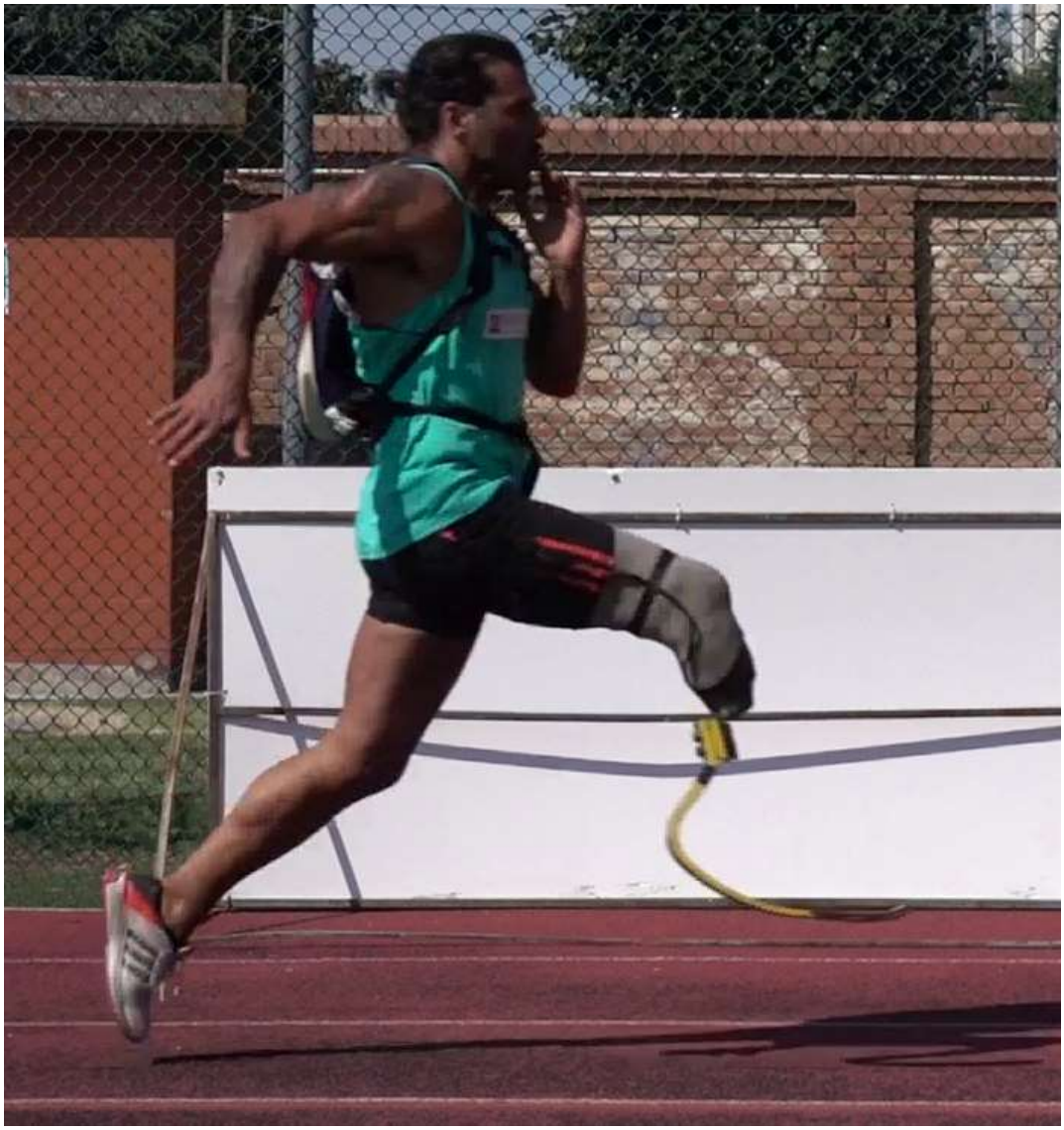

Figure 1 | Roberto La Barbera, Italian Paralympic athlete.

To help athletes who wear RSPs to improve performance and comfort, it is first necessary to know the mechanical characteristics of the prostheses, in terms of mechanical stiffness

and energy released during running, to evaluate which is the most suitable and performing prosthesis according to the athlete and the sport discipline carried out. Furthermore, a profound knowledge of the prostheses during the different stages of the stance, is the first step to develop a prostheses adjustment technique to maximize the athlete's performance.

To date, prosthetic manufacturers do not report the mechanical stiffness values of RSPs. They classify RSPs into stiffness categories, from 1 to 7, based on body weight and discipline performed (slow or fast running); the greater the weight and the speed of running, the higher the recommended category. The rigidity of the prosthesis is essential for running mechanics and performance, therefore, it is imperative to quantify and disseminate stiffness values to further understand prosthetic function. The measurement of rigidity must be performed by reproducing the angles and observable running speeds over the athlete's run. To date, there are no standardized tests for the measurement of stiffness, consequently there are sometimes inconsistent measurements in literature.

The prosthetic foot is constructed with different shapes and the material is a carbon fiber composite. As a result, the mechanical behaviour is very complicated, and this is evidenced by the numerous studies that have tried to give a definitive answer to the question: how do running specific prostheses work?

In the literature there are few studies in which the machines used for the measurement of mechanical stiffness are monoaxial traction machines for testing materials adapted to the purpose [20,21,23], or more simply vertical carriages in which the force of compression of the prosthesis is given by weight of barbells [22,24].

The ambitious objective of this thesis is the development and realization of a test bench able to reproduce as closely as possible the biomechanics of the running, to evaluate in detail and in a complete way the mechanical performances of the RSP. Only with a tailor-made test bench can investigate all the various aspects of the prosthetic foot.

INDEX

1. INTRODUCTION: RSP'S state of art

The Flex-Foot was first running specific prosthesis in elite sports at the 1988 Paralympic Games (Figure 1.1). Four years later, the prosthetic heel was absent in some athletes, creating the first sprint prosthesis. In fact, the first specialized running foot, the Flex-Sprint I (Figure 1.2 -A; Össur, Reykjavik, Iceland), was developed by eliminating the heel portion and altering the stiffness configuration with the layup sequence of carbon while still maintaining the J-shaped outline of the carbon forefoot. There are now several different sprint foot designs available, all with a similar basic shape (Figure 1.1 -A to N), which has changed little since 1992. [19]

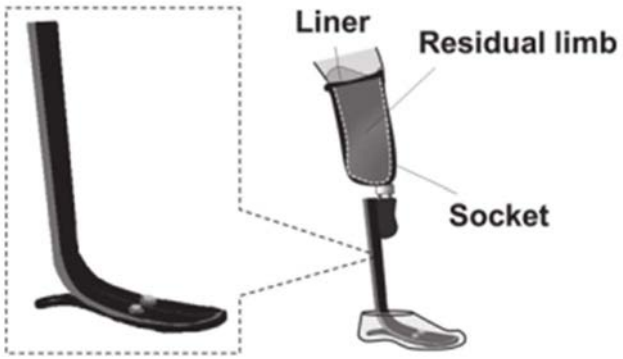

Figure 1.1 | Schematic representation of "Flex-Foot®" and prosthetic components (socket and liner) with representation of a residual limb. The schema is based on transtibial (below-knee) amputees. (Hobara, 2014). [19]

For the last 15 years, technical advances in prostheses have been a main factor in the increased performance of athletes with lower-limb amputations. The use of materials such as carbon fiber, titanium, and graphite has provided added strength and energy storage capabilities to prostheses while decreasing the weight of prosthetic components. Today, carbon fiber prostheses are most popular in elite running and jumping events. These prostheses allow lower-limb amputees to actively participate in sporting activities including competitive sports.

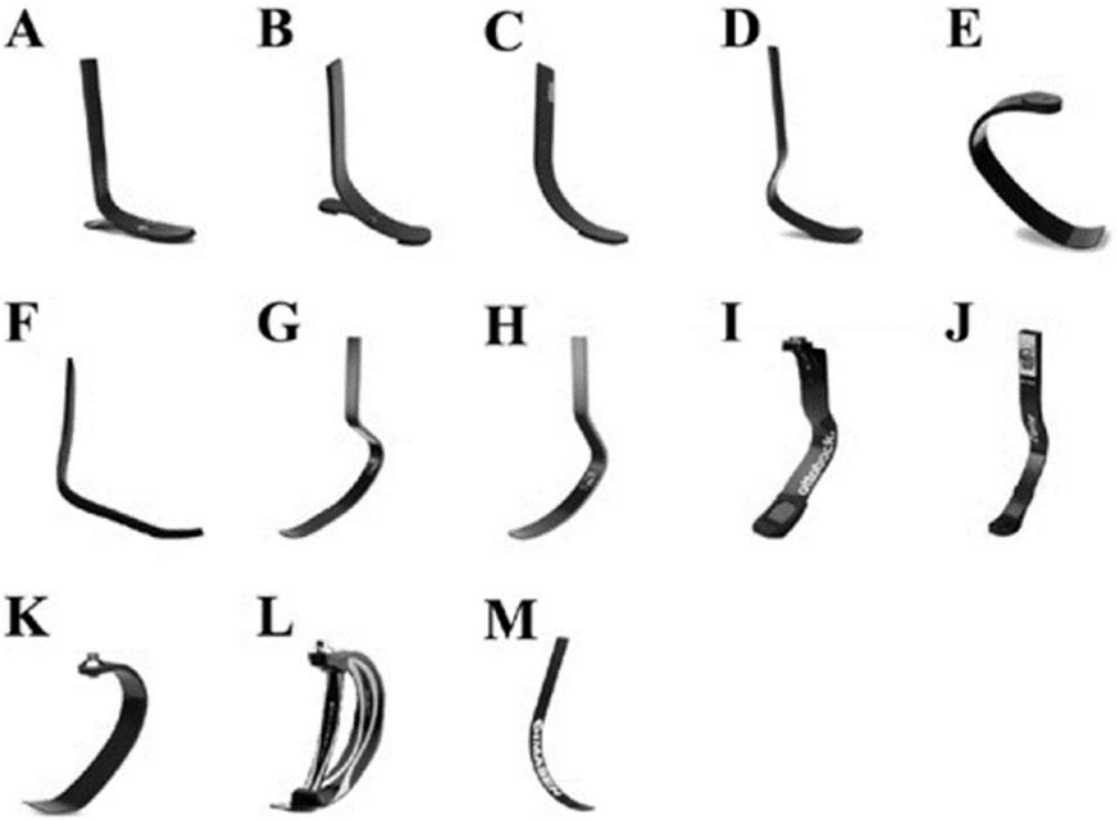

Figure 1.2 | A: Flex-Foot® (Modular III; Össur), B: Flex-Sprint II (Össur), C: Flex-Sprint I (Össur), D: Flex-Sprint III® (Cheetah; Össur), E: Flex-RunTM (Össur), F: Symes-Sprint (Össur), G: Cheetah Xtreme®, H: Cheetah Xtend®, I: 1E90 (Sprinter, OttoBock), J: 1C2 (C-Sprint®), K: Nitro (Freedom Innovation), L: CatapultTM (Freedom Innovation), M: SP1100 (KATANA, IMASEN Engineering Corporation), N: Rabbit (IMASEN Engineering Corporation). (Hobara, 2014) [19]

1.1. BIOMECHANICS OF RUNNING

Running is a bouncing gait that is well-characterized by a spring-mass model [1-14]. The spring-mass model portrays the stance leg as a mass-less linear spring supporting a point mass representing the runner's centre of mass.

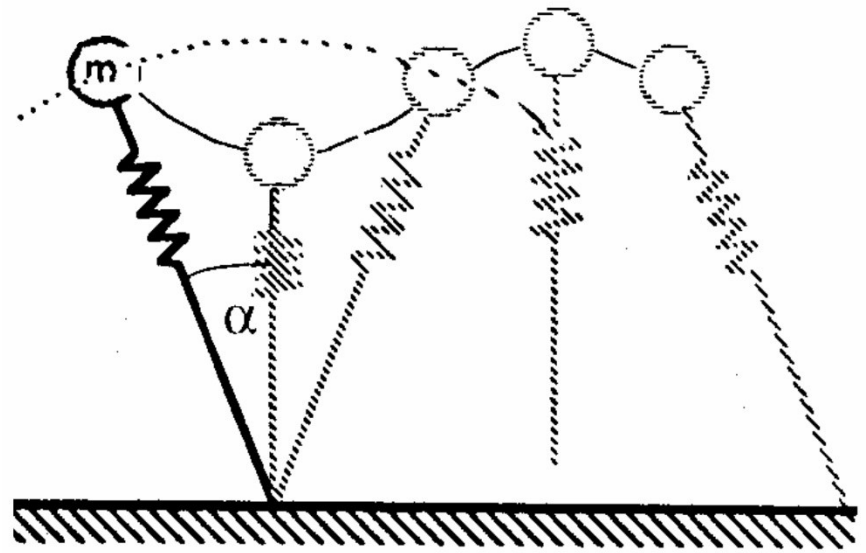

Figure 1.1.1 | Schematization of the running with the spring mass-model. (Blickhan, 1989) [1]

In this model the leg stiffness k_{leg} is equals the quotient of the peak applied force (F) and the change in leg length (Δl) from touchdown to mid-stance (Figure 1.1.2):

$$k_{leg} = \frac{F}{\Delta l}$$

The vertical motions of the system during the ground contact phase can be described in terms of an 'effective vertical stiffness' (k_{vert}). The effective vertical stiffness was calculated from the ratio of the peak vertical force (F) to the peak vertical displacement of the centre of mass during the stance phase (Δy) (Figure 1.1.2):

$$k_{vert} = \frac{F}{\Delta y}$$

The effective vertical stiffness (k_{vert}) does not correspond to any physical spring in the model. Rather, k_{vert} describes the vertical motions of the centre of mass during the ground contact time and is determined by a combination of the stiffness of the leg spring (k_{leg}), half the angle swept by the leg spring (θ) and the compression of the leg spring (Δl).

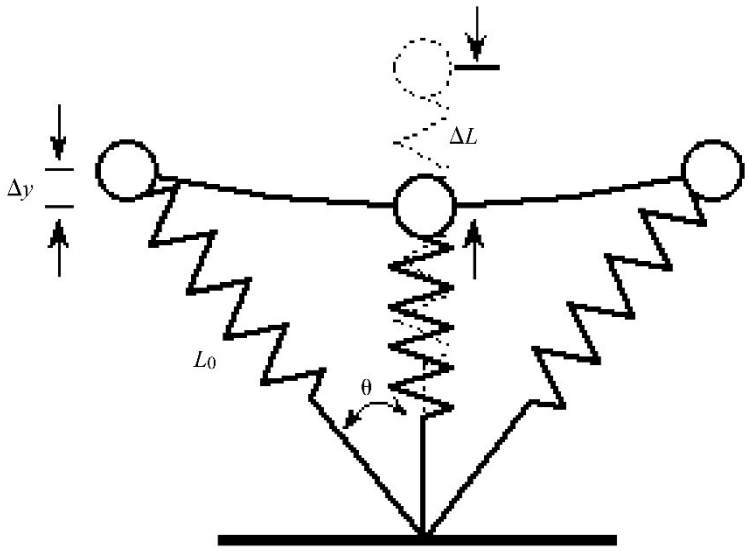

Figure 1.1.2 | Stiffness in the spring-mass model [2]

Upon ground contact, the leg spring compresses and stores elastic energy until mid-stance, and then returns mechanical energy from mid-stance through the end of ground contact [10]. In this model, the leg spring is completely elastic, however the structures of a biological leg are viscoelastic and therefore only a portion of the stored potential elastic energy is returned (due to hysteresis). The spring-like action of the leg conserves a portion of the runner's mechanical energy, theoretically mitigating the additional muscular force and mechanical energy input necessary to maintain running speed [10,11]. The magnitude of the stored and returned mechanical energy is inversely related to leg stiffness (resistance to compression) and is influenced by the magnitude and orientation of the external force vector acting on the leg.

1.2. RSP HISTORY

For many years, people are searching for a mechanical solution for amputees, with the aim of enabling the amputees to walk with two legs. A simple solution for this was the peg leg, a wooden stick attached to the stump and tight. (Figure 1.2.1) However, the design of the peg-leg created a certain stigma (Melville's Captain Achab) and only focusses on connecting the stump with the ground and not on ergonomic aspects. It is uncomfortable for the amputees and it may cause chafing, muscle- and bone aches and more.

Figure 1.2.1 | The captain Achab with his wooden leg. (Ventura and Shvo, 2017) [15]

The purpose of the prosthesis is to hide the missing leg, but it is more difficult to recreate a prosthesis that imitating a leg and even a shoe, because it is a more sophisticated product linked to socio-cultural context and fashion.

Along the years, the designers try to build prosthesis that resembles a human limb, but not really close to it, and the other hand avoiding the cyborg connotation.

In the figure 1.2.2 it is possible to see the evolution along time and different eras of the prosthesis. [15]

Figure 1.2.2 | A mixture of simple function and mimesis of the human leg in different eras. (Ventura and Shvo, 2017) [15]

There are many prosthetic feet designed over time. The Federal Government's Artificial Limb program converted various designs into one standard manufactured production model: The Solid Ankle and Cushioned Heel (SACH) foot. In 1957 this model was approved for male amputees. The SACH foot has a simple design and gives amputees many foot and ankle functions that are required. Therefore, it is and will be a valuable product for patients. [16].

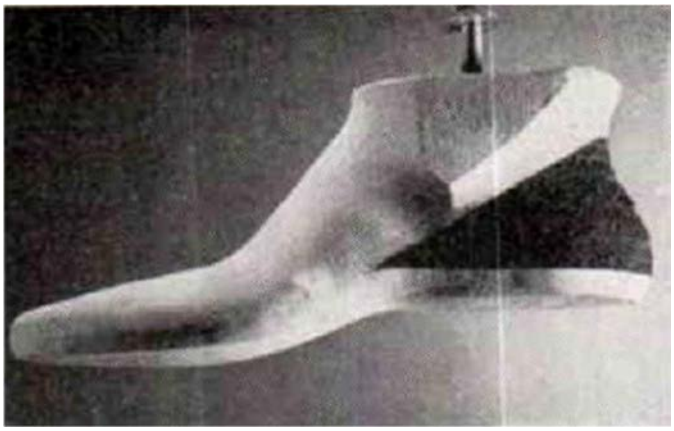

Figure 1.2.3 | SACH Foot [16]

A special mention goes to the Canadian Terry Fox, which ran the Marathon of Hope in 1980, a cross-country run dedicated to raising awareness and money for cancer research. Fox, whose right leg had been amputated in 1977, performed this incredible feat using a prosthesis designed primarily for walking. His accomplishment inspired Canadians across the country as well as amputees and para-athletes around the world.

It also motivated researchers to develop prostheses better suited for running. Since 1980, developments in materials manufacturing and computer/bionic technology have led to more comfortable, stable and responsive prostheses, both for recreational and elite athletes [17]

Figure 1.2.3 | Terry Fox [17]

After the invention of SACH foot (Ohio Willow Wood, Ohio, USA) in the late 1950s, prosthetic foot designs and materials changed little for approximately 20-30 years. According to the previous studies [18], the usefulness of lower-limb prostheses improved tremendously in the 1980s, when advances in composite materials flooded the prosthetics industry. Carbon composite materials, used extensively in the aerospace industry, brought lightness, durability, and strength to the design of prosthetic feet, pylons, and sockets. In 1984, Van Phillips, an American inventor of prostheses, created the "Flex-Foot®" made of carbon graphite. The innovative artificial foot allowed users to store and then return elastic energy during the ground-contact phase of gait. [19]

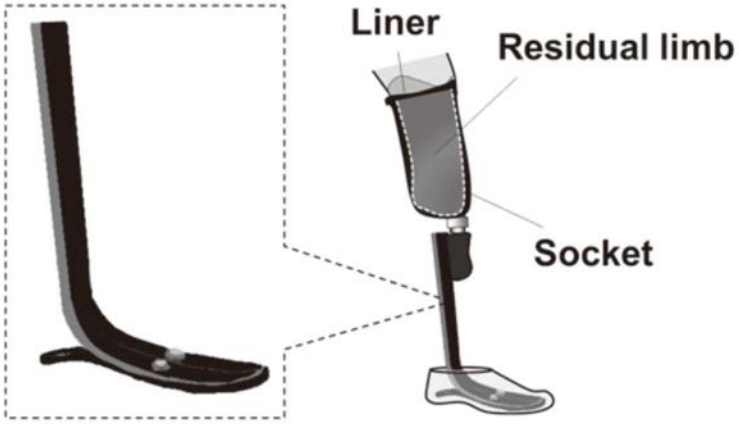

Figure 1.2.4 | Schematic representation of "Flex-Foot®" and prosthetic components (socket and liner) with representation of a residual limb. The schema is based on transtibial (below-knee) amputees. (Hobara, 2014) [19]

1.3. HOW THE RSP WORKS

Inspired by the spring-like nature of running, passive-elastic running-specific prostheses (RSPs) were developed to enable athletes with lower-limb amputations to run. These carbonfiber devices are attached to the sockets that encompass the residual limbs, are in-series with the residual limbs, and mimic the mechanical energy storage and return of tendons during ground contact. Unlike biological ankles, RSPs cannot generate mechanical power anew and only return 63% to 95% of the stored elastic energy during running [29,30,31]. For context, biological ankles generate mechanical power through use of elastic structures as well as muscles, and thus appear to return 241% of the energy stored while running at 2.8 m/s [29].

Athletes with leg amputations may adapt similar leg spring mechanics as non-amputees by using RSPs that emulate biological lower leg stiffness. Individually, non-amputees adopt a constant, metabolically optimal leg stiffness during running [12]. Non-amputee runners maintain leg stiffness across speeds by exhibiting constant ankle joint stiffness (sagittal plane torsional stiffness) [13,14]. It has been assumed that prosthetic stiffness is also constant across speeds [25,31,34,38], which if true, RSPs would act like that of biological ankles. It is unknown whether the force-displacement profiles of RSPs are linear, or curvilinear, which would infer that stiffness is contingent upon the applied force magnitude.

When athletes with transtibial amputations run, they generate peak vertical ground reaction forces (GRFs) with their affected legs that are 2.1 to 3.3 times body weight at speeds of 2.5 m/s to 10.8 m/s [31,34-36]. During running, peak resultant GRFs typically occur around mid-stance and are oriented vertically. At the same instant, the proximal end of the stance leg's RSP is rotated forward in the sagittal plane relative to the peak resultant GRF vector. Therefore, the proximal bending moment acting on shorter RSPs may be less than that on taller RSPs for a given applied force, due to a reduced moment arm length. A smaller moment (torque) associated with shorter RSPs may reduce vertical displacement, and in turn increase prosthetic stiffness. Nonetheless, the peak resultant GRF magnitudes and sagittal plane orientations relative to RSPs are unknown, as is the influence of prosthetic height on stiffness.

1.4. REFERENCE SYSTEMS AND NOMENCLATURE ADOPTED

There is no reference standard for RSPs, so in literature there is no standardization of reference systems, axes, angles, forces, etc; in this paragraph are presented the ones we have developed. The definitions below are taken from the site [47]. An extended version of the medical terms is present in Appendix A.

1.4.1.Medical lexicon [47]

AK (above-the-knee): A specific level of amputation—also known as **transfemoral**.

alignment: The position of the prosthetic socket in relation to the foot and knee.

amputation: The cutting off of a limb or part of a limb.

anterior: The front portion of a shoe or foot.

bilateral amputee: A person who is missing or has had amputated both arms or both legs. For example, a person that is missing both legs below-the knee is considered a bilateral BK.

biomechanics: Applying mechanical principles to the study of human movement; or the science concerned with the action of forces on the living body.

BK (below-the-knee): A specific level of amputation—also known as transtibial.

bumper: Rubber like, polymer based devices that are available in varying degrees of density, depending on an amputee's desired level of stiffness in a prosthetic knee or heel. As with other prosthetic componentry, basic maintenance or replacement may be required as a result of wear and tear.

C-Leg: The Otto Bock C-Leg features a swing and stance phase control system that senses weight bearing and positioning to provide the knee's microprocessor information about the amputee's gait, thus promoting smoother ambulation. The outer shell houses a hydraulic cylinder, microchip, and rechargeable battery.

definitive, or **permanent prosthesis**: The definitive prosthetic replacement for the missing limb or part of a limb, meeting standards for comfort, fit, alignment, function, appearance and durability.

distal: (1) The end of the residual limb. (2) The end that is farthest from the central portion of the body. Distal is the opposite of **proximal**.

donning and doffing: Putting on and taking off a prosthesis, respectively.

lateral: To the side, away from the median plane of the body.

Foot or **prosthetic foot**: carbon fiber blade.

Liner (roll-on liner): Suspension systems used to hold the prosthesis to the residual limb and to provide additional comfort and protection for the residual limb. Roll-on liners can also accommodate volumetric changes in the residual limb. These liners may be made of silicon, pelite, or gel substances.

medial: Motion of a body part toward the median plane of the body.

neuroma: When a nerve is severed during amputation, the nerve endings form a mass (neuroma) reminiscent of a cauliflower shape. Neuromas can be troublesome, especially when they are in places that are subject to pressure from the socket. They can also cause an amputee to experience sensory phenomena in or around the residual limb, which can be aggravating and/or painful.

nylon sheath: A sock interface worn close to the skin on the residual limb to add comfort and deter perspiration.

prosthesis: An artificial limb, usually an arm or a leg, that provides a replacement for the amputated or missing limb. **Prostheses** is plural. The prosthesis includes the socket, the connecting parts and the carbon fiber composite foot.

proximal: Nearer to the central portion of the body. Proximal is the opposite of distal.

pylon: A rigid member, usually tubular, between the socket or knee unit and the foot that provides a weight bearing, shock-absorbing support shaft for the prosthesis.

quad socket: A socket designed for an AK amputee that has four distinctive sides. The design allows the muscles to function as much as possible as it works to improve the AK amputee's ability to control knee function. The distal end of the socket should match the shape and size of the residual limb and should provide secure contact, alleviating edema and other skin problems.

residual limb: The portion of the arm or leg remaining after an amputation, sometimes referred to as a stump or residuum.

shuttle lock: A mechanism that has a locking pin attached to the distal end of the liner, which locks or suspends the residual limb into the socket.

socket: The portion of the prosthesis that fits around and envelopes the residual limb and to which the prosthetic components are attached.

stance control knee: These prosthetic knee joints typically offer a weight-activating friction brake that locks the knee into place during pivotal points of ambulation, offering stability and balance where needed.

stump: A word commonly used to refer to the residual limb.

suction socket: Mainly for use by AK level amputees, this socket is designed to provide suspension by means of negative pressure vacuuming. This is achieved by forcing air out of the socket through a one-way valve when donning and using the prosthesis. In order for this type of socket to work properly, the soft tissues of the residual limb must precisely fit the contours of the socket. Suction sockets work very well for those whose residual limbs maintain a constant shape and size.

transmetatarsal amputation: An amputation through the metatarsal section of the foot bone. (see partial foot amputation)

unilateral: An amputation that affects only one side of the body (opposite of bilateral).

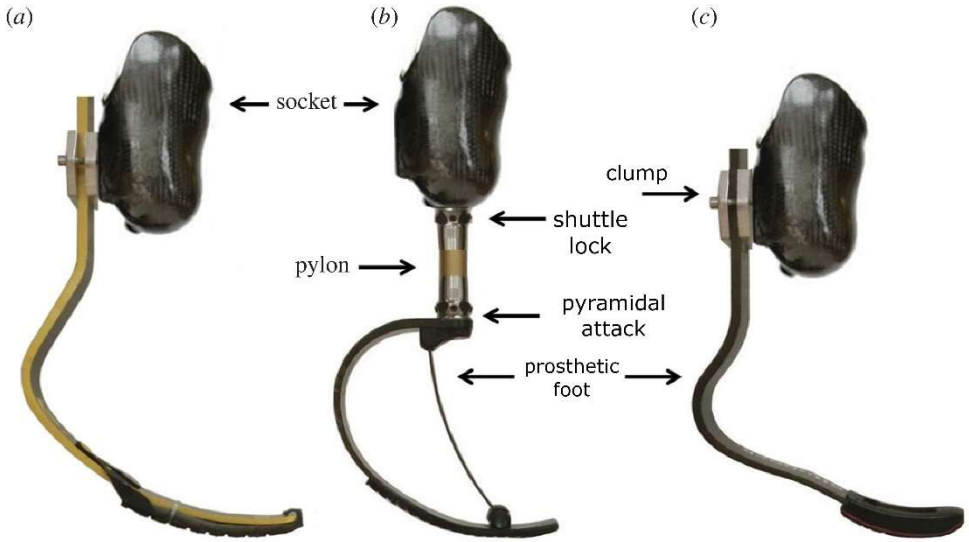

Figure 1.4.1 | Main components of the prosthesis [37] a) Ossur Cheetah Xtend prosthesis (J-shaped), b) Freedom Catapult FX6 prosthesis (C-shaped), c) Ottobock 1E90 Sprinter prosthesis (J-shaped)

1.4.2.Reference systems

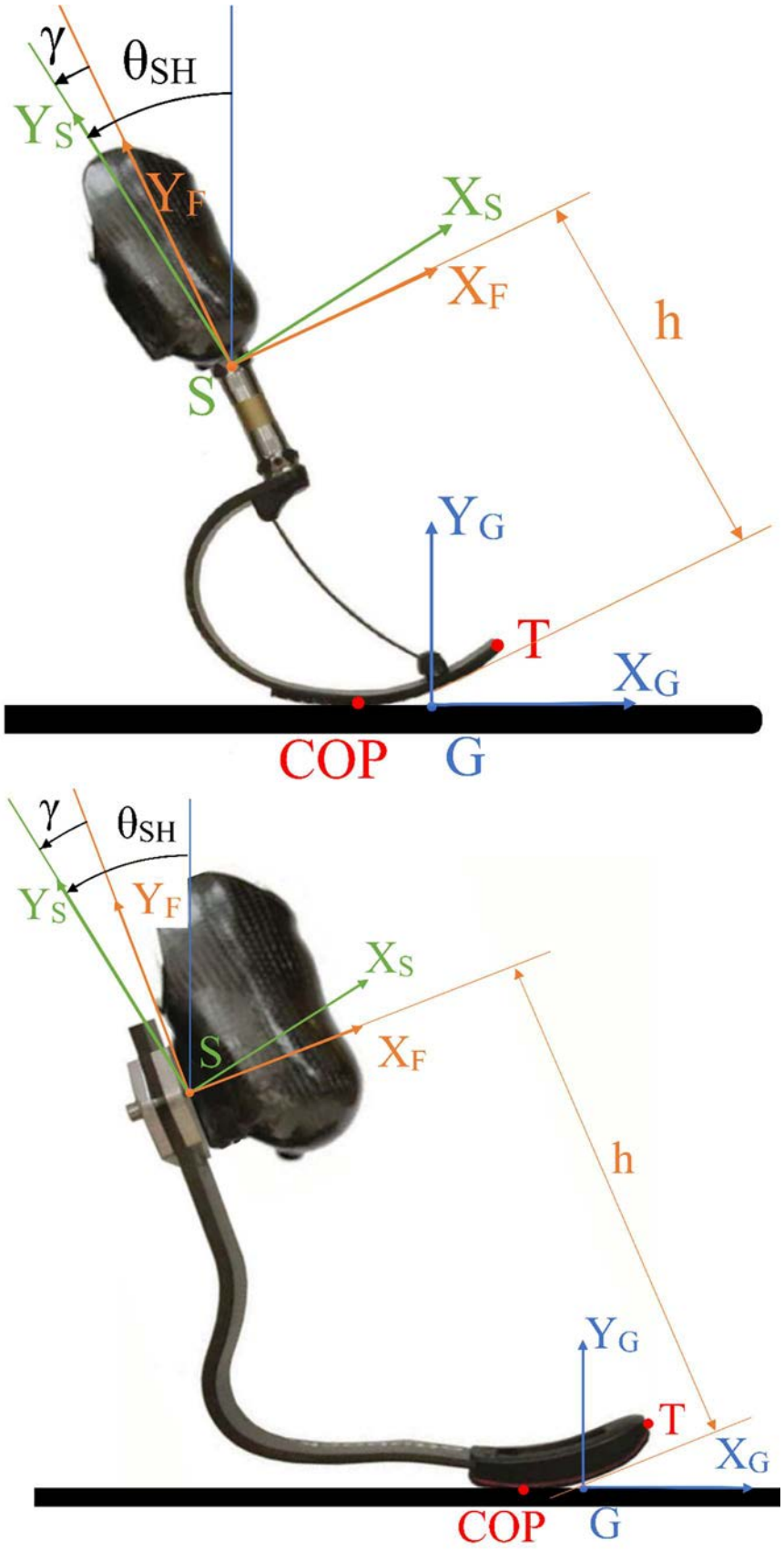

Figure 1.4.2.1 | Reference system in C-shaped RSP (upward) and in J-shaped (below)

Figure 1.4.2.1 shows the reference systems used.

- Ground reference system (G $X_G Y_G Z_G$)

The origin of the reference system G is located at a fixed point of the ground. As will be shown below, point G will be the point where the ground is hinged on the test bench. The X_G axis is parallel to the ground in the sagittal plane, the Y_G axis is orthogonal and directed upwards. The Z_G axis derives from the right-hand rule.

- Socket reference system (S $X_S Y_S Z_S$)

The origin of the reference system S is located in the shuttle lock in the case of C-shaped prostheses, in the middle of the contact surface between the foot and the socket in the case of j-shaped prostheses. The Y_S axis is the axialsimmetry axis of the socket, approximating the shape of the socket to an axisymmetric solid. The X_S axis is orthogonal to the Y_S axis with a posterior-to-anterior direction. The Z_S axis derives from the right-hand rule.

- Foot reference system (S $X_F Y_F Z_F$)

The origin of the reference system is the same of the socket reference system. The Y_F axis, for C-shaped prostheses, is the axis of the pyramidal attachment or the pylon axis when present, for the J-shaped prostheses, is the axis of the proximal straight stretch. The X_F axis is orthogonal to the Y_F axis with a posterior-to-anterior direction. The Z_F axis derives from the right-hand rule.

- Angle θ_{SH}

It is the angle that defines the position of the leg with respect to the ground in the sagittal plane. Is defined as the angle between the Y_G axis and the Y_S axis, positive if counterclockwise.

- Angle γ

It is the fixed angle of alignment of the prosthetic foot with respect to the socket in the sagittal plane. Is defined as the angle between the Y_F axis and the Y_S axis, positive if counterclockwise.

- Centre of pressure COP

It’s a point on a surface contact through which the resultant force due to pressure passes. This point changes during the stance phase with respect to the ground reference system, both with respect to the socket reference system

- Point T.

It is the toe of the prosthetic foot.

- Height of the prosthesis h

Is defined as the distance between the X_F axis and the furthest point of the sole.

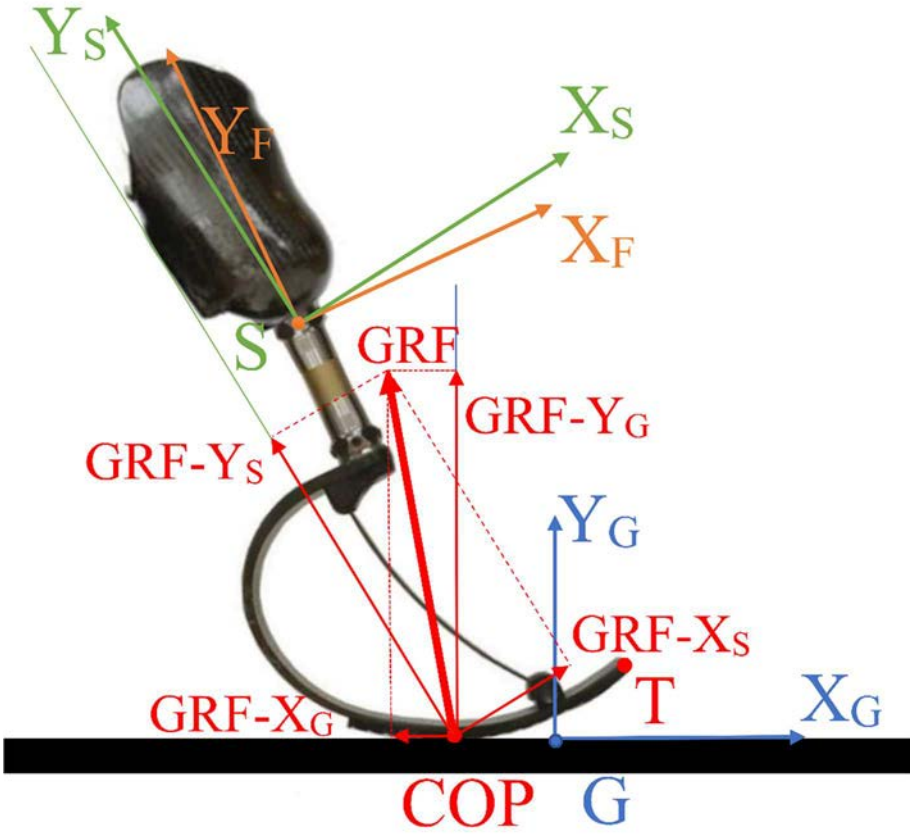

Figure 1.4.2.2 | Ground reaction force GRF.

Figure 1.4.2.2 shows the ground reaction force GRF in the sagittal plane. The point of application of the GRF is the COP point. The decomposition of the GRF along the X_G and Y_G axes creates the forces GRF-X_G and GRF-Y_G. It is useless to break down the GRF even in the socket reference system obtaining the forces GRF-X_S and GRF-Y_S. The direct measurement of the GRF ground reaction force is performed with a force platform. Below, to indicate that the measurement is performed using a force platform, the prefix FP will be applied (es FP-GRF-X_s).

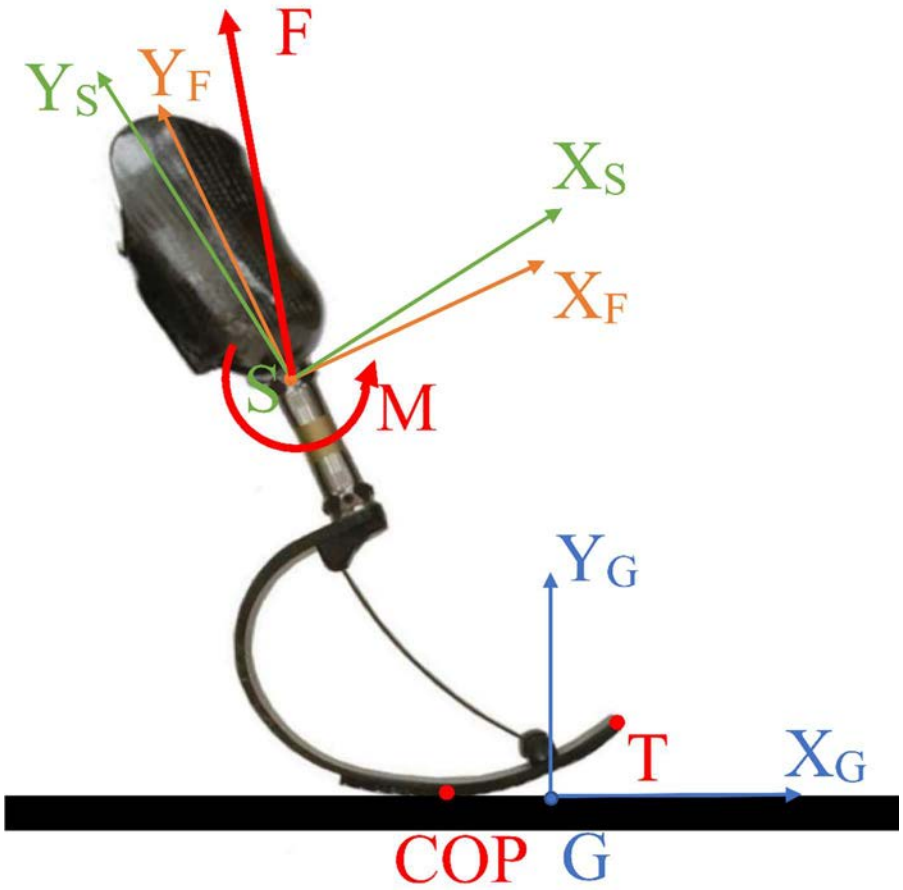

Figure 1.4.2.3 | Ground reaction force GRF

The force F and the moment M are defined as the stresses that the prosthetic foot transmits to the socket and therefore to the leg in the sagittal plane (Figure 1.4.2.3). The point of application of F is the point S. The axis of the moment is the Z axis, common to both the socket and the foot reference system, positive if anticlockwise. F can be decomposed into the socket reference system, in the F-X_S and F-Y_S components, while decomposing it with respect to the socket reference system the F-X_F and F-Y_F are obtained. To measure F and M we will use load cells interposed between the foot and the socket. Below, when we refer to F and M measured with the load cell, we will add the prefix LC (es LC-F-Y_S).

2. CONCEPT OF THE TEST BENCH

The aim of this study is to develop a test bench capable of producing on the prosthesis the complex cycle of stresses that it undergoes during the running of an athlete, in terms of the forces magnitude, imposed deformations and application times. Our research aims to develop a test bench capable of stressing the prostheses in the sagittal plane, either by compressing them along the longitudinal axis or orthogonally to it. Furthermore, the ground must be able to vary the angle of inclination to explore the behavior during the different phases of the stance.

2.1. TEST BENCH'S STATE OF ART

2.1.1. Beck, Taboga and Grabowski, 2016. Characterizing the Mechanical Properties of Running-Specific Prostheses [20]

In the research of Beck, Taboga and Grabowski, 2016 [20] the objective is to determine the mechanical stiffness of the prostheses and the hysteresis in the condition of maximum GRF, varying the travel speed and the height of the prosthesis. They therefore measured GRFs from 11 athletes with unilateral transtibial amputations while they ran at 3 m/s and 6 m/s on a force-measuring treadmill, and the angle β, defined as the angle between the longitudinal axis and the peak resultant GRFs in the sagittal plane, using a motion capture system. Each athlete used their own personal RSP. They found that the beta angle varies between 10 ° and 25 °, depending on the type of prosthesis and the speed of running, while the GRF peak is 2.5 to 2.8 times the body weight. To obtain the stiffness curve they used a material testing machine with an aluminium rotating base to performe each tests at different beta angles, with a upper limit of peak GRFs 3 times the body weight to simulate a 3m/s running, and 3.5 times the body weight to simulate a 6m/s running [25] (Figure 2.1.1.1). To minimize shearing forces, they used a low-friction roller-system beneath each RSP that allowed anterior and posterior translation while maintaining the angle of the applied force relative to the longitudinal axis, justifying this choice by referring to ISO 10328 2016 [42], which, however, does not refer specifically to RSPs. In our opinion, it is also essential to evaluate the whole stance phase, between heel strike

and mid stance to evaluate how the prosthesis is loaded, and especially between mid stance and toe off to evaluate how energy is released, a fundamental step to optimize athlete's performance.

Beck, Taboga and Grabowski suggest that "it is possible that the inverse relationship between affected leg stiffness and running speed found in McGowan et al. [25] can be attributed to decreased prosthetic stiffness via increased angles between the resultant GRF vectors and RSPs at faster speeds" and olso "the discrepancies with different research suggest that prostetic stiffness testing procedures should be standardized".

It is important to point out how the inclination of the floor in the test bench has nothing to do with the inclination of the ground during the run. More precisely, the inclination of the plane, together with a soil capable of sliding on it, is an expedient to generate a GRF that is always orthogonal to the ground, because precisely the cutting forces can not be transmitted due to the trolley. So they have reproduced a GRF with a definite inclination with respect to the prosthesis, precisely the beta inclination, but they are certainly not the same conditions in which the participants of their test have run. In fact, in normal running conditions there is always a friction between the sole of the prosthesis and the floor, so that the cutting forces are generally not null. Obviously there is an instant in which they cancel, and correspond to the moment when the GRF-XG passes from negative to positive, that is when it passes from braking to propulsive. In conclusion therefore, their test faithfully reproduces the conditions of stresses provided that it is assumed that at that moment the ground is orthogonal to GRF.

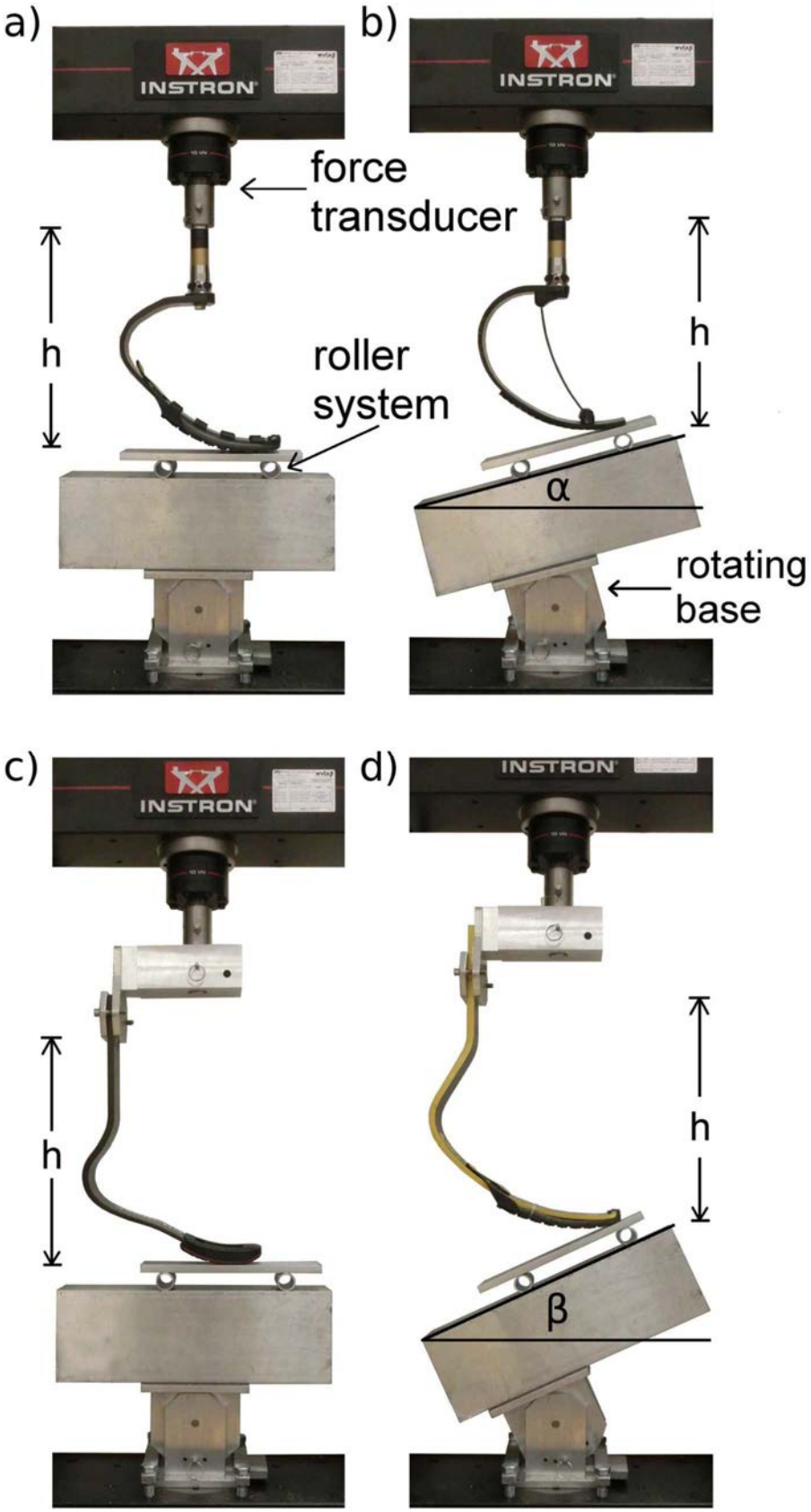

Figure 2.1.1.1 | Test bench of Beck, Taboga and Grabowski, 2016 [20]

2.1.2. Dyer, Sewell and Noroozi, 2014. An Investigation into the Measurement and Prediction of Mechanical Stiffness of Lower Limb Prostheses Used for Running.[21]

Methodology: Two Elite Blade composite lower limb energy storage and return prostheses (ESRP's_Chas A Blatchford & Sons Ltd., Basingstoke, UK) were used in this study as typical examples of high activity prostheses.

This is the same technology in principle as those used in elite competition. They have a split toe design that sometimes utilizes an attached "heel." This heel component was omitted from these studies to focus solely on the carbon "blade" itself. The lengths of the prostheses are approximately 405 mm from end to tip. The thickness of the composite material is approximately 10 mm along the length of their shanks but then progressively tapers down to 3 mm at their distal ends (Figure 2.1.2.1).

Figure 2.1.2.1 | Prosthesis design test piece. Dyer, Sewell and Noroozi, 2014 [21]

They were numbered prostheses 1 and 2. Their exact performance specification was not known prior to these experiments.

The prostheses were vertically compressed in a fixed, inverted position using a Testometric strength testing machine (Testometric Company Ltd., Lancashire, UK).

Taking the length of the supplied prostheses into account, both were mounted to an aluminum fixing block that aligned the prostheses shank at a 60-degree angle from a horizontal plane. This selected angle ensured correct alignment creating a theoretical centerline that would run from the distal end of the prostheses through the midpoint of

the fixing bolts that would normally attach to the prosthesis socket. An example image of the experiment setup is shown in Figure 2.1.2.2.

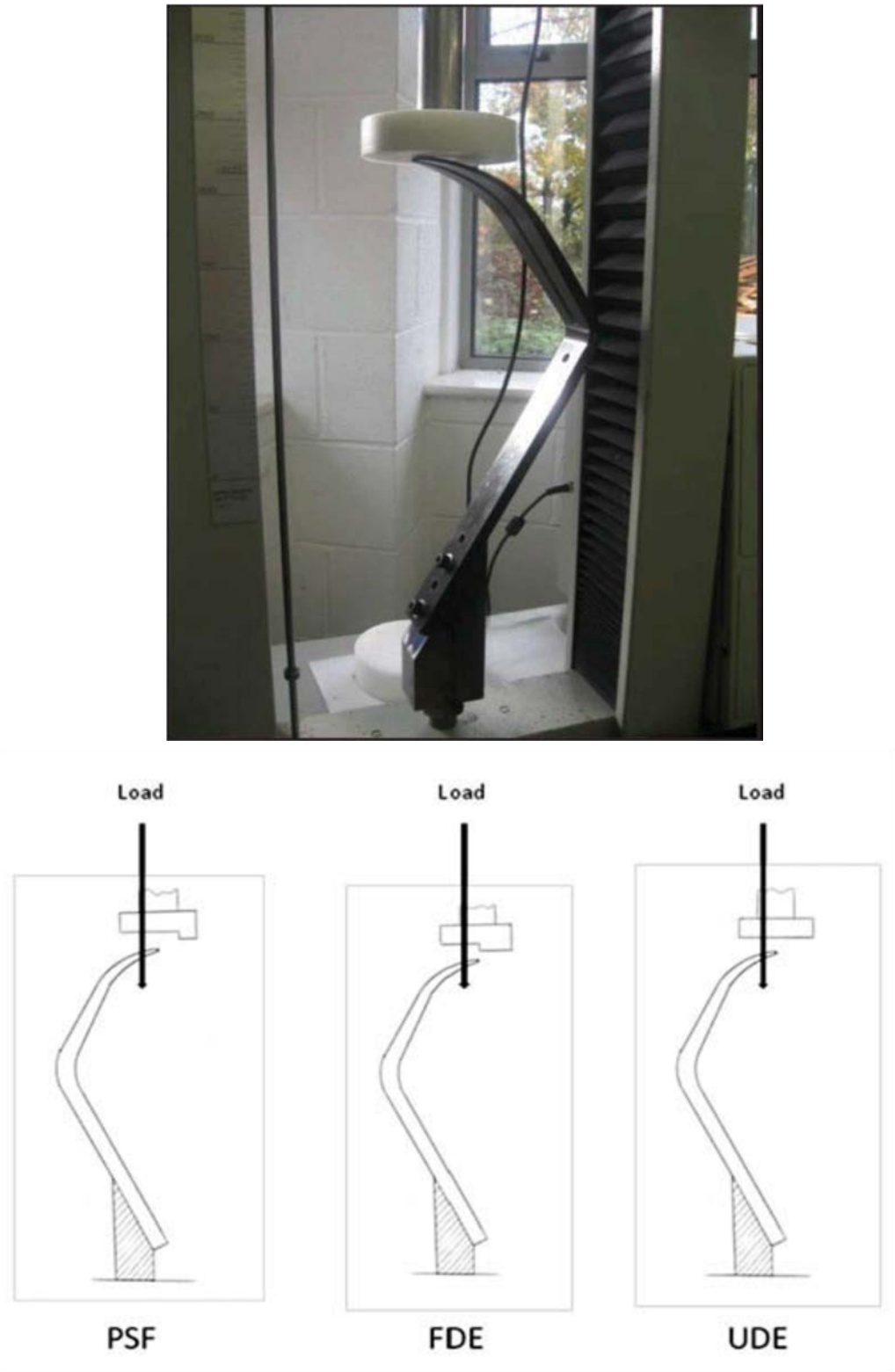

Figure 2.1.2.2 | To the left, Prosthesis loading test machine. To the right, Testometric loading formats. Dyer, Sewell and Noroozi, 2014 [21]

Both prostheses were loaded in compression 10 separate times up to a load of 1500÷2000 N and applied at a rate of 50 mm/min. Due to the lateral shear forces imposed when loading the prostheses in test trials prior to these experiments, these were the safest maximum loads it was felt to impose in these experiments. Each test took approximately 1 minute to complete.

The three different prostheses compression static loading techniques, illustrated in Figure 2.1.2.2, are as follows:

1. FDE: Fixed at the prostheses distal end. The distal end of the prosthesis butts against a ledge that prevents it from sliding when compressed.

2. PSF: Partial slide then fixed. The prosthesis can slide 28 mm before the distal end butts against a ledge preventing further slide when compressed.

3. UDE: Unfixed distal end. The distal end of the prosthesis is unfixed and can slide freely under the load cell platen when compressed.

The coefficient of variation (CV) is used to calculate the data's variability in this study. The CV has been defined as a measure of absolute consistency when evaluating a series of results [26] and is calculated as the Standard Deviation divided by the Mean Average and then multiplied by 100. The lowest possible percentage is most desirable.

Next, it is investigated to see if a limited subset of load and deflection data could be used to accurately predict the stiffness response of higher loads. This would be corroborated with an additional load and resultant deflection test to the targeted higher load. This is useful as it was proposed in this papers introduction that lower limb stiffness changes based on running speed [27] and in addition, it has been proposed that sprinting witnesses bodyweight impacts of 4÷5 times bodyweight [28]. Therefore, a successful method of prediction would allow prosthesis stiffness to be calculated for greater loads than those investigated in this study or for different running events based on a smaller subset of data.

The predictions will use prosthetic loading data from experiment 1 but be corroborated with a second data set loaded to the higher load of 3500 N. The experiment 1 data will have two trend lines extended from the first experiment data of the FDE method to help predict the response. These are:

- A 2nd order polynomial line of the entire load and deflection graph trace.

• A linear line extended from a 450 N loading sample taken at the end of the load and deflection graph trace.

	Prostheses 1: FDE	Prostheses 1: PSF	Prostheses 1: UDE	Prostheses 2: FDE	Prostheses 2: PSF
Stiffness at 1,950 N (1,500 N UDE)	60	58	34	48	42
Average stiffness of total load cycle (N/mm)	51	30	26	39	26
Percentage increase of peak load stiffness over average stiffness	18	93	31	23	61
CV (%) of Stiffness at 1,950 N	0.6	0.5	0.2	1.1	0.2
CV (%) of average stiffness of total load cycle	1.6	0.9	0.6	1.7	0.1

Figure 2.1.2.3 | Stiffness (N/mm) data of five tests. Dyer, Sewell and Noroozi, 2014 [21]

With both prostheses, the FDE method demonstrated the highest recorded average stiffness.

The UDE method only used on prostheses 1 highlights a vastly inferior recorded average stiffness. However, in this specific case, the distal end is not fixed meaning the prosthesis is constantly slipping or "arching through" as it is compressed. The recorded deflection is therefore a relative rather than a true deflection. In addition, due to the controlled slippage, the prostheses total length is effectively shortening as it is being compressed. Due to the amount of bend evident, it was decided for safety reasons to cease loading at 1500 N.

Typical behavior of all the tests of prosthesis 1 are shown in Figure 2.1.2.4

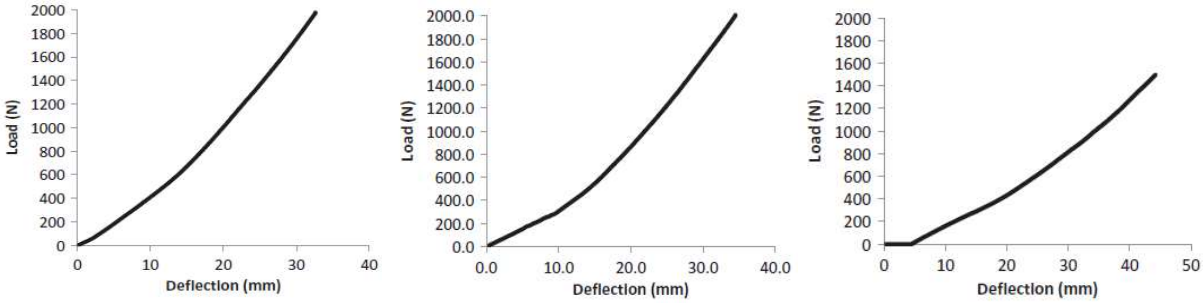

Figure 2.1.2.4 | First graph: Prosthesis 1 FDE test; Second graph: Prosthesis 1 PSF test; Third graph: Prosthesis 1 UDE test. Dyer, Sewell and Noroozi, 2014 [21]

One prosthesis (prosthesis 2, FDE method) is used to ascertain whether a predictive stiffness can be generated from a smaller load and deflection data set that stops at a lesser amount (2000 N). By then applying both a 2nd order polynomial trend line and a linear trend line to the final 450N "linear like" sample of section 3's data, the following result from one of the tests can be seen in Figure 2.1.2.5.

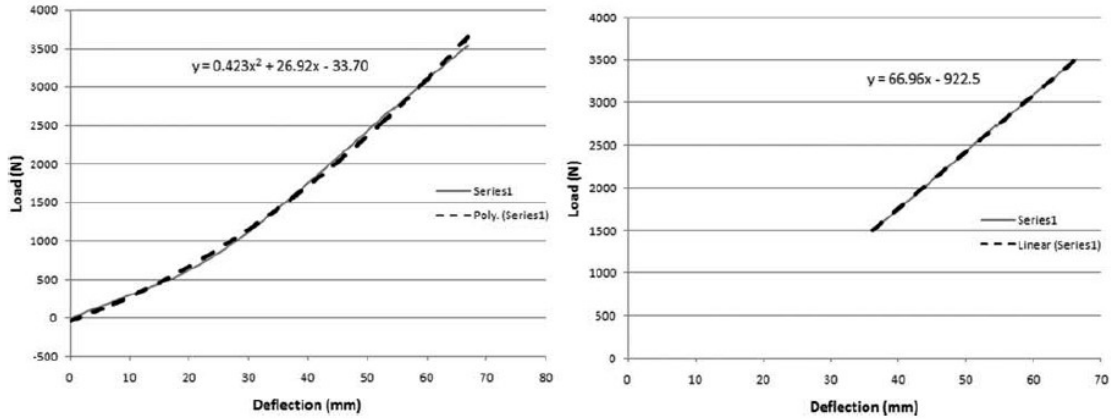

Figure 2.1.2.5 | Second order polynomial and 450 N linear 3,500 N predictive load examples. Dyer, Sewell and Noroozi, 2014 [21]

The predictive stiffness values at 3500 N were calculated by rearranging the polynomial and linear line trend line calculations displayed inside the graphs in Figure 9. This was achieved by determining the resultant deflection when 3,500 N is applied. The mechanical stiffness was recalculated and then compared to new actual loading cycles of prosthesis 2 performed up to 3500 N of load. This data can be compared in Table 2.1.2.1 below.

Data Set	Sample	Stiffness (N/mm)
st Experiment FDE test	Average stiffness of 0–1,950 N sample	39
	Actual stiffness at 1,950 N loading	48
2nd Experiment FDE test	Average stiffness of 0–1,950 N sample	37
	Actual stiffness at 1,950 N loading	45
	Actual stiffness at 3,500 N loading	53
Predictive stiffness @3500N	2nd order polynomial trend line	55
	1,500–1,950 N loading linear trend line	49

Table 2.1.2.1 | Prosthesis 2—FDE test 3,500 N loading and prediction. Dyer, Sewell and Noroozi, 2014 [21]

Discussion: Both prostheses 1 and 2 produced different levels of stiffness to each other. This only highlight how composite manufacture can be altered by changing parameters such as cloth lay-up, fiber orientation or resin application to change the mechanical properties of a prosthesis - despite looking physically identical.

Despite some differences between the three measuring methods prostheses stiffness, all experiments each generated extremely low coefficient of variation of the data in a 0.2–1.1% range. This value is extremely low and suggests that each experiments data was stable and repeatable. It is also suggested that less than 10 tests are sufficient for each experiment test method. This low level of data variation did include the PSF and UDE methods that had incorporated intentional slippage of the distal end. While the boundary conditions of each method are slightly different, the compression and slide characteristics of the methods are clearly stable.

The highest recorded stiffness with both prostheses 1 and 2 occurred when using the FDE method. This is likely due to both the UDE and PSF methods having controlled slippage of the distal end causing a relative rather than an actual displacement to be recorded by the loading machine. It is possible that such slippage of the PSF and UDE methods may effectively shorten the spring length causing further measurement inaccuracy.

Under load, the “foot” and “ankle” zones of the prosthesis with a tapered thickness will compress first, then causing an initial non-linear response. The increased (yet uniform) thickness of the shank/calf related areas in the prosthesis used here will create an increase in stiffness and will therefore produce a more linear load/deflection relationship.

At a loading of 1,950 N, the prosthesis 1 FDE and the PSF methods had stiffness's of 60 N/mm and 58 N/mm, respectively, a difference of 3.3%, while the prosthesis 2 had FDE and PSF stiffness's of 48 and 42, a difference of 12.5%.

This demonstrates that while the prosthesis performance itself is repeatable, the change in methods produces a significant enough change in the experiments boundary conditions not to make the data referenceable between methods.

The FDE method is recommended for use in the future because its stiffness was both higher than the PSF method coupled with the knowledge that its distal end was fixed and therefore likely a more accurate representation of mechanical performance.

It could be argued however, that measuring stiffness by fixing the prosthesis at the distal end is not representative of it in actual use as the ground reaction strike point will likely not be at the absolute distal end. However, because this strike point would be different between all runners, an alternative approach is to identify a standardized point along the prosthesis length that correlates to the strike point of the human foot.

The UDE method will likely lead to an underestimation of the prosthesis performance or a misprescription of such technology to athletes. An unfixed distal end when measuring stiffness of a prosthesis is not recommended.

For the prediction of the stiffness response of higher loads, starting from lower loads, the initial 1950 N maximum load was increased by 45% to 3500 N (or roughly 4.4 times the bodyweight of 80 kg sprinter).

The 2nd order polynomial trend line of the whole trace slightly overestimated the 3,500 N load stiffness. It is felt that this is because the latter section of the graph becomes increasingly linear.

Instead, when taking the upper, more linear section of the load deflection graph and then extending it to a loading of 3500 N, the obtained stiffness from the mechanical testing and corroborated data was 45 N/mm and 48 N/mm, respectively. The predicted performance was a stiffness of 49 N/mm that is much closer to the actual performance.

The best method would be to take the highest load and deflection data graph trace available and then apply a linear line to that aspect to predict higher load stiffness.

2.1.3. GROBLER,2015. Characterisation of running specific prostheses and its effect on sprinting performance. [22]

Methodology: Two different models (E and X) of commercially available RSPs from the same company were tested. Four different stiffness categories of each of the models were used (Table 2.1.3.1).

Stiffness category	Cat 3	Cat 4	Cat 5	Cat 6
Weight (kg)	60 – 68	69 - 77	78 - 88	89 - 100

Table 2.1.3.1 | Stiffness categories used in this study and the patient weight scale for which each RSP is prescribed. GROBLER,2015 [22]

The ground reaction forces were measured when dropping these RSPs onto a force platform, while two-dimensional video analyses, recording at 120 frames per second, was utilized to determine the compression of the RSP. The RSPs were attached to a prosthetic socket made specifically for this testing setup (Figure 2.1.3.1).

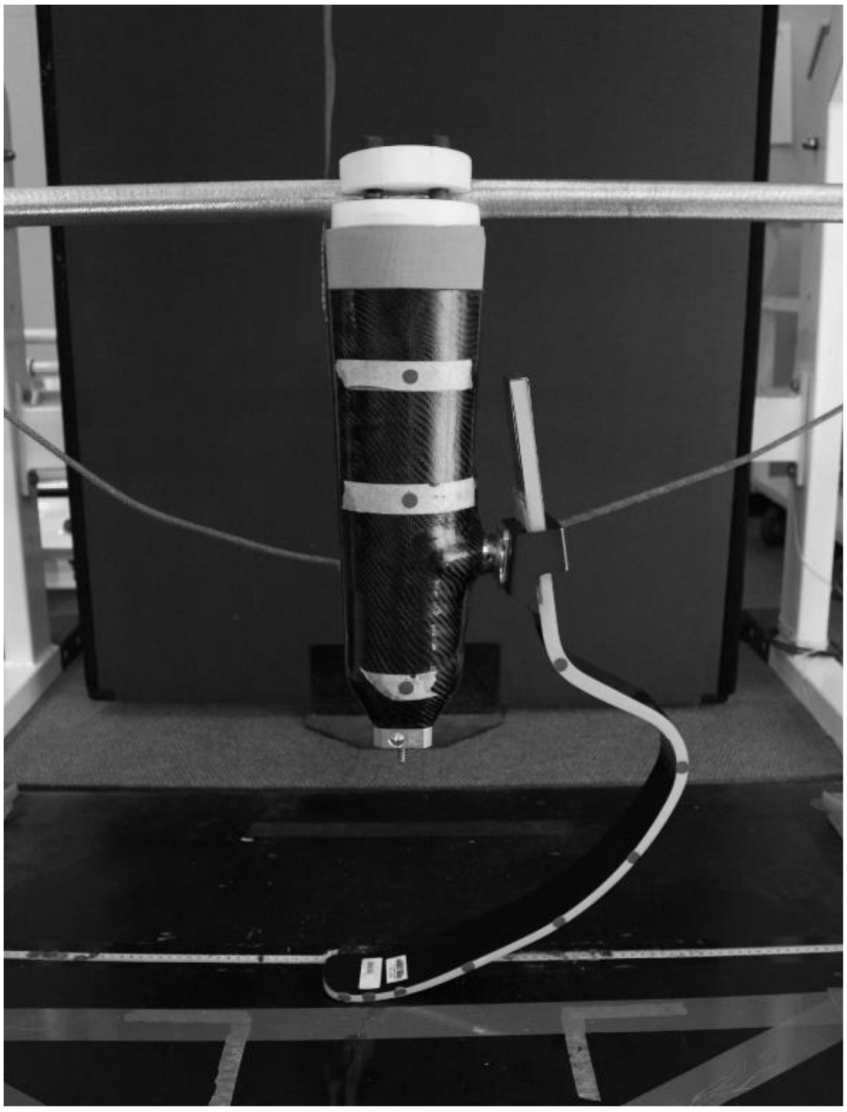

Figure 2.1.3.1 | Custom-built prosthetic socket and RSP blade attached to a Smith Machine®. GROBLER,2015 [22]

The socket-RSP attachment allowed for variations in the plantar flexion angle, as well as the attachment height of the RSP on the socket. The RSP socket complex was then attached to a rig and kept in an upright position while dropped onto a force platform. The RSPs were dropped with three different masses attached to it, namely 28, 38 and 48 kg. Selection of the 28 kg mass was since the prosthetic socket weighed 8 kg and the Olympic bar used with the rig weighed 20 kg. For each of these masses, seven alignment setups were used per RSP (baseline with two heights and five angle variations). Each drop was repeated three times, adding up to a total of 63 drops per blade.

Category: For each of the RSP models (E and X), four stiffness categories were tested. These categories are determined by the manufacturer (Table 1). For the purpose of the current study, categories 3, 4, 5 and 6 were used (Ecat 3-6, Xcat 3-6), with 3 being least stiff and 6 being most stiff.

Height: The length of the RSP was adapted by sliding the RSP up and down the attachment on the socket. The maximum height of the shorter of the two RSPs (model E) was used as the baseline (H0) height setup. The distance from the tip of the toe to the bottom of the socket in this baseline setup was replicated in the model X RSP (7 cm longer than model E), so that the baseline heights were similar for the two models. From here the RSP height was adjusted to three and six centimeters below baseline (H3 and H6, respectively). All height testing was done at a 7° plantar flexion angle.

Plantarflexion angle: According to the manufacturer's guidelines, the RSP should preferably be set at a 7° flexion angle in the sagittal plane as a starting point, with adjustments being made from this position to suit the athlete. Thus, a 7° flexion angle (A7) was used as the baseline setup and the angle was increased and decreased by one and two degrees for variation (A5, A6, A8, A9). All of these tests were completed at the baseline (H0) height.

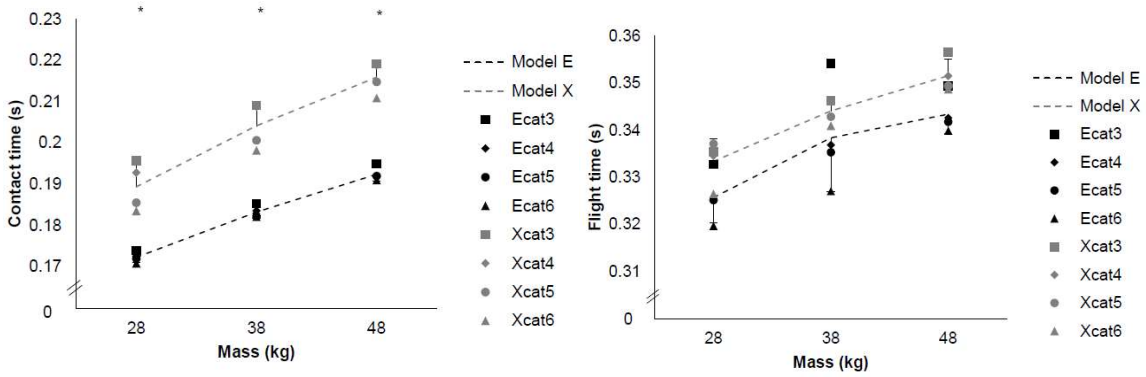

Figure 2.1.3.2 | Left graph: Mean ± SD ground contact time (s) measured in the two RSP models (E and X), as well as the categories of each model, using three different masses (kg). * Statistically significant difference between E and X ($p < 0.05$). Right graph: Mean ± SD flight time (s) measured in the two RSP models (E and X), as well as the categories for each model, using three different masses (kg). * Statistically significant difference between E and X ($p < 0.05$). GROBLER,2015 [22]

	RSI			ΔL (cm)		
Mass	28 kg	38 kg	48 kg	28 kg	38 kg	48 kg
Model E	1.89 ± 0.02	1.85 ± 0.05	1.78 ± 0.01	7.94 ± 0.49	8.90 ± 0.56	9.83 ± 0.68
E_{cat3}	1.91 ± 0.05	1.91 ± 0.04	1.79 ± 0.04	8.14 ± 0.49	9.91 ± 0.67	10.06 ± 0.78
E_{cat4}	1.88 ± 0.06	1.84 ± 0.03	1.79 ± 0.03	8.22 ± 0.41	9.08 ± 0.43	10.11 ± 0.65
E_{cat5}	1.89 ± 0.03	1.89 ± 0.03	1.78 ± 0.03	7.68 ± 0.43	8.48 ± 0.57	9.33 ± 0.58
E_{cat6}	1.87 ± 0.03	1.80 ± 0.03	1.78 ± 0.01	7.71 ± 0.46	8.83 ± 0.34	9.84 ± 0.49
Model X	1.76 ± 0.05	1.69 ± 0.03	1.63 ± 0.02	9.90 ± 1.21	11.27 ± 1.22	12.24 ± 1.14
X_{cat3}	1.71 ± 0.07	1.66 ± 0.06	1.63 ± 0.08	11.29 ± 0.49	12.55 ± 1.15	13.49 ± 0.89
X_{cat4}	1.74 ± 0.03	1.66 ± 0.04	1.61 ± 0.04	10.47 ± 0.41	11.79 ± 0.52	12.45 ± 0.79
X_{cat5}	1.82 ± 0.02	1.71 ± 0.01	1.63 ± 0.02	9.60 ± 0.37	10.94 ± 0.44	12.07 ± 0.51
X_{cat6}	1.78 ± 0.03	1.72 ± 0.04	1.65 ± 0.03	8.26 ± 0.36	9.82 ± 0.43	10.94 ± 0.55

Table 2.1.3.2 | Reactive strength index (RSI) and maximal compression (ΔL) measured in the two RSP models (E and X) whilst dropped with three different weights (kg).GROBLER,2015 [22]

Discussion

The results of this study indicated that there is a significant difference in the maximal ground reaction force (GRF peak), contact time (tc), and compression (ΔL) between the two tested models.

In order to simulate different body masses of athletes, three different masses were attached to the experimental setup. No statistically significant interaction effect was found between the model of RSP, the mass dropped and the setup of the RSP. This finding suggests that the attachment angle and height does not affect the way in which the prosthetics react to the applied load. Therefore, the RSP setup is only dependent on the athlete's personal preference and comfort, since the properties of the RSP are not influenced by setup changes.

Significant differences in the different categories were found for the variables with the 38 kg drops. The RSP stiffness categories are specified by the manufacturers as a means of accounting for variations in athletes' body mass. Therefore, the greater the body mass of the athlete, the greater the stiffness of the RSP in order to prevent excessive compression leading to prolonged contact times while running. This is evident in the data, as both the tc and ΔL decreased with an increase in stiffness category. The compression of the RSP acts similarly to a spring and decreases the impact by allowing for compression of the RSP. Thus, less compression leads to shorter contact time.

The GRF peak results showed that the stiffer the RSP, the less energy is stored as elastic potential energy in the RSP, and more energy is transferred as force into the ground. In this case, the stiffer the RSP, the greater the GRF peak. However, the storage of elastic potential energy in the softer RSPs did not result in greater jump heights (tf) in the softer prosthetic compared to the stiffer prosthetic. This indicates that the elastic energy stored compensates for the decreased GRF peak.

The model E RSP also had a significantly shorter ground contact time in comparison to the model X RSP. Shorter contact time has been found to have a moderate correlation to higher running speed.

The prosthetics used in this study were chosen for its specificity to sprint running. The model X prosthetic is specifically designed for short sprints, such as the 100 and 200 m, whereas the model E prosthetic is designed for longer sprints (≥ 400 m).

The results of this study suggest that the model of prosthetic (E or X) has a significant effect on the vertical ground reaction force when bouncing the prosthetic. In this case the use of the longer distance prosthetic E, resulted in greater vertical ground reaction forces in comparison to the shorter distance prosthetic X. This finding is in contrast to what would intuitively be expected, namely that the prosthetics for a short sprint would produce greater vertical ground reaction forces than prosthetics for a long sprint.

Perhaps the answer relates to the different phases of each race. The 100 [m] sprint can be divided into three main phases, namely the acceleration phase (0 to ~ 60 [m]), the speed maintenance/ maximal velocity phase (60 to 80 [m]) and the deceleration phase (80 to 100 [m]). Thus, the largest proportion (60%) of the 100 [m] sprint is spent in the acceleration phase. Although a 400 [m] race has the same three main phases, the acceleration phase lasts about 25% of the race (0 to ~100 [m])20. A significantly larger proportion of a 400 [m] sprint is spent in the speed maintenance phase (50%)20, compared to the 20% in the 100 [m] (20%). This may therefore explain why the model E prosthetic is prescribed for longer distance sprints and the model X prosthetics for shorter distances.

Conclusion

It was concluded from the results that there were differences between the two tested RSP models, however, variations in the setup of the RSP had minimal influence on performance of the prosthetic. Therefore, from a practical point of view, setting up the RSP to the athletes' comfort will not influence the performance of the prosthetic. The results further indicate that these two models of prosthetic significantly differ from each other, and that more research is needed to further the knowledge of the different RSPs available in order to assist athletes and coaches in determining the optimal RSP for the athletes' demands.

2.1.4. Nishikawa, Hobara, 2018. Mechanical stiffness of running-specific prostheses in consideration of clamped position. [23]

The prosthesis was mounted to two sets of steel jigs, which could change the clamped condition of the prosthesis. Figure 2.1.4.1 show the composition of the testing jigs.

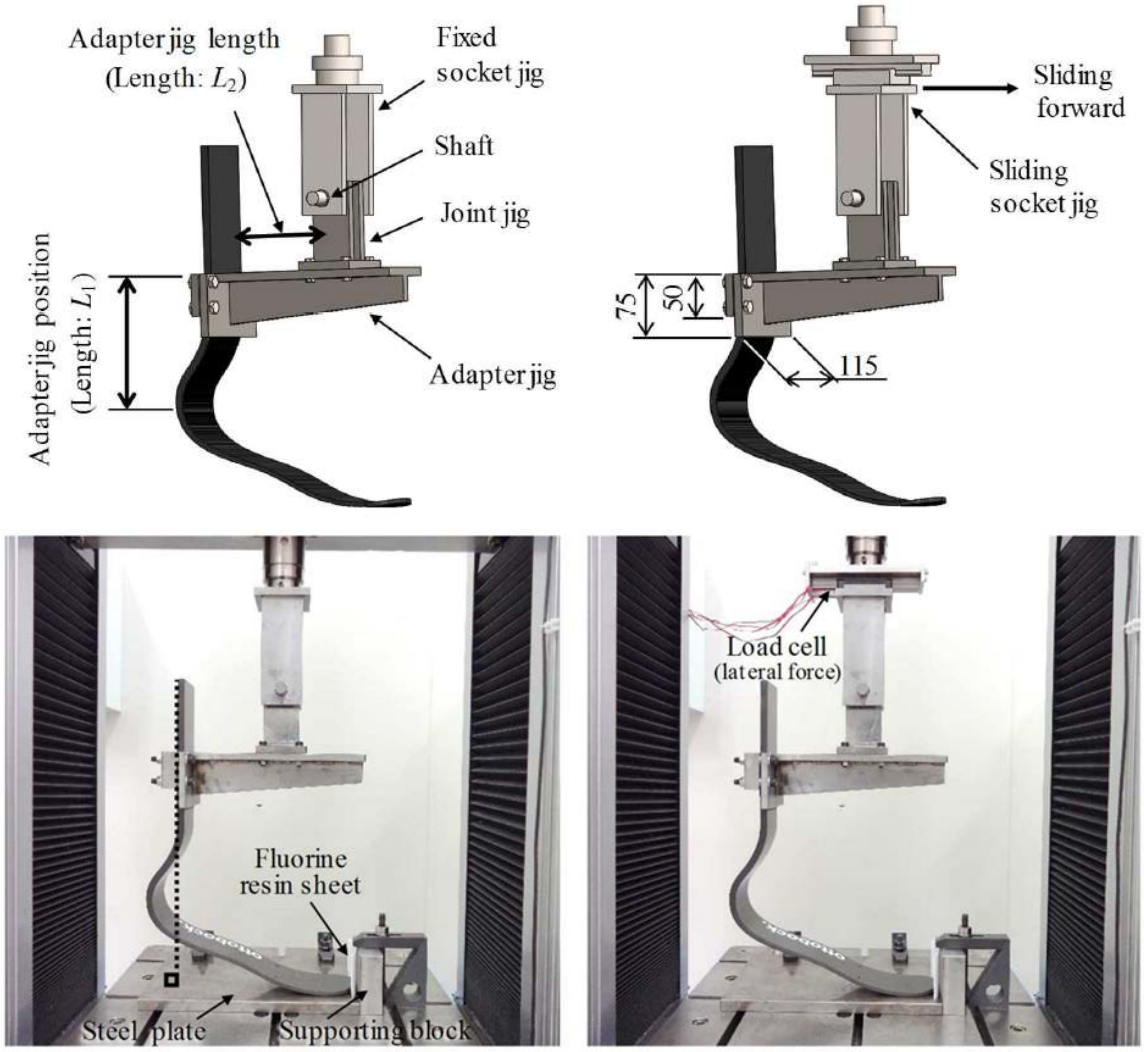

Figure 2.1.4.1 | Composition of testing jigs. To the left: fixed socket jig type. To the right: sliding socket jig type. Nishikawa, Hobara, 2018 [23]

The fixed socket jig was completely fixed to the testing machine, while the sliding socket jig could only slide forward. The joint jig was combined with the socket jig by a shaft. The prosthesis was mounted on the adapter jig. The angle between the adapter jig and prosthesis shank was 90 °. These jigs were extremely rigid as compared with the prosthesis; therefore, the deformation of the jigs themselves was neglected in comparison with the test results.

Fifteen testing conditions were employed in this study. As shown in Figure 2.1.4.1, the length L1 from the top of the calf part to the adapter jig position was set at 205, 255, and

305 mm. These are the same lengths as those from the shank edge to the adapter jig positions of 100, 50, and 0 mm, respectively. The adapter jig length L2 from the prosthesis to the joint jig was set at 75, 100, 125, 150, and 175 mm. Hereafter, the clamped condition is written as L1-L2 (for example, in the case of L1 = 205 mm and L2 = 75 mm, the clamped condition is denoted as 205-75).

L1 and L2 are determined optionally based on the physical characteristic and running-performance of the prosthetic user; therefore, both the parameters do not have a standard length. In this study, the range of L1 was assumed to be the longest possible (from 205 mm to 305 mm) in the test prosthesis. In addition, the range of L2 was set from 75 mm to 175 mm to clarify the influence of L2 on mechanical stiffness in practical use.

Static compression test.

All tests were conducted under laboratory conditions (23 ± 2℃ and 50 ± 5 % relative humidity). The prosthesis was vertically compressed using a universal material testing machine (AutoGraph AG-100kNX; Shimadzu co.). The crosshead speed was 100 mm/min. The prosthesis shank was aligned at a 90 ° angle from the horizontal table of the testing machine. The prosthesis toe contacted the supporting block with a fluorine resin sheet. Immediately after loading, the prosthesis toe separated from this block; therefore, the supporting block and the fluorine resin sheet did not influence the test results. The prosthesis bottom surface contacted a steel plate in a line. The surface of the steel plate without surface treatment was smooth.

Figure 2.1.4.2 show the situations after the compression tests.

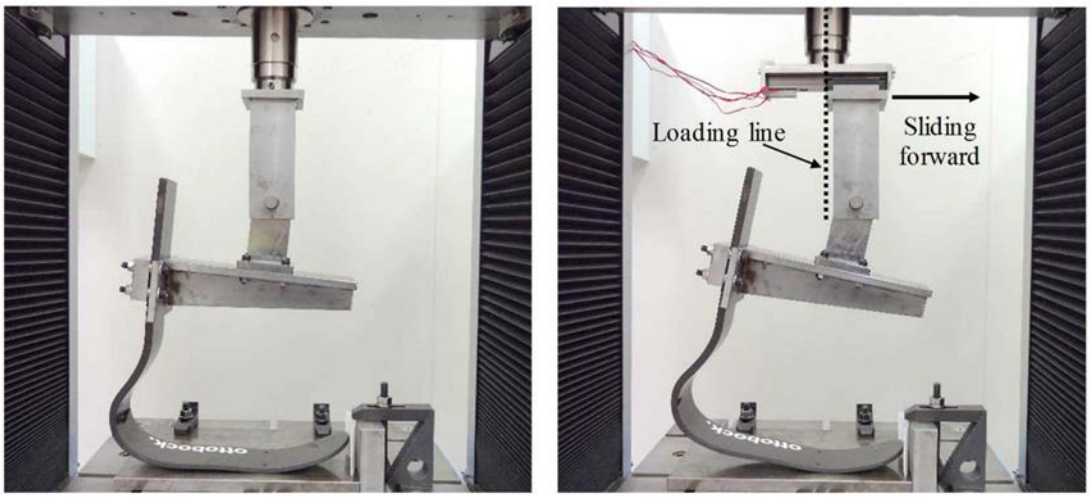

Figure 2.1.4.2 | Images of situations after compression tests. To the left: fixed socket jig type. To the right: sliding socket jig type. Nishikawa, Hobara, 2018 [23]

The prosthesis was loaded in compression for three separate times up to a maximum load of 2500 N; this value was chosen as this was approximately four times the bodyweight of the intended user for the prostheses specification. Under the compressive load of 2500 N, the prosthesis bottom surface contacted the steel plate in a line as shown in Figure 2.1.4.2, left image. However, the compression test stopped when the prosthesis slipped backward or slid forward, as shown in Figure 2.1.4.2, right image.

Result and discussion

Load-deflection relation

Figure2.1.4.3 show the typical load-deflection diagrams in the case of using the fixed socket jig.

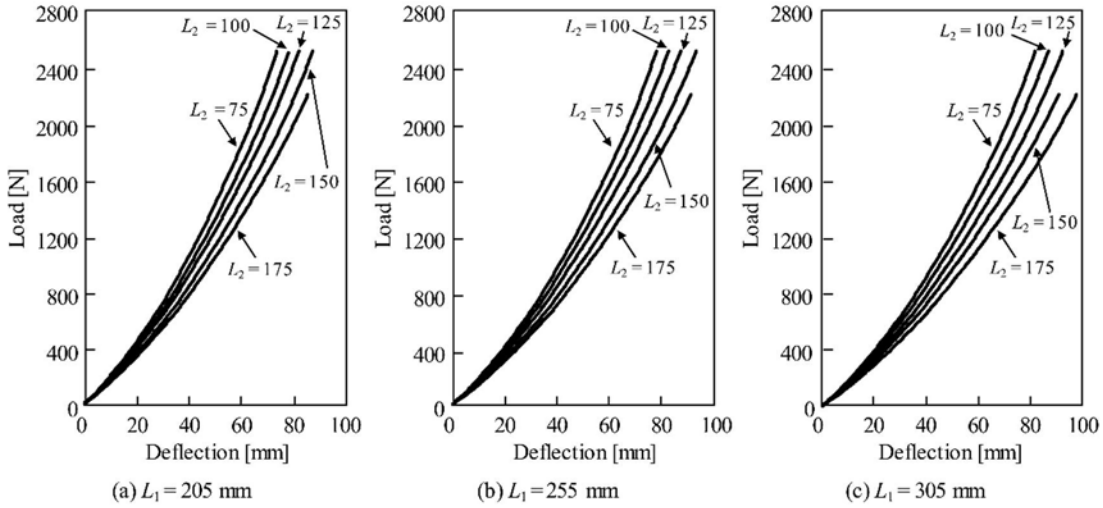

Figure 2.1.4.3 | Typical load-deflection diagrams (using fixed socket jig). Nishikawa, Hobara, 2018 [23]

All load and deflection relations were non-linear; this tendency has also been witnessed in other studies [21,24]. This may be due to a combination of the tapered thickness of the toe region and the change in prosthesis length with the movement of the contact line. The mechanical stiffness of the prosthesis is defined as load divided by deflection. In consideration of this definition, as the applied load increased, mechanical stiffness increased independently of the clamped condition. In comparison, at the same load, the stiffness increased with decreasing adapter jig length. Unlike the previous studies [21,24], the testing jigs in the present study applied both vertical load and moment to the prosthesis. Therefore, the moment and deflection decreased with decreasing adapter jig length, leading to higher mechanical stiffness under the same load.

Figure 2.1.4.4 show the typical load-deflection diagrams in the case of using the sliding socket jig.

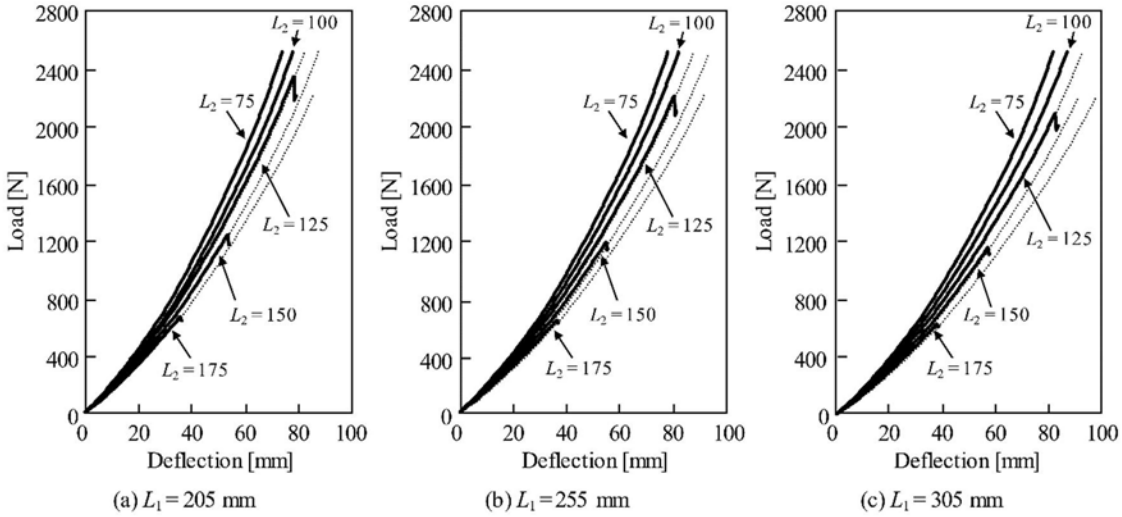

Figure 2.1.4.4 | Typical load-deflection diagrams (using sliding socket jig). Nishikawa, Hobara, 2018 [23]

The prosthesis was slid forward at the maximum load. Figure 7 shows the relations between the applied load and lateral force, which was measured at the sliding socket jig in the case of L1 = 205 mm.

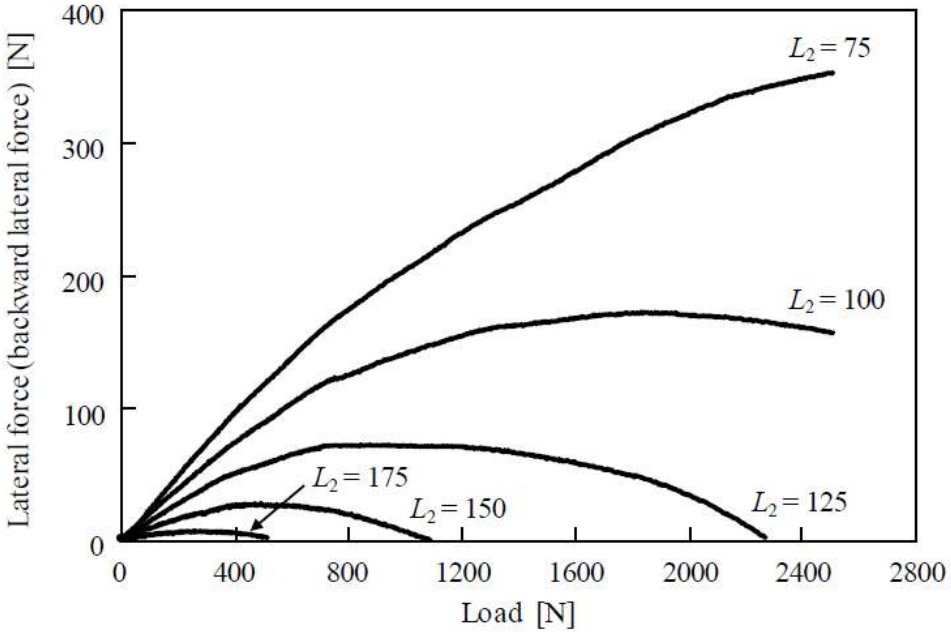

Figure 2.1.4.5 | Relations between applied load and lateral force (L_1 = 205 mm). Nishikawa, Hobara, 2018 [23]

Immediately after loading, the backward lateral force (acting in the direction opposite to that of RSP) was applied to the prosthesis shank. After the backward lateral force reached the peak, the forward lateral force (propulsive force) was generated. When the backward lateral force decreased and only the forward lateral force was applied to the shank, the

prosthesis was pushed out forward. This means that the minimum necessary vertical load to effectively propel the RSP exists.

Effect of clamped condition on mechanicall stifness

Figure 2.1.4.6 shows fifteen load-deflection diagrams under all clamped conditions using the fixed socket jig (as shown in Figure 2.1.4.3). Each load-deflection behavior corresponded under the certain clamped conditions (for example, 205- 125, 255-100, and 305-75). According to the interaction of the adapter jig position and length, fifteen load-deflection diagrams were classified into seven tendencies.

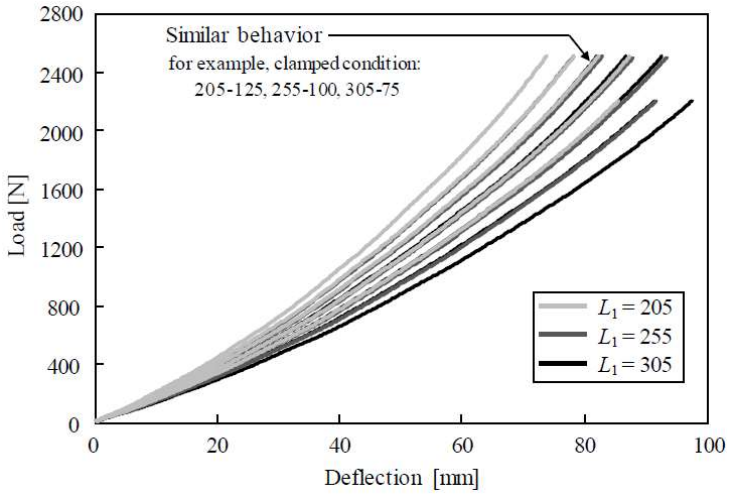

Figure 2.1.4.6 | Fifteen load-deflection diagrams classified into seven tendencies (using fixed socket jig). Nishikawa, Hobara, 2018 [23]

Figure 2.1.4.7 shows the relations between the deflection and inclined angle of the shank obtained from the observation results of the deformation behavior. Except for the clamped condition 205-75, the inclined angle was quite proportional to the deflection in all cases. Therefore, the inclined angle can become the key factor influencing the load-deflection behavior. In the case of clamped condition 205-75, an increment in the inclined angle decreased with an increment in deflection because the vertical load as compared with the moment was strongly applied to the prosthesis.

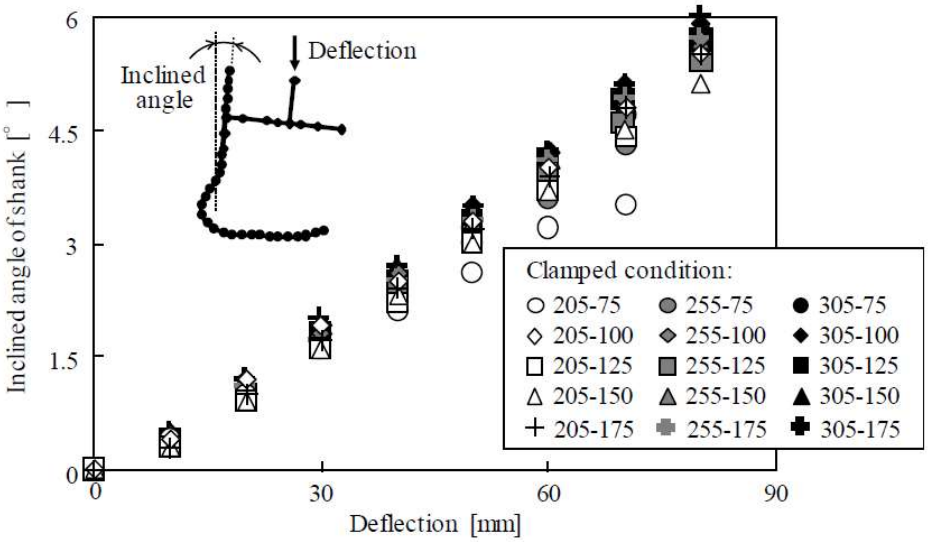

Figure 2.1.4.7 | Relations between deflection and inclined angle of shank. Nishikawa, Hobara, 2018 [23]

The prosthesis shank side is assumed to be a simple truss structure. In this model, the inclined angle was calculated using the product of L1 and L2, which is defined as a positional parameter (indicating the clamped condition quantitatively). Figure 2.1.4.8 shows the relations among L1, L2, and the positional parameter. Each positional parameter value corresponded under the certain clamped conditions (for example, 205-125, 255-100, and 305-75). The seven classified tendencies of the positional parameter were same as those shown in the load-deflection diagrams.

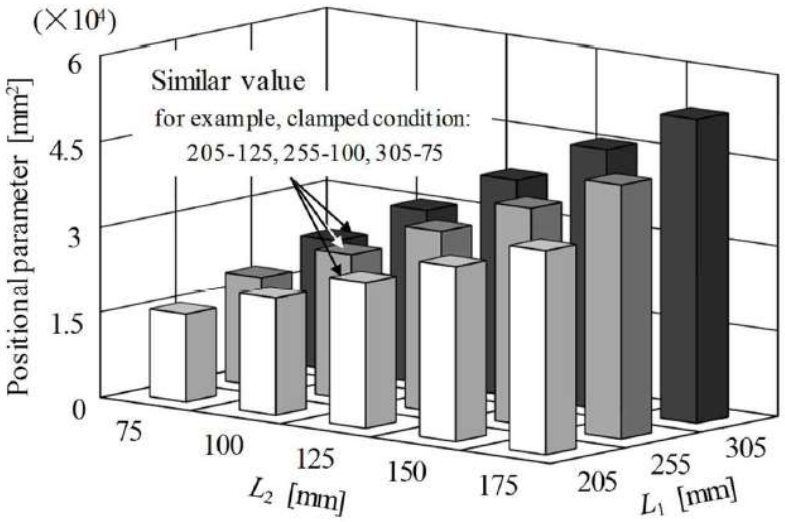

Figure 2.1.4.8 | Relations among L_1, L_2 and position parameter. Nishikawa, Hobara, 2018 [23]

Figure 2.1.4.9 shows the relations among mechanical stiffness, applied load, and the positional parameter. The mechanical stiffness was calculated as the average load divided by average deflection in the load range of ± 25 N. The minimum necessary vertical load to propel the RSP is also shown in Fig. 13. As for these relations, it can guide the athletes with lower extremity amputations in selecting the RSPs with the most suitable mechanical stiffness in consideration of their clamped condition. Consequently, the evaluation method of mechanical stiffness correlated with the applied load and positional parameter was proposed.

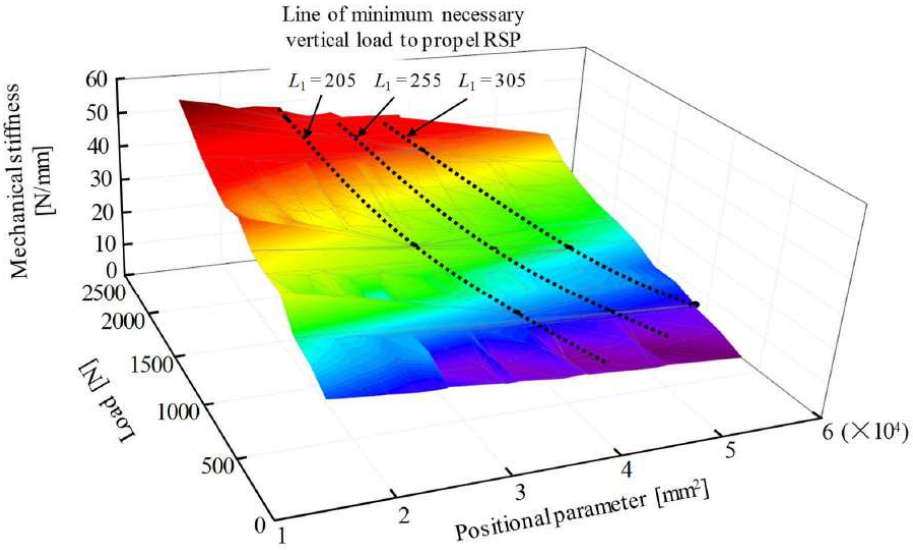

Figure 2.1.4.9 | Relations among mechanical stiffness, applied load, and positional parameter. Nishikawa, Hobara, 2018 [23]

Conclusion

In this study, mechanical stiffness of RSP was evaluated under fifteen clamped conditions by changing the adapter jig position and length. The results are summarized as follows.

1) All load-deflection relations were non-linear. The mechanical stiffness increased with increasing applied load and decreasing adapter jig length.

2) Immediately after loading, the backward lateral force was applied to the prosthesis shank, and then, the forward lateral force was generated in continuing loading. We also confirmed that there was a minimum necessary vertical load to effectively propel the RSP.

3) According to the interaction of the adapter jig position and length, fifteen load-deflection diagrams were classified into seven tendencies. From the observation results of the deformation behavior, the product of the adapter jig position and length was defined as positional parameter, which quantitatively indicated clamped condition. Consequently, the evaluation method of mechanical stiffness correlated with the applied load and positional parameter was proposed.

2.1.5. Dyer, Sewell and Noroozi. 2013. How should we assess the mechanical properties of lower-limb prosthesis technology used in elite sport? An initial investigation. [24]

This article shows a test to evaluate the part of energy returned by an RSP of the type Elite Blade. The prosthesis, fixed to a body in which the masses are positioned, is dropped to the ground, in order to evaluate the response to the impact. Reflective markers have been placed on the prosthesis to grasp the displacements with a motion capture system. A rubber layer has been placed on the ground to guarantee a high coefficient of attrition between the prosthesis sole and the floor, to avoid slipping.

Figure 2.1.5.1 | Prosthesis drop test rig. Dyer, Sewell and Noroozi. 2013 [24]

2.2. VIDEO ANALYSIS OF AN ATHLETE'S RUNNING WITH RSP

To design the test bench, it was first necessary to understand how the RSP is stressed during the running. For this preliminary study I used the graphs of the ground reaction forces (GRFs) during the stance phase published in a recent article (Makimoto *et al.*, 2017) [39] , of which I also had a slow motion video recording of an athlete's running. The objective of the research is to compare the GRFs between the intact limb and the prosthetic limb of athletes with unilateral amputation (Figure 2.2.1).

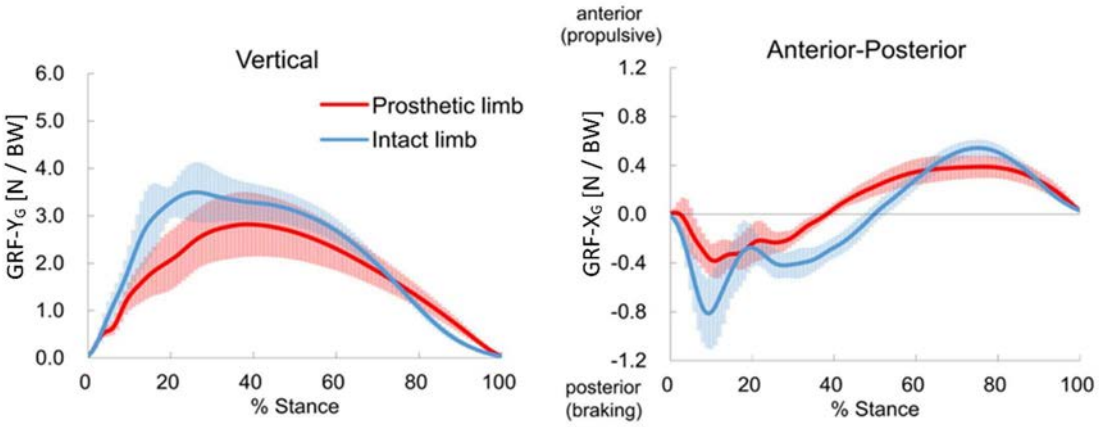

Figure 2.2.1 | GRFs . Average time-course profiles of ground reaction forces (GRFs) of prosthetic (red line) and intact (blue line) limbs during maximal sprinting recorded from 9 participants. Shaded area indicates standard deviations. Positive values indicate the vertical (A) and anterior (B)component of the GRFs, respectively. GRFs are normalized with respect to the athlete's weight force, BW. (Makimoto et al., 2017) [39]

This and many other articles [20,22,24,25,30-32,34-36,38] show how the prosthetic limb is not able to reproduce the same peak of strength of the GRF with respect to the intact limb, moreover the prosthetic limb has as a greater interval of the stance phase.

I then extracted from the video the frames of the stance fase, equispaced over time, starting from the instant of heel strike up to the toe off passing through the mid stance (Figure 2.2.2).

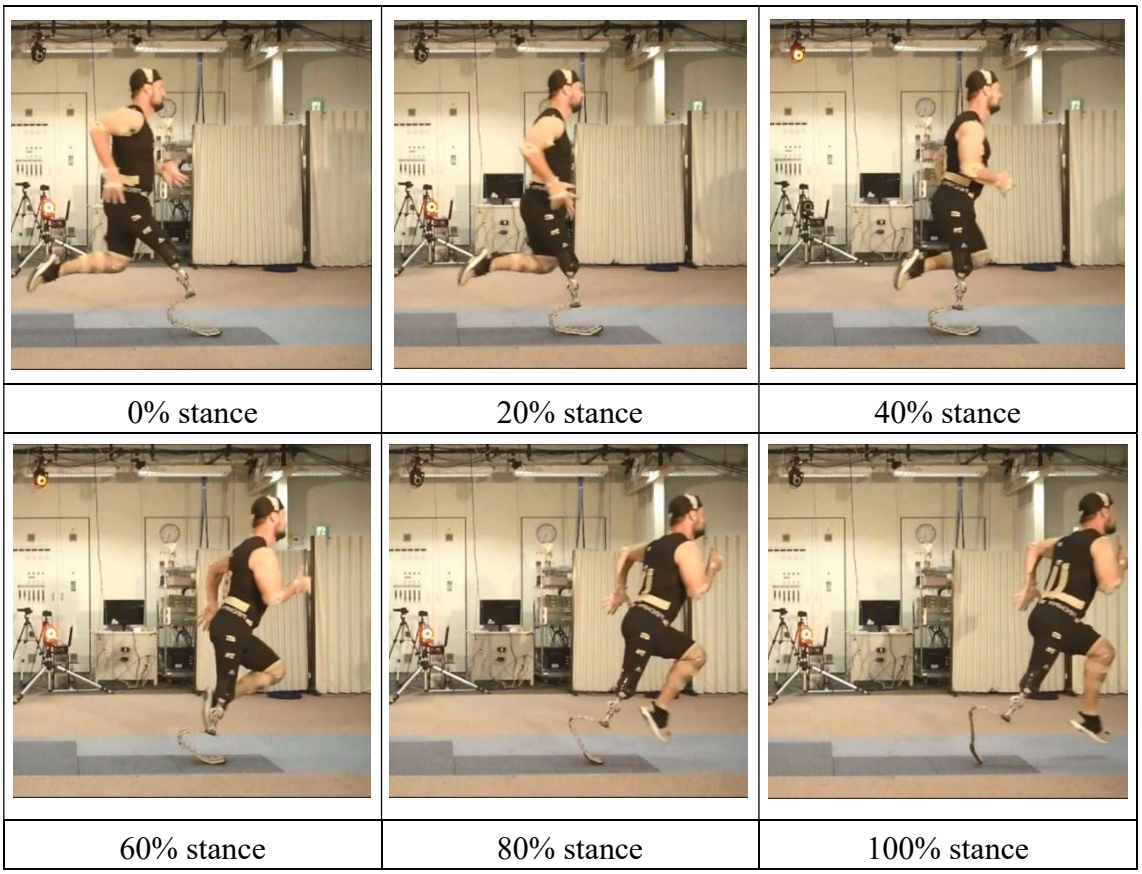

Figure 2.2.2 | Slow motion video frames taken from Makimoto et al., 2017. (Makimoto et al., 2017) [39]

On each frame I traced in red:

A) Y_F: Foot axis of the prosthetic foot

B) Y_S axis of the socket

C) $X_{G:}$ axis of the ground

while in blue I traced the GRF-X_G and GRF-Y_G whose values have been obtained from the graph in Figure 2.2.1, applied in the pressure centre (COP) (Figure 2.2.3).

The first frame and the last represent respectively the first contact between the prosthesis and the ground and the moment of the detachment of the prosthesis from the ground, for which the GRFs are void, as also shown in Figure 2.2.1

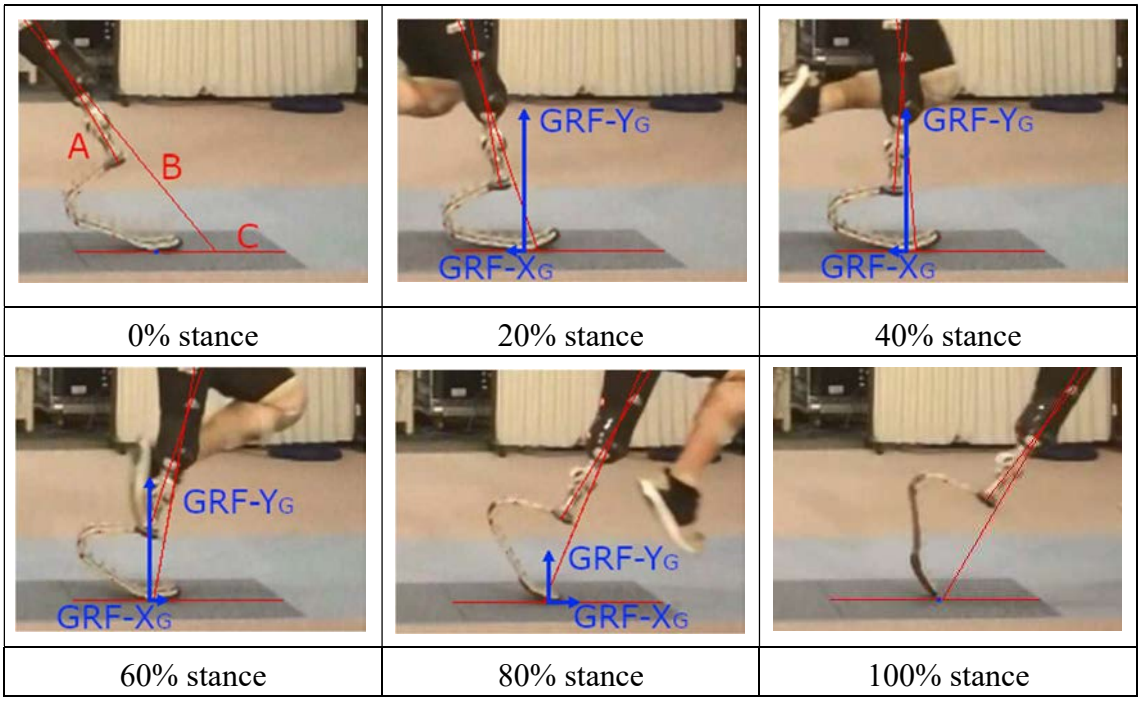

0% stance	20% stance	40% stance
60% stance	80% stance	100% stance

Figure 2.2.3 | Video frames with reference axes and GRFs. (Makimoto et al., 2017) [39]

The representation on each frame of the GRFs obtained from the paper provides a visual and immediate idea of the type of stress that the prosthesis undergoes.

From video measurements I have obtained the absolute angle of the leg, θ_{SH} defined as the angle that the axis of the socket forms with the normal on the ground, Y_G, and the angle γ, defined as the fixed angle of alignment in the sagittal plane between the foot and the socket (Figure 2.2.4)

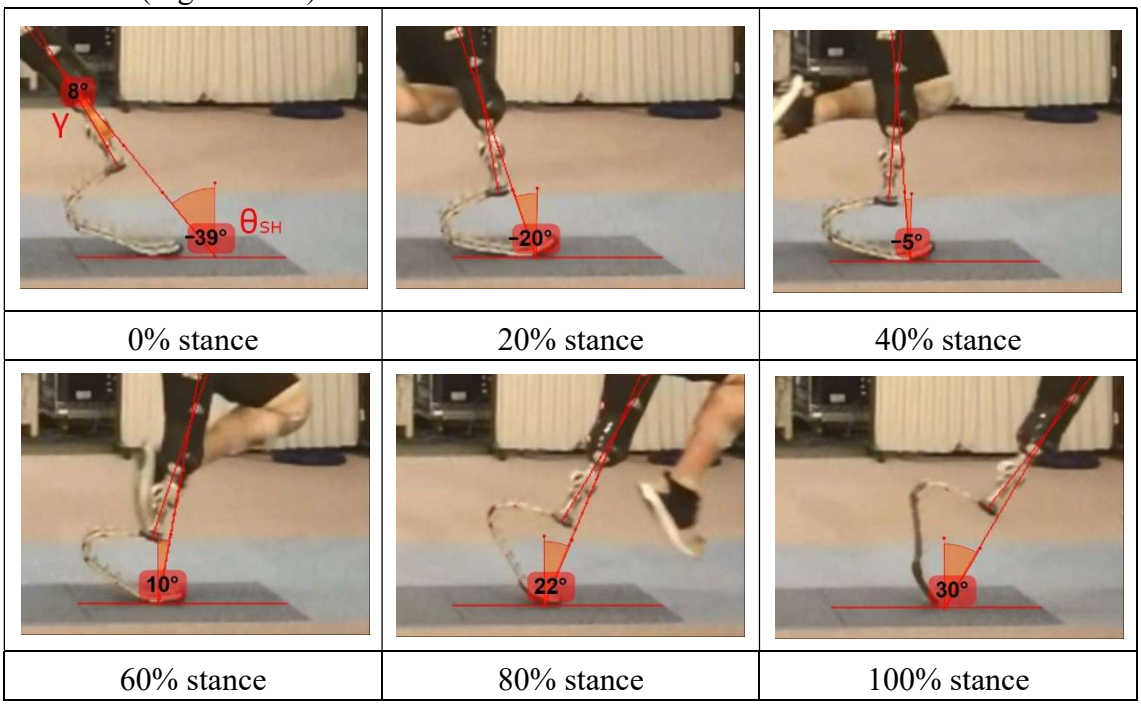

0% stance	20% stance	40% stance
60% stance	80% stance	100% stance

Figure 2.2.4 | Video frames with angles. (Makimoto et al., 2017) [39]

In Figure 2.2.5 is represented θSH trend during the stance phase.

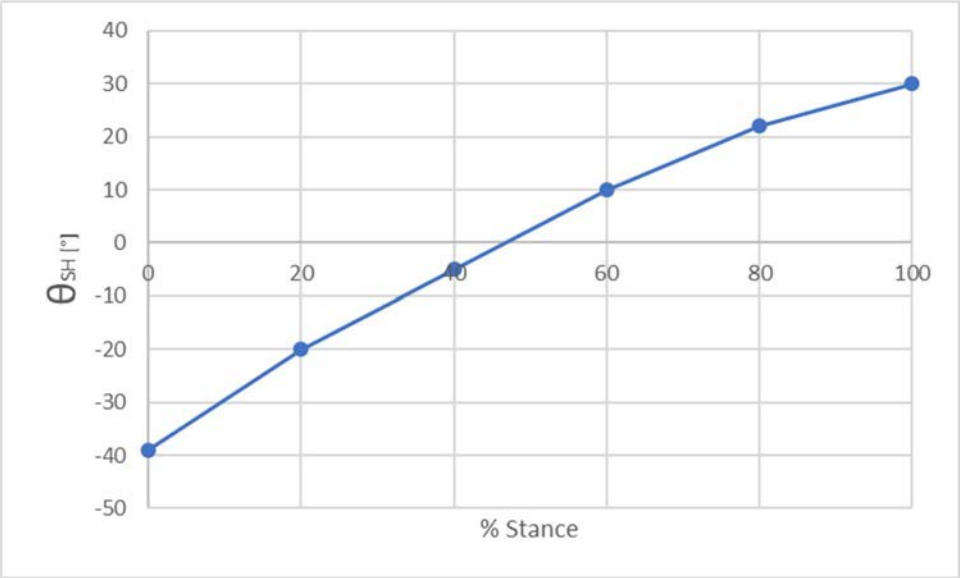

Figure 2.2.5 | θ_{SH} trend during the stance phase.

Known the GRF and the absolute angle of the leg I have decomposed the GRFs in the sagittal plane along the axis of the soket, Y_S, and orthogonally to it, X_S (Figure 2.2.6).

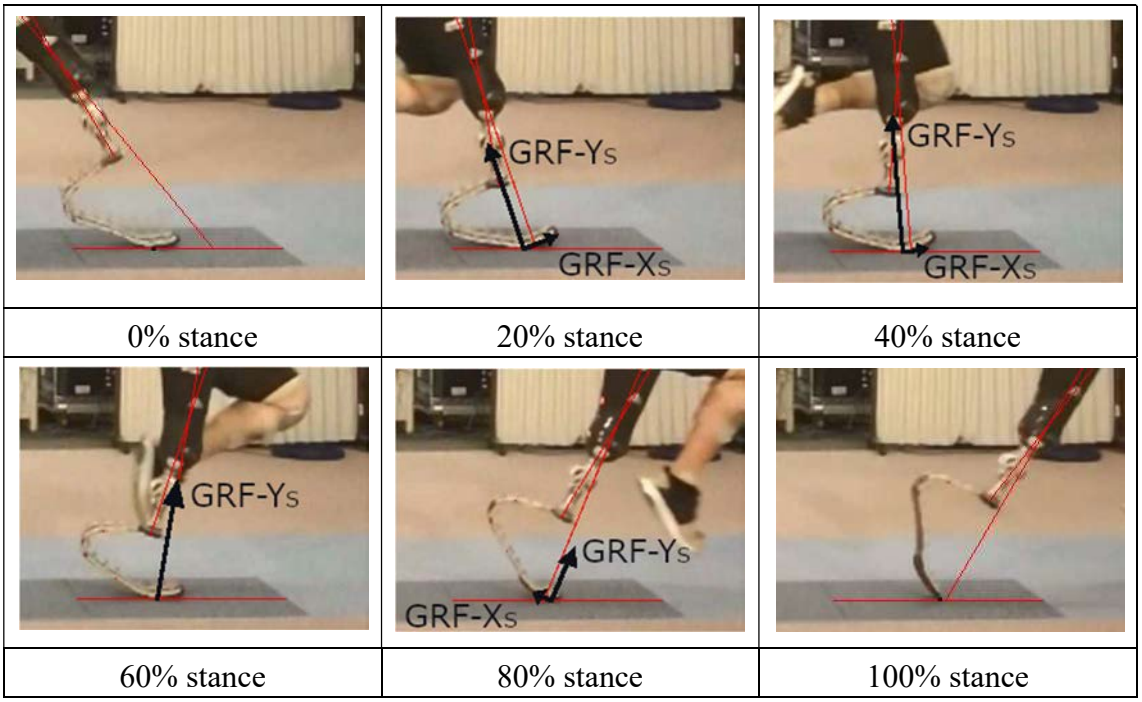

Figure 2.2.6 | Video frames with GRFs GRF projected into the socket reference system. (Makimoto et al., 2017) [39]

This has allowed me to highlight a first aspect: the prosthesis is mainly stressed in the direction of the axis of the soket, and this is reflected in the spring model. However the shearing forces it is not negligible, even if there is a moment in which it is annulled to

change its sign, from braking to propulsive. This confirms the need to characterize the prostheses by applying both components.

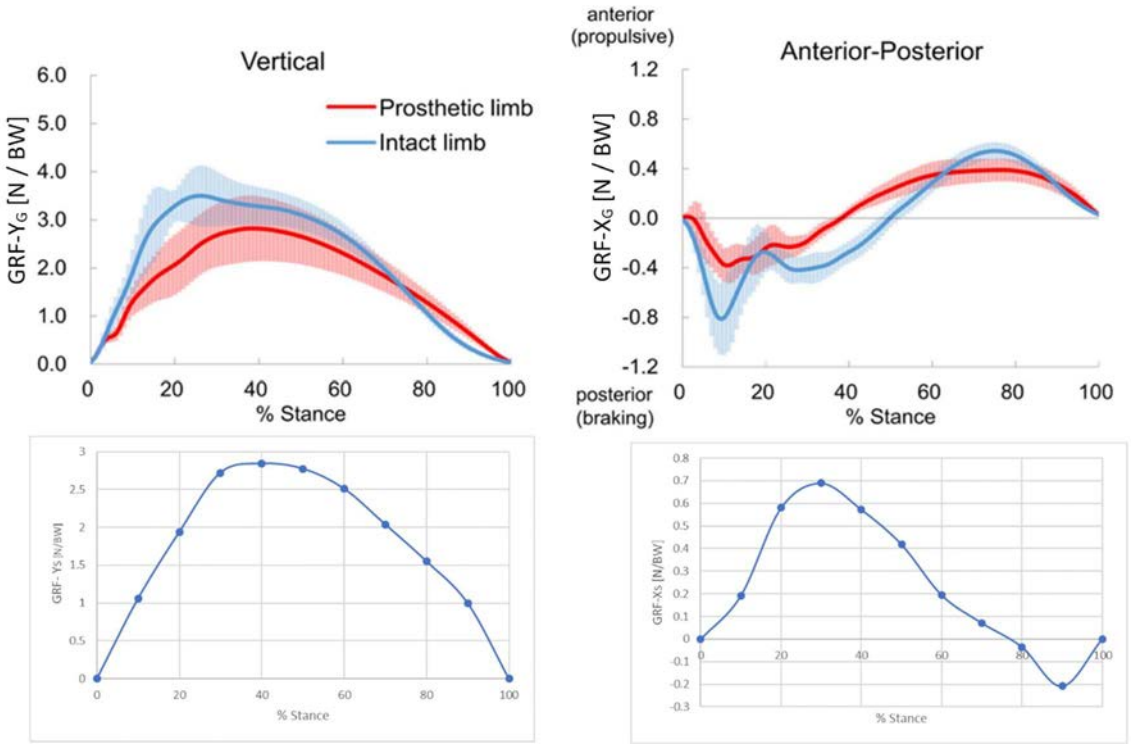

Figure 2.2.7 | Comparison between the GRF components expressed in the soil reference system and the components with respect to the socket reference system.

At this point I derived from the frames the pixel position of easily recognizable points of the socket, the foot and the laboratory. Knowing the size of the prosthesis, I could estimate the width of each pixel. This operation, although approximate, allowed me to obtain a first evaluation of the movements that test bench should have allowed. Observing the kinematism of the socket, I notice that the rigid motion of the socket is not a pure rotation but a rototranslation in the sagittal plane, therefore the degrees of freedom of the socket in the sagittal plane are three. A test bench capable of reproducing a rototranslation in the plane is not easy to implement, moreover the stance phase lasts on average 0.2s [34,35].

I rotated all the frames so that the socket reference system would be fixed. (Figure 2.2.8).

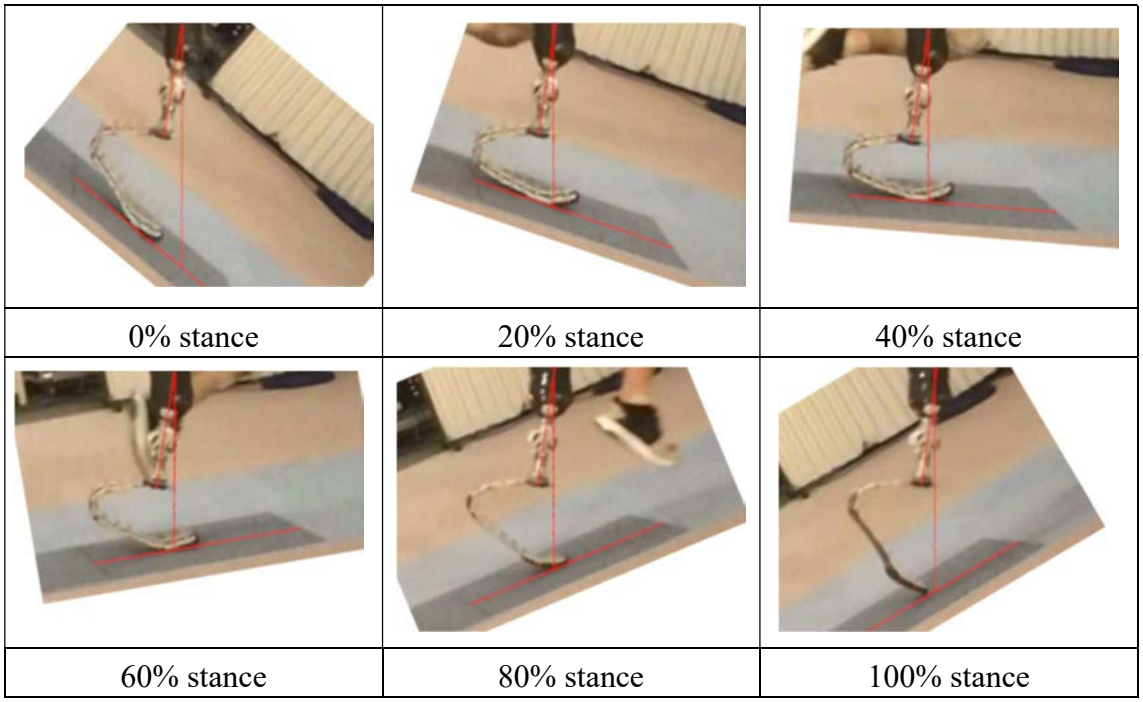

Figure 2.2.8 | Rotated video frames. (Makimoto et al., 2017) [39]

In Figure 2.2.9 I have schematically represented the prosthesis and the horizontal axis of the ground X_G of all six frames of Figure 2.2.8

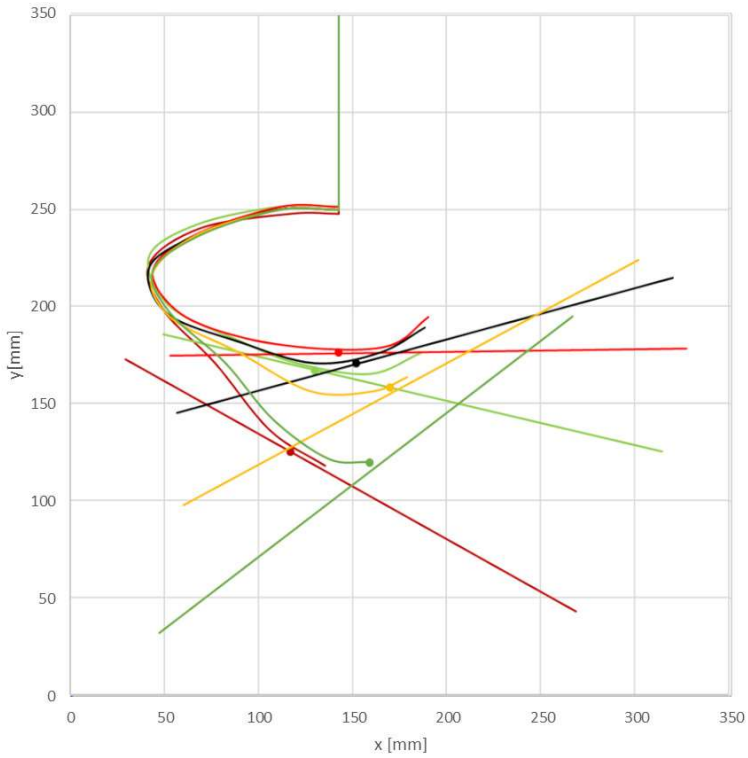

Figure 2.2.9 | Schematic representation of the kinematism of the prosthesis during the stance phase considering the socket reference system as fixed.

To simplify the movement of the ground I studied the solution in which the ground is hinged in a point that translates along an axis orthogonal to the axis of the socket. To do this it was necessary for the prosthesis to translate along the axis of the socket. The kinematics of the prosthesis is schematized in the Figure 2.2.10. The kinematism of the ground has remained a rototranslation but much simpler than in previous cases.

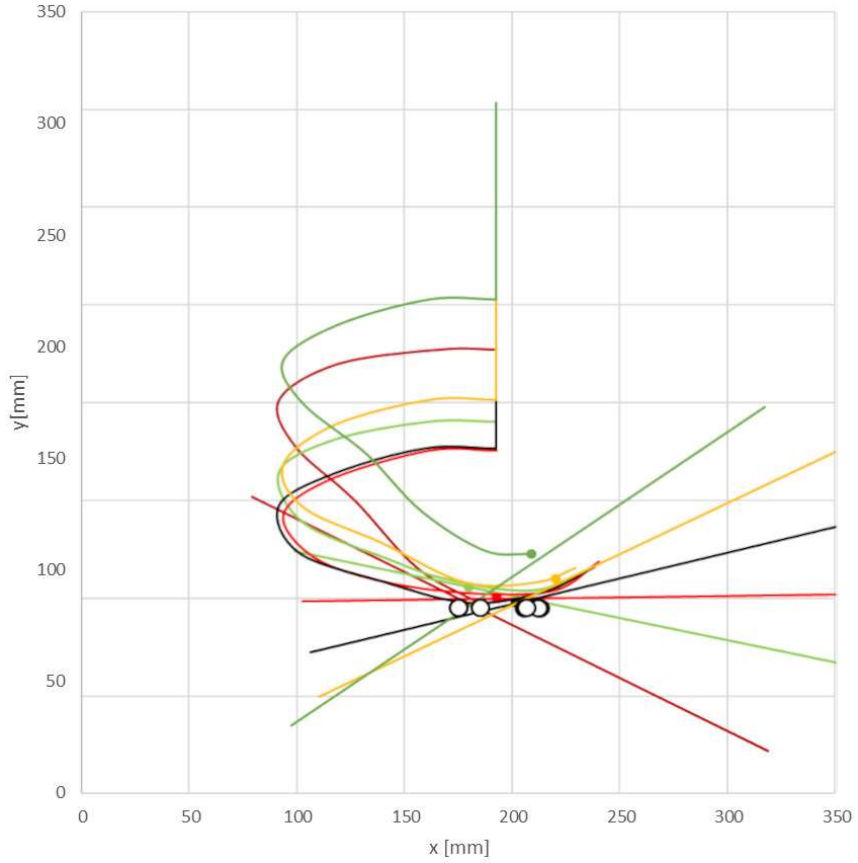

Figure 2.2.10 | Schematic representation of the test bench concept.

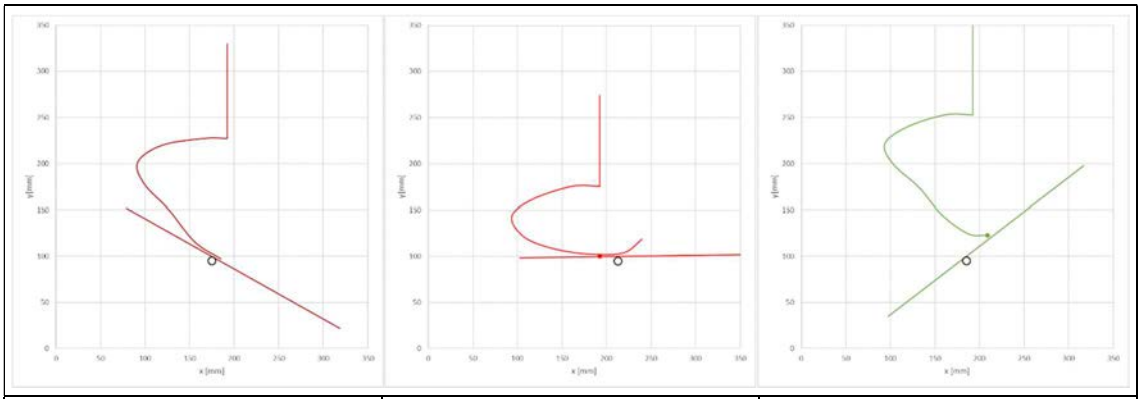

Heel stike	Mid stance	Toe off

Figure 2.2.11 | Schematic representation of the test bench concept during the three fundamental events.

At this point the movements are:

1) Prosthesis translation along the Y_S axis, defined as the displacement C1.

2) Rotation of the ground around the G point, corresponding to the already defined rotation θ_{SH}.

3) Translation of the G point along X_S axis, defined as the displacement C2.

A new reference system is defined, called the laboratory reference system ($O\ X_L Y_L Z_L$), corresponding to the fixed reference system of the laboratory on which the test bench will be built (Figure 2.2.11)

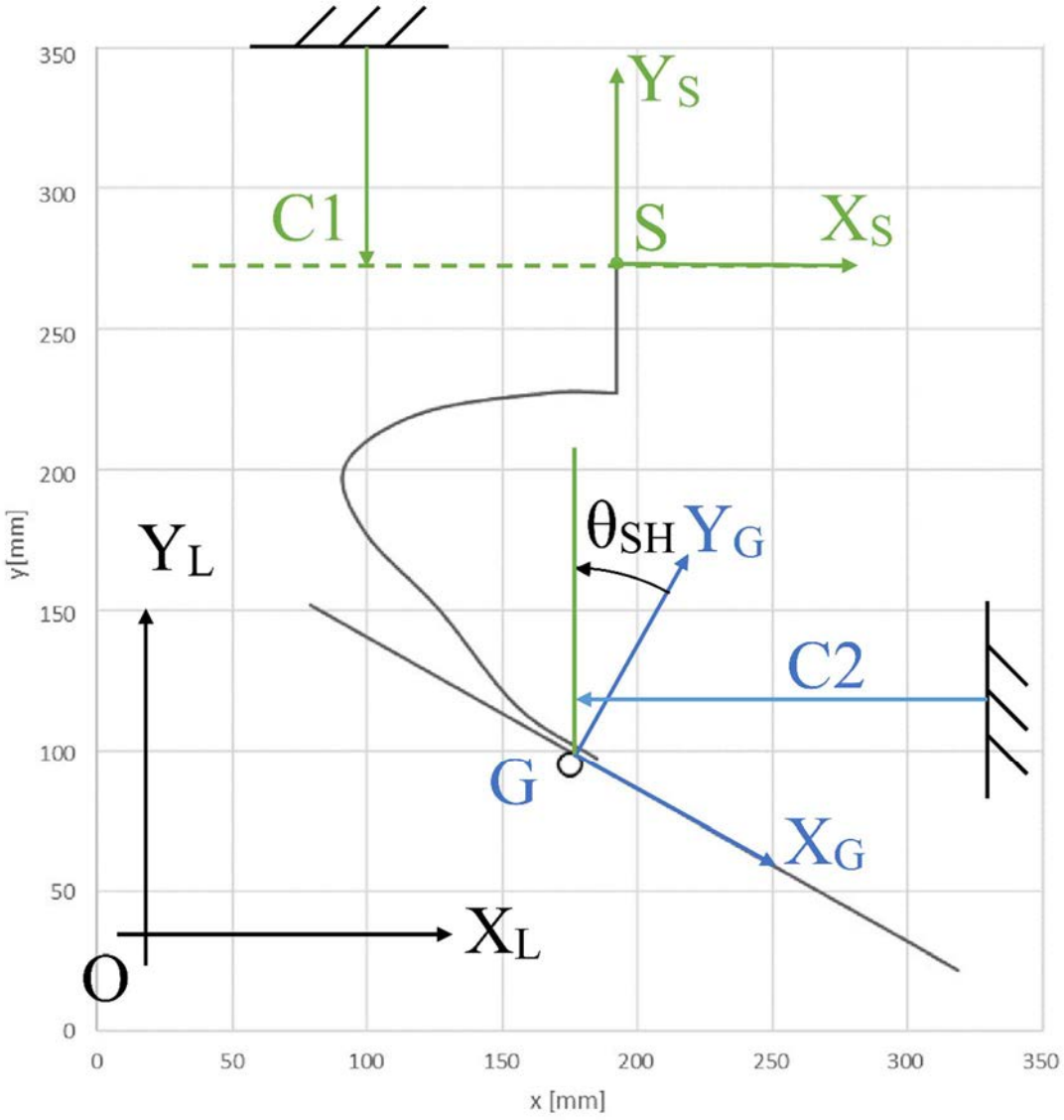

Figure 2.2.10 | Test bench reference systems.

As shown later, except for the rotation of the ground, the displacements C1 and C2 depend on the point where the hinge is to be positioned. At this point it was fundamental to understand where the hinge of the ground goes. To find the optimal point in which to hinge the ground I tried to:

a) Minimize the variation of the displacement C1

b) Minimize the variation of the displacement C2

c) Minimize the variation of the displacement $\theta_{SH.}$

d) Minimize the moment that must be transmitted to the ground to balance the stress transmitted by the prosthesis, ground moment, GM

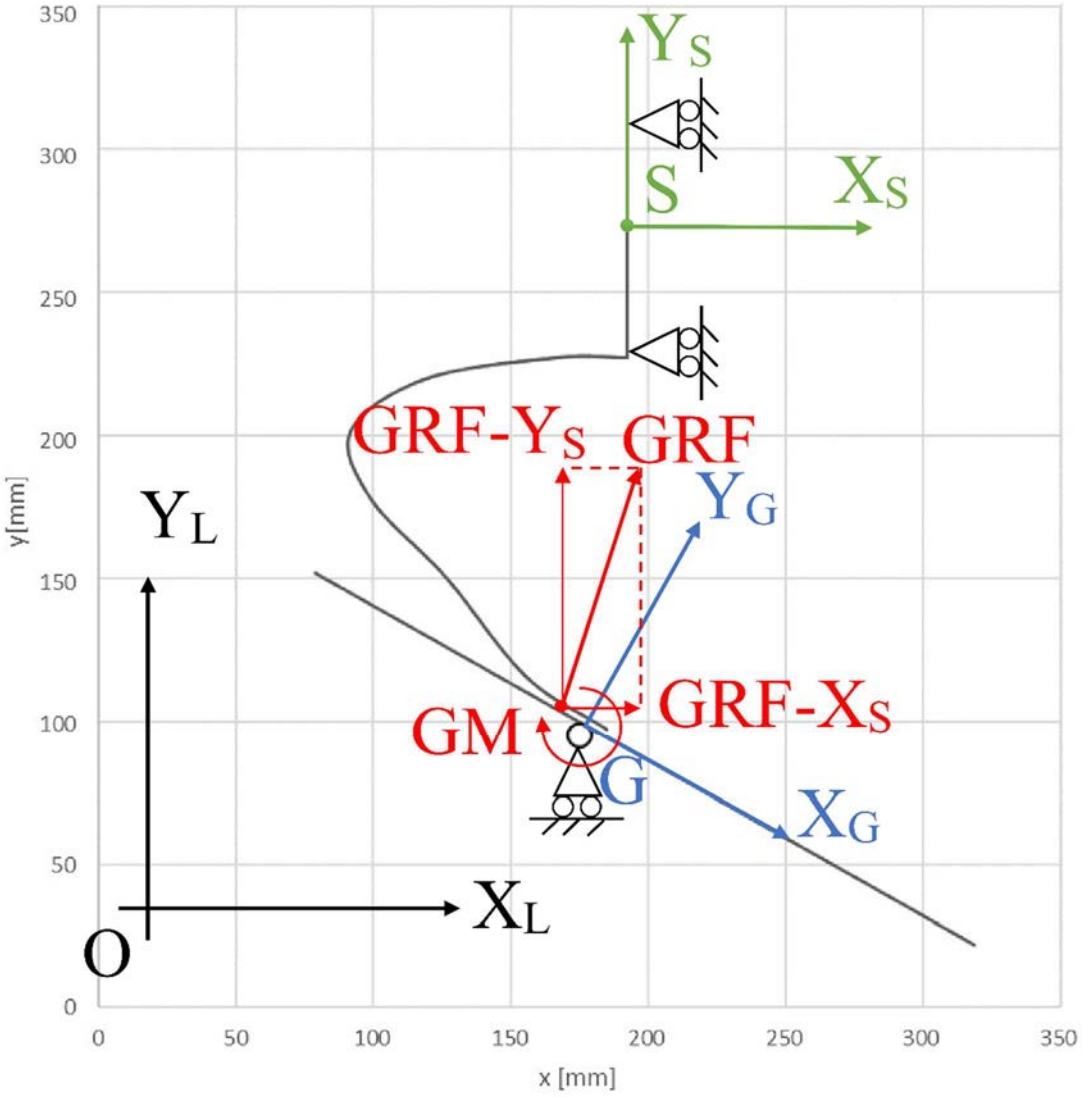

Figure 2.2.11 | Ground reaction moment, GRM.

Point d) immediately suggests placing the hinge as close as possible to the center of pressure (COP) of the prosthesis to minimize the GM necessary.

In Figure 2.2.12 in the left column, there are C1, C2 and $\theta_{SH,}$trends along the stance fase, in the right-hand column there are GRF-Y_S, GRF-X_S and GM trends along the stance fase (stance fase time 0.14s). Applying the same deformations to video and with the same speed we expect the same forces to be developed from the force plates during the in vivo tests. It is not yet known whether using a longer stance phase, in the order of seconds, the stresses produced are the same. This is an interesting aspect of investigation that we intend to explore.

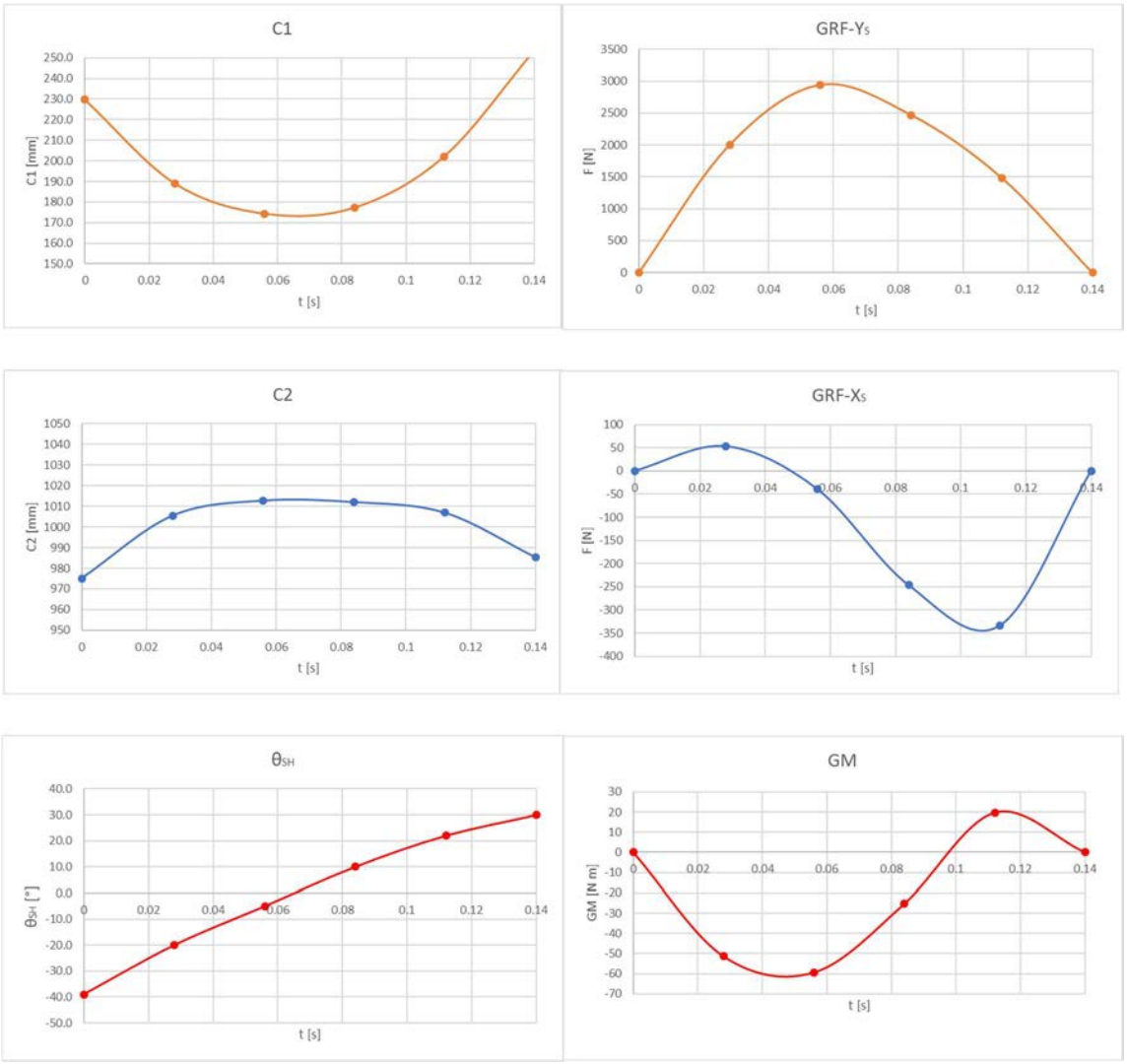

Figure 2.2.12 | Kinematic and dynamic analysis of the test bench

As can be inferred from the kinematic and dynamic analysis, the optimal configuration foresees that the hinge of the ground is very close to the COP as can be seen from the graphs in Figure 2.2.12. The parameter "hinge position" varies from 0 to 1 and represents the position of the hinge with respect to two points on the ground, one in the rear position (to which corresponds a value of zero), the other in anterior position with respect to the zone of contact between the prosthesis and the ground (to which a value of one corresponds).

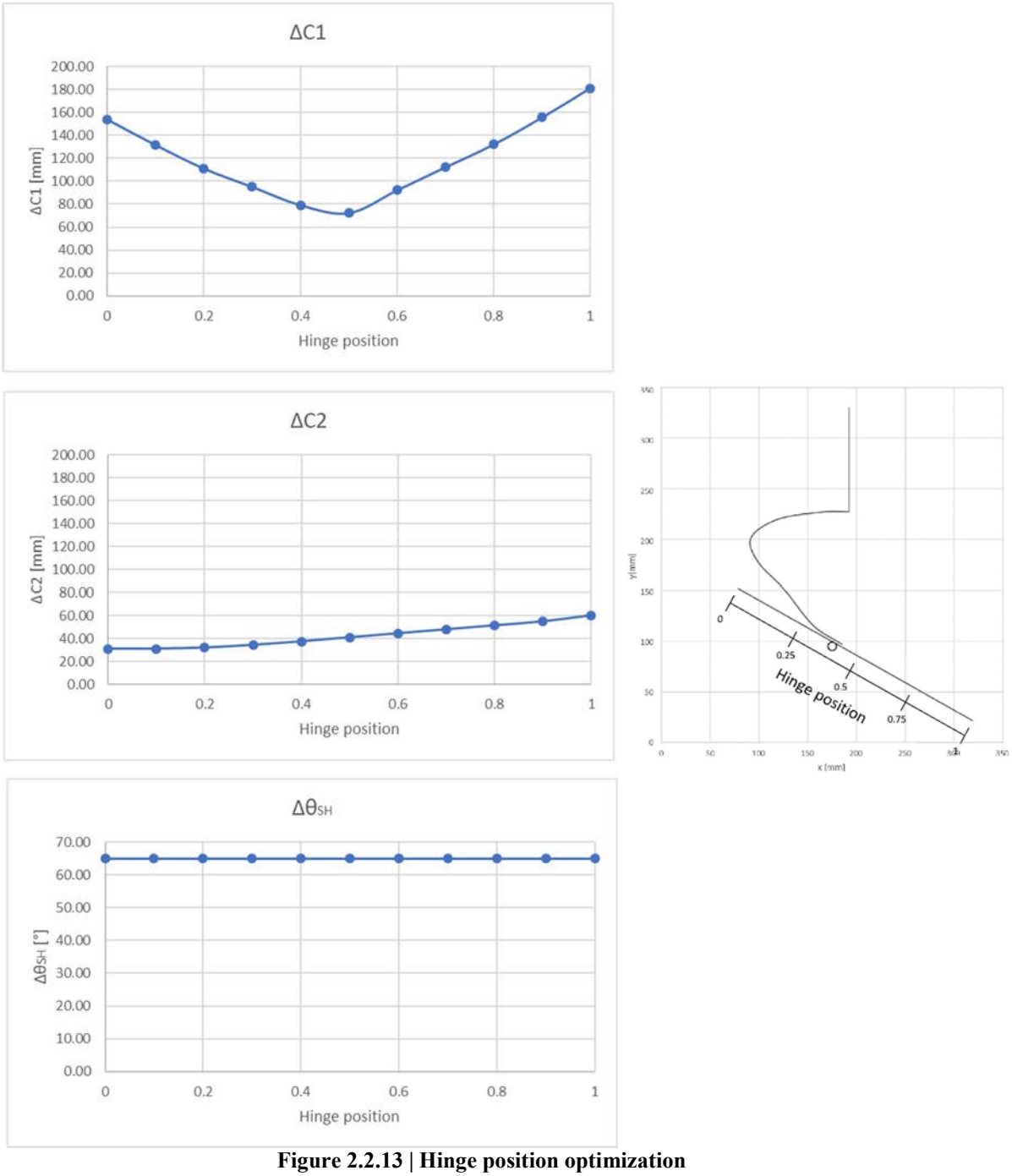

Figure 2.2.13 | Hinge position optimization

This study, although spoiled by not inconsiderable approximations, allowed me to reach a concept of the test bench that proved to be successful.

The ambitious goal of this research, unlike what can be found in literature, is to build a test bench capable of stressing the prosthesis in the most similar way to the real one. Neglecting the medial lateral stress, the test bench must therefore allow three degrees of freedom of the soket, consequent to the rototranslation in the sagittal plane, to allow the rotation of the prosthesis and the axial and orthogonal compression.

The simplest mechanism is: the prosthesis is mounted on a cart that translates vertically with respect to the laboratory reference system, while the ground rotates around a hinge. The hinge mounted on a cart moves horizontally. The movement of the carriages is made by hydraulic jacks, while the rotation of the ground is operated by an electric motor. The carriages are necessary to absorb the bending moments which otherwise would bend the hydraulic jack stem, which should always be avoided because it would produce oil leakages from the gaskets, asymmetric wear of the gaskets. To measure the GRFs that the prosthesis generates on the ground, it is planned to use a three-axis cell capable of measuring the three forces.

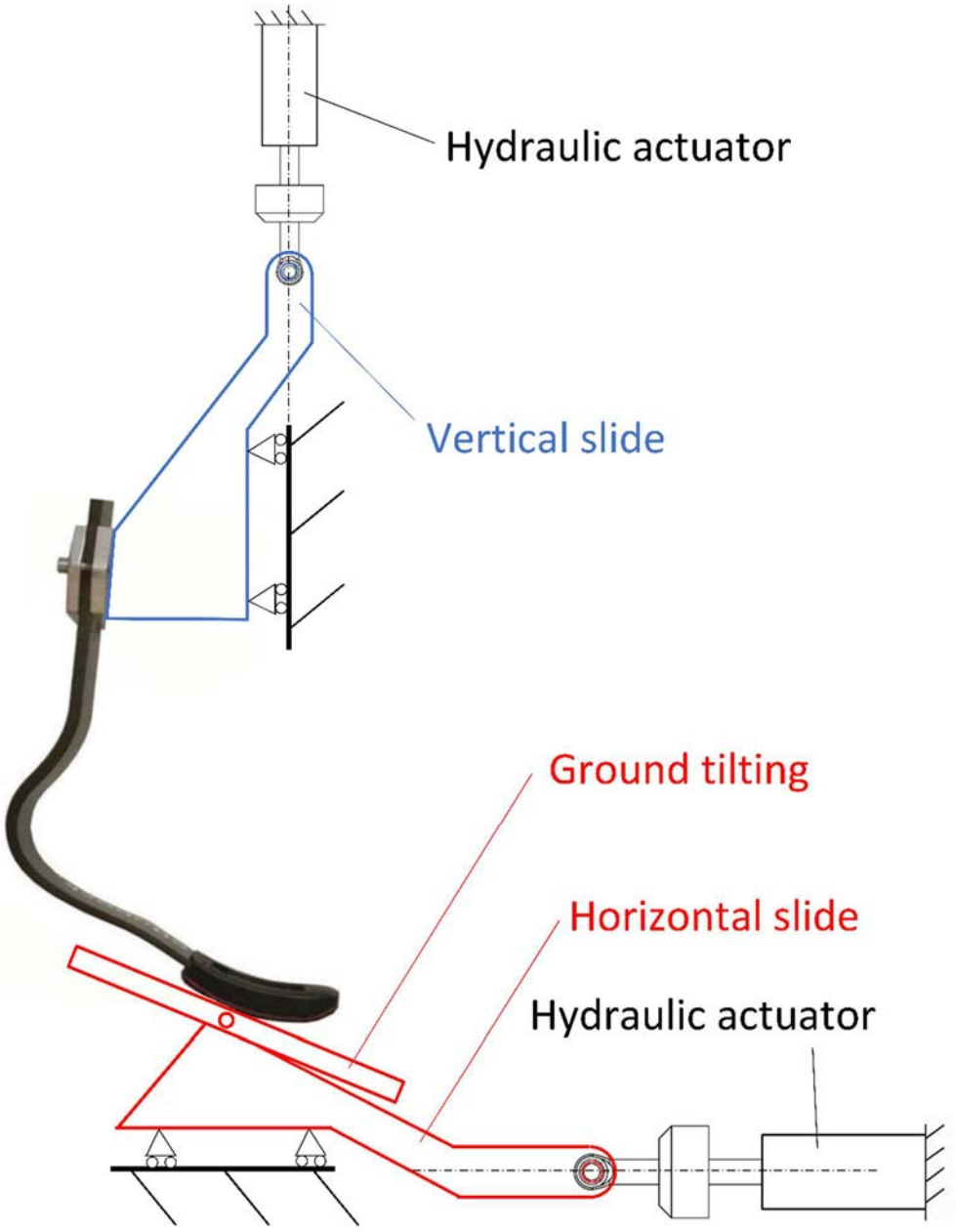

Figure 2.2.14 | Test bench concept.

3. DESIGN OF THE TEST BENCH

A test bench or testing workbench is an environment used to verify the correctness or soundness of a design or model.

In our case we must measure the mechanical stiffness of a device, applying a known deformation and measuring the corresponding reaction force generated. It's essential when applying the deformation that the test bench has a rigidity of at least one order of magnitude higher than the device, otherwise the instrumental load will invalidate the measurement [26]. The first requirement of the test bench is that it must be much stiffer than the device to be measured. Obviously, aspects of an economic nature and simplicity of construction require that the test bench be made lighter and simpler, compatibly with the design specifications.

As anticipated, the test bench is made of two slides, one on which the prosthesis is fixed, the other carries the ground on which the prosthesis goes to rest. Considering that the speeds involved can be very high (see kinematic analysis of the paragraph 2.2) the two slides as well as being rigid must also be light, in order to minimize the forces of inertia that are generated when the accelerations are high.

Ultimately the basic design requirements are two: stiffness and lightness. The massive use of aluminum alloy materials is therefore obvious.

3.1. TEST BENCH AIMS

In the literature there are some examples of bench tests performed on the RSPs, but there are very few test benches specific to the RSPs, as discussed in detail in paragraph 2.1. The most innovative aspect we wanted to introduce was the possibility to load the prostheses not only in axial direction (with respect to the YF axis of the prosthesis), but also orthogonally to it (XF axis), so as to be able to evaluate the stiffness of the prosthesis in axial direction also according to the applied orthogonal load. In Beck's work, Taboga and Grabowski, 2016, [12] (see Figure 2.1.1.1 on page 18) they focused on measuring the stiffness of the prosthesis by imposing loading conditions in which the GRF forms a precise angle with the prosthetic foot axis (YF axis). To do this they neglect cutting stress, reproducing a purely axial stress. Instead, in Dyer's work, Sewell and Noroozi, 2014, [21], (see Figure 2.1.2.2 on page 20), different tests were carried out taking into account the presence or absence of shearing forces. In this case, however, more than imposing

conditions on the cutting forces impose conditions on the slippage of the sole. Another innovative aspect to be introduced was the study of the stiffness of the prosthesis also when the angle of inclination between prosthesis and ground changed (theta SH). Finally, as also suggested by Dyer, Sewell and Noroozi, 2013, [24] "static load testing should not be recommended to regulate energy return prostheses for athletes with lower limb amputation"; as the ultimate goal we set ourselves the task of creating a test bench to reproduce the stresses while also respecting the load application times. Ultimately, a test bench capable of reproducing the stresses on the prostheses, in terms of forces, angles, displacements and times.

3.2. FIRST VERSION OF THE TEST BENCH

Before proceeding with the construction of the test bench, a temporary one was created, adapting an existing test bench. This allowed us to verify the feasibility of the project.

In this version, the prosthesis was mounted on a cart that moves horizontally from the laboratory reference system, moved by a hydraulic jack mounted on a abutement. The ground instead was mounted on a vertical cart, moved by a hydraulic jack fixed on a portal. The ground does not have the possibility to rotate, so the tests essentially concern the midstance phase of the runnig.

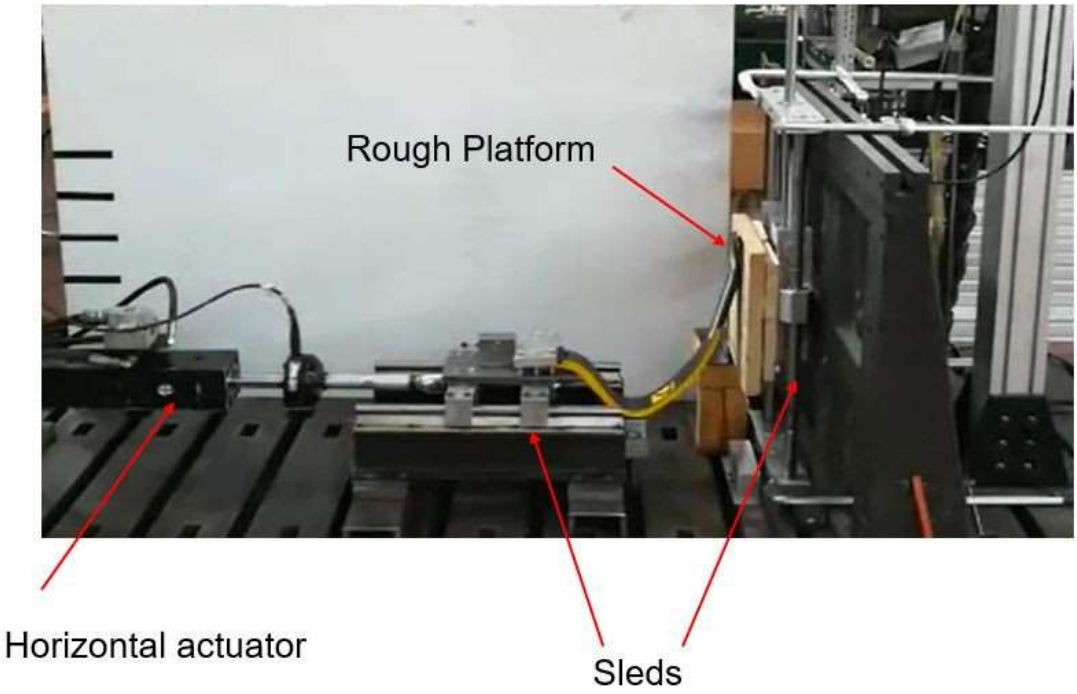

Figure 3.1 | Beta version of the test bench

The realization of this temporary test bench was made in collaboration with a group of students as part of a project of the course SPORTS ENGINEERINGS AND REHABILITATION DEVICES held by professor Nicola Petrone.

The prosthesis is clamped on the horizontal slide, which is moved by a hydraulic actuator. The soil is composed of a wooden board on which a layer of rough paper has been glued to maximize the friction between the denture sole (rubber) and the ground. The board is mounted on a vertical slide, which can be connected to a second hydraulic actuator.

Tests were carried out to collect a first estimate of the stiffness of the two prostheses in our possession (Ottobock «Runner 1E91», size 5; Össur's «Cheetah Xtreme», size 7).

We measured the mechanical stiffness under conditions of zero shearing forces. To do this we left the vertical slide free to flow, canceling the gravitational force on it through

a counterweight system. We used 0 ° as the alignment angle of the prosthesis in the sagittal plane. As we expected, by compressing the prosthesis along the Fooy axis (see paragraph 1.4 REFERENCE SYSTEMS AND NOMENCLATURE ADOPTED) the prosthetic foot tip, as well as obviously in the direction of the proximal part, also in the anterior direction, dragging the ground by friction.

Figure 3.2 and 3.3 shows the displacement force curves of the two prostheses, obtained with a feed speed of the horizontal actuator of 5 mm/s, up to a maximum of 1000N.

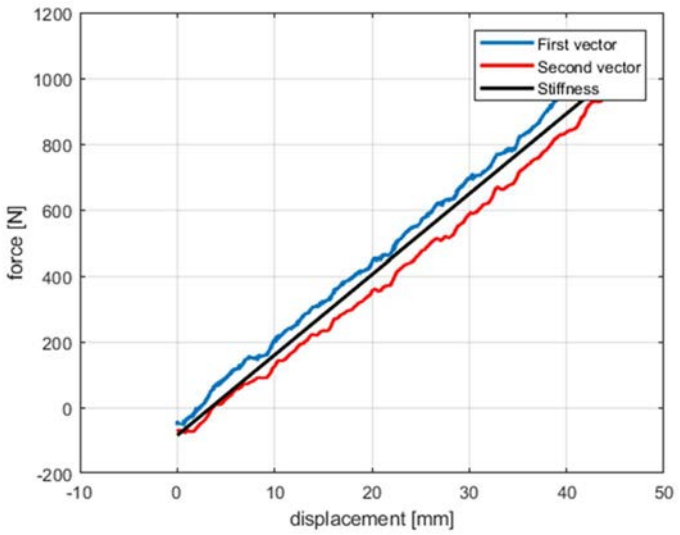

Stiffness= 24,4 N/mm

H8ysteresis= 4.08J

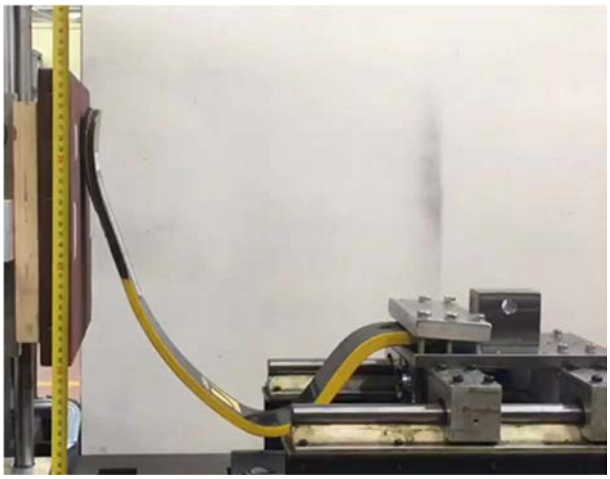

Figure 3.2 | Loading / unloading curve (5mm/s) Össur's «Cheetah Xtreme», size 7, test bench set up.

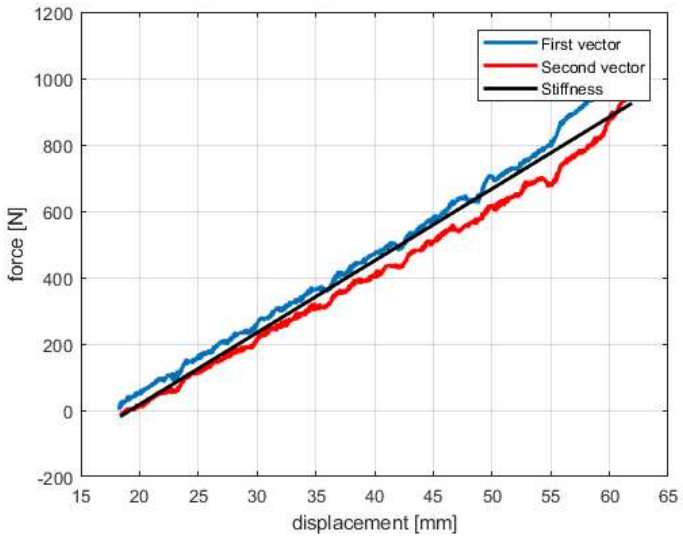

Stiffness= 21.8 N/mm

Hysteresis= 2.9J

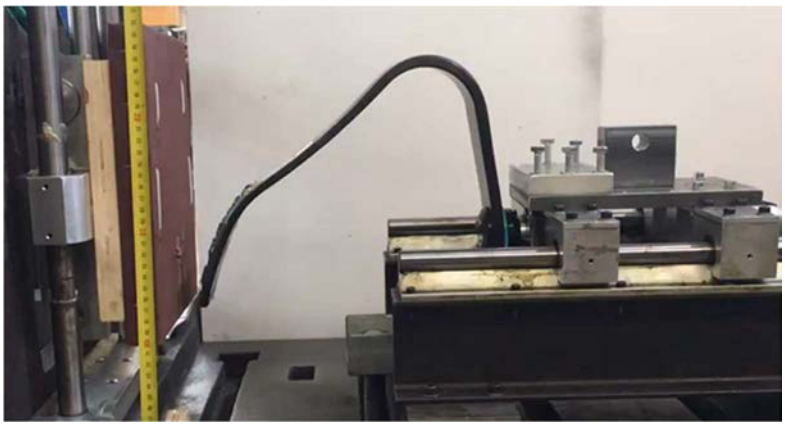

Figure 3.3 | Loading / unloading curve (5mm/s) Ottobock «Runner 1E91», size 5, test bench set up.

As we expected, Össur's «Cheetah Xtreme» size 7 has a higher stiffness than Ottobock «Runner 1E91» size 5, being of a higher category. As far as the hysteresis is concerned, it is useful to quote here (Beck, Taboga and Grabowski, 2016): *prosthetic hysteresis was 42% lower when we removed the rubber soles, indicating that the rubber soles were responsible for almost half of the dissipated energy.*

3.3. HYDRAULIC ACTUATOR AND CONTROL SYSTEM

In our laboratory we have hydraulic actuators from MTS Systems Corporation, capable of producing up to 14700 N with MOOG servovalves. The control software and control station is always of MTS Systems Corporation, which operates the feedback control on servovalves. The movement of the piston can take place under force control by means of a uniaxial force trasducer positioned the head on the stem, or in displacement control by means of a petentiometer inside the cylinder.

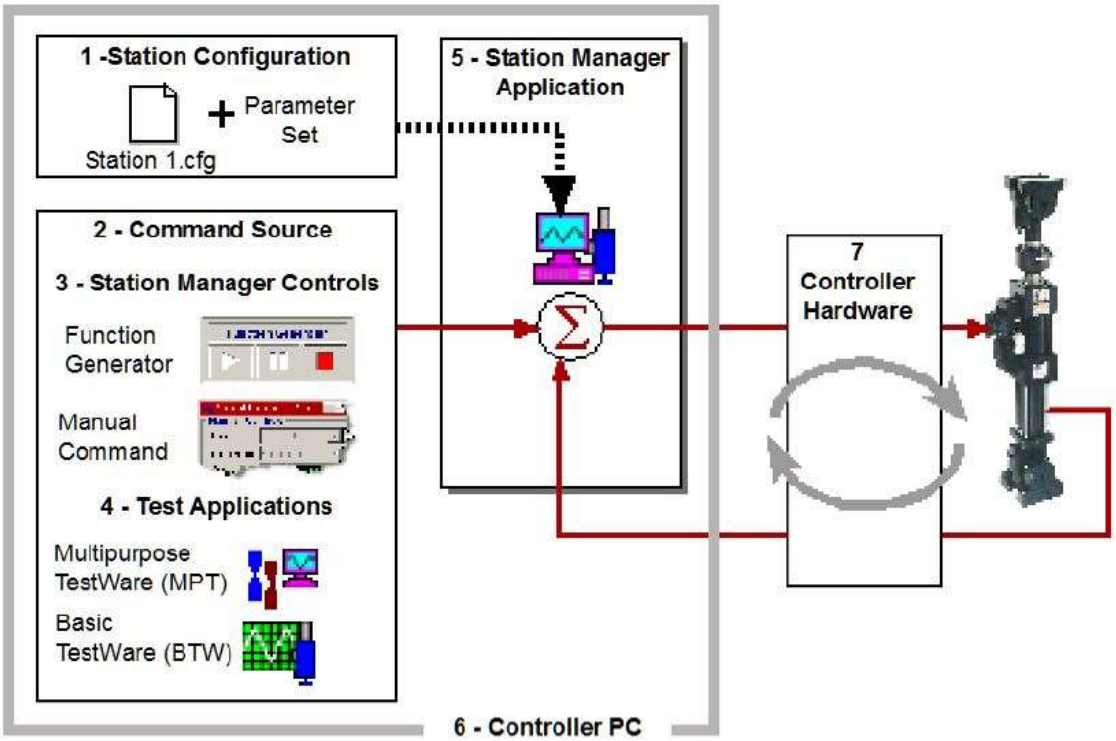

Figure 4.1.1 | MTS control system [MTS manual].

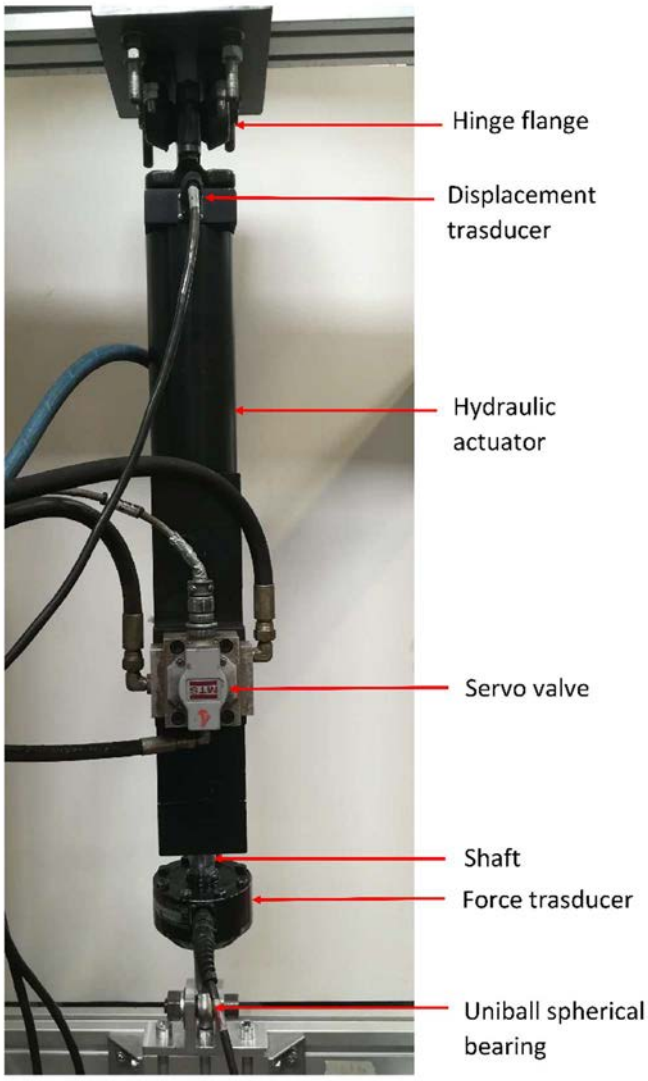

3.4. DOUBLE PORTAL DESIGN

progettazione del portale, le diverse versioni della slitta vertical

To support the hydraulic actuator that moves the vertical slide, a portal has been designed with structural aluminum profiles. In addition to the structural strength of these beams, there is the advantage of being able to create flexible solutions making use of the ease of assembly and disassembly and the possibility of changing the configuration of the project at any time, and there is the possibility of being dismantled and reused for new projects. The structural profiles are made of aluminum alloy, of square section, with unified T-slot on each side to allow the insertion of the fixing nuts. The internal slots are designed to minimize weight while maintaining a high moment of inertia of the section.

The structural profiles PMA 88X88 SN supplied by the UMS (Figure 4.2.1) [44] have been used for the portal.

In Figure 4.2.2 we report the physical characteristics as reported by the supplier.

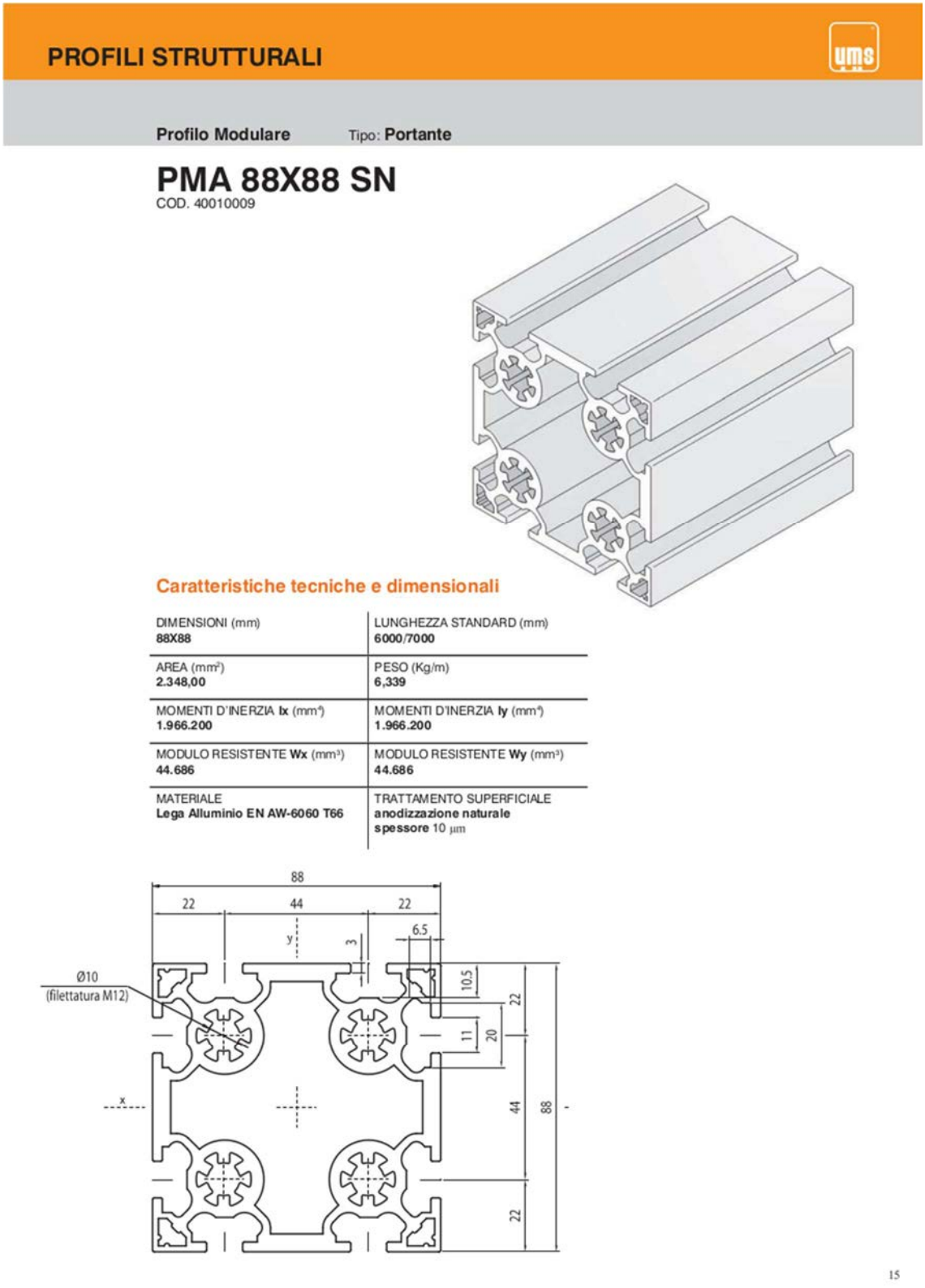

PROFILI STRUTTURALI

Profilo Modulare Tipo: **Portante**

PMA 88X88 SN

COD. 40010009

Caratteristiche tecniche e dimensionali

DIMENSIONI (mm) **88X88**	LUNGHEZZA STANDARD (mm) **6000/7000**
AREA (mm^2) **2.348,00**	PESO (Kg/m) **6,339**
MOMENTI D'INERZIA **Ix** (mm^4) **1.966.200**	MOMENTI D'INERZIA **Iy** (mm^4) **1.966.200**
MODULO RESISTENTE **Wx** (mm^3) **44.686**	MODULO RESISTENTE **Wy** (mm^3) **44.686**
MATERIALE **Lega Alluminio EN AW-6060 T66**	TRATTAMENTO SUPERFICIALE **anodizzazione naturale** **spessore** 10 µm

88 22 44 22 y 3 6.5 Ø10 (filettatura M12) 10.5 22 11 20 x 44 88 22

15

Figure 4.2.1 | Supporting profile PMA 88X88 SN [44]

CARATTERISTICHE FISICHE

Materiale:	**Lega di alluminio: EN AW-6060 T66**
Tolleranze di estrusione:	**EN 755-9**
Trattamento termico:	Invecchiamento artificiale
Trattamento superficiale:	Anodizzazione : E6/EV1 (chimicamente decapato e anodizzato color argento) Strato spessore: 10 µm Le sezioni tagliate non sono anodizzate
Modulo di elasticità:	**70000 N/mm²**
Peso specifico:	**2,7 Kg/dm³**
Durezza:	**75 HB 2,5/62,5**
in direzione dell'estrusione	
Resistenza a trazione minima:	**Rm = 215 N/mm²**
Limite di snervamento:	**Rp 0,2 = 160 N/mm²**
Allungamento alla rottura:	**A = 8% A_{50} = 6%**
Coefficiente di dilatazione lineare:	**23,38•10⁻⁶/°C mm per metro (da o° a 100° C)**

Figure 4.2.2 | Physical characteristics [44]

About the type of connection between the beams, a 90 ° connection was used by means of corner brackets made of die-cast aluminium (Figure 4.2.3). All the screws used for the adhesives are M8 8.8 screws in cylindrical-head galvanized steel with hexagon socket (ISO4762).

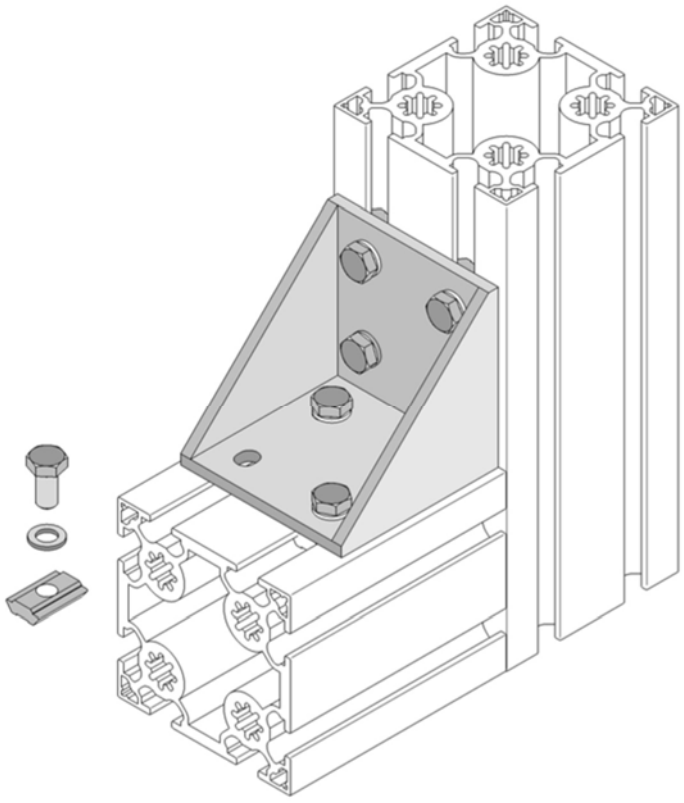

Figure 4.2.2 | Corner brackets [44]

To avoid the overturning of the portal, a double portal was used.

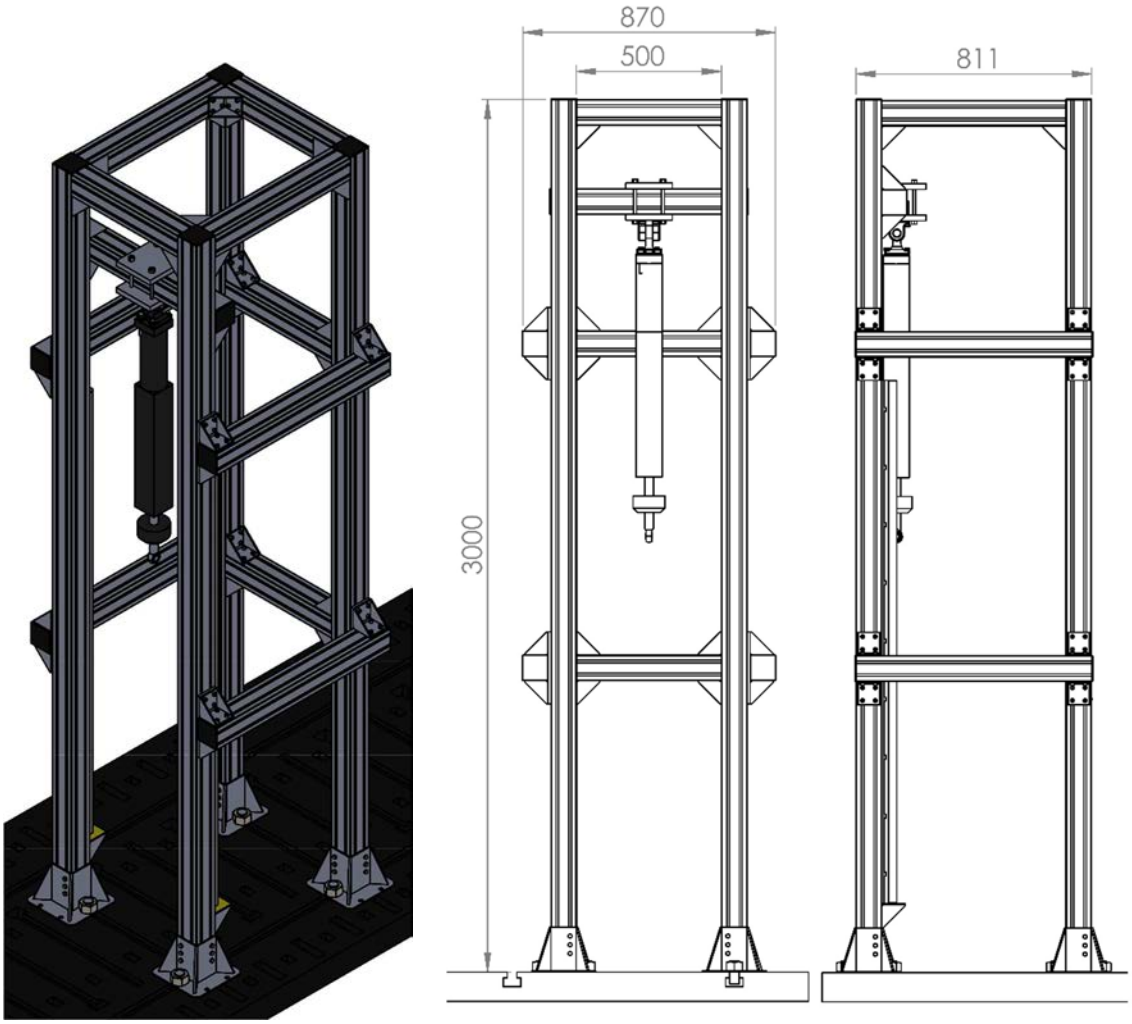

Figure 4.2.3 | Double portal designs with hydraulic actuator. Quotes are in mm.

The height of the portal is three meters because under it must be the actuator (1m long), the vertical slide on which the prosthesis is fixed, including load cells (0.6m), the prosthesis with eventually the reservoir (maximum 1m), the horizontal slide with tilting ground (max 1m). The width is such as to have an internally useful space of 0.5m, so as to comfortably accommodate the horizontal slide.

3.4.1. Double portal structural verifications

verifiche sul portale, sulla slitta e sulle guide

Static structural check on the transverse of the portal on which the hydraulic actuator is mounted (Figure 4.2.1.1).

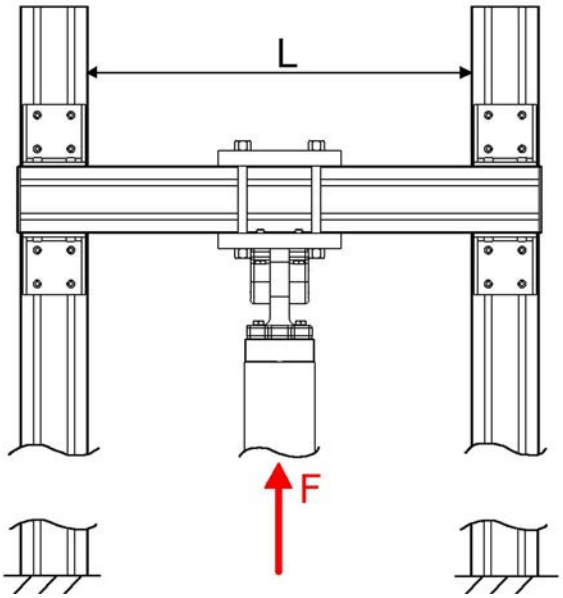

Figure 4.2.1.1 | Load acting on portal transverse

Theoretical model: double beam trapped with centre line load (Figure 4.2.3)

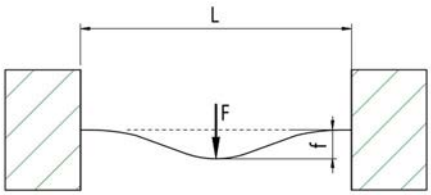

$$f = \frac{F \cdot L^3}{192 \cdot E \cdot I} \qquad \sigma = \frac{F \cdot L}{8 \cdot W} \leq \sigma_{max}$$

Figure 4.2.3 | Double beam trapped [44]

According to the data in the literature [9,16,23], the peak GRF reaches a maximum of 4 times the body weight of the athlete. Assuming an athlete of 120kg, multiplicative factor 4, the maximum force is:

$$F = 120 * 9.81 * 4 \cong 4700\ N$$

The length L of the beam is:

$$L = 500\ mm$$

Elastic module, moment of inertia and resistant module:

$$E = 70\ GPa\ ,\ I = 1966200\ mm^4\ ,\ W = 44686\ mm^3$$

The maximum permissible stress is calculated as the yield stress at 0.2%, reduced by a safety factor $\nu = 1.5$:

$$\sigma_{max} = \frac{\sigma_{s\ 0.2}}{\nu} = \frac{160}{1.5} = 107\ MPa$$

Conditions of static security:

$$\sigma = \frac{F * L}{8 * W} = \frac{4700 * 500}{8 * 44686} = 6.6\ MPa\ <\ \sigma_{max} = 107\ MPa$$

is verified.

The maximum displacement of the center line because of the load is:

$$f = \frac{F * L^3}{192 * E * I} = \frac{4700 * 500^3}{192 * 70000 * 1966200} = 0.02\ mm$$

it is negligible.

Static structural checks on bolted joints (Figure 4.2.1.2).

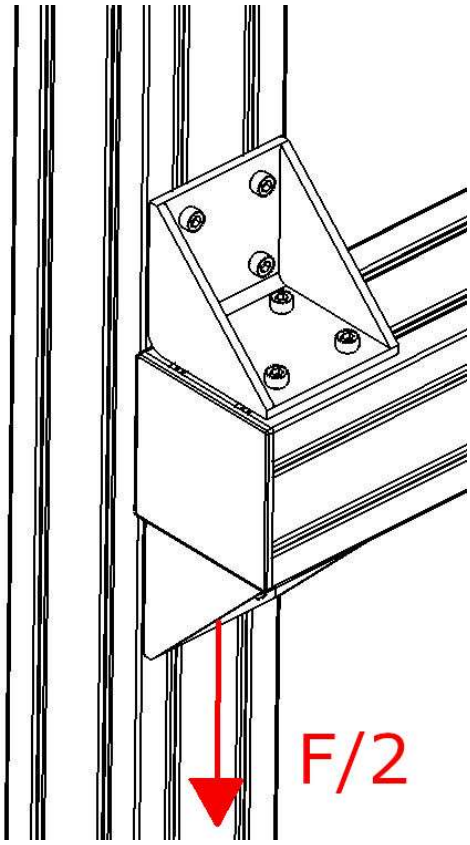

Figure 4.2.1.2 | Bolted joint.

Verification is carried out under friction sealing conditions.

Total number of bolts per junction:

$$n_b = 8$$

Number of friction surfaces:

$$n_s = 2$$

Load transmitted by every single screw:

$$V_f = \frac{F/2}{n_b * n_s} = \frac{4700/2}{8 * 2} = 146.9\ N$$

Tightening load:

$$N_s = 12000\ N$$

Estimated coefficient of friction for untreated surfaces:

$$\mu = 0.3$$

Maximum transmissible load per screw:

$$V_{f,0} = \frac{\mu * N_s}{1.25} = \frac{0.3 * 12000}{1.25} = 2880\ N$$

Conditions of static security:

$$V_f = 146.9\ N < V_{f,0} = 2880\ N$$

is verified.

3.5. VERTICAL SLIDE DESIGN

The design of the vertical slide on which the prosthesis is fixed has required a rather long processing. In fact, we were looking for a rigid and at the same time light structure. The sliding mechanism is made up of two cylindrical bars, one on each column of the portal, made of tempered steel with a superficial carburizing treatment, on which bushings linear recirculating ball bearings (Figure 4.3.1).

Figure 4.3.1 | Linear motion: rail with slide bush.

The two rails have been fixed directly on the columns of the portal to increase the rigidity of the rails and prevent the guides from flexing under load, thus compromising the normal operation of the bearings. The Figure 4.3.2 shows the versions developed for the vertical slide. In the end we used the same structural profiles of the portal, with a lower section. This has allowed us to significantly reduce the weight compared to the use of aluminium plates, has also simplified the construction. To avoid an irregular consume of the bushes

the actuator's axis must be aligned with the sliding axis. To minimize the moment produced by GRFs, a horizontal beam has been added, so that the point of contact between the prosthesis and the ground falls in the plane identified by the two axes of the rails (Figure 4.3.3).

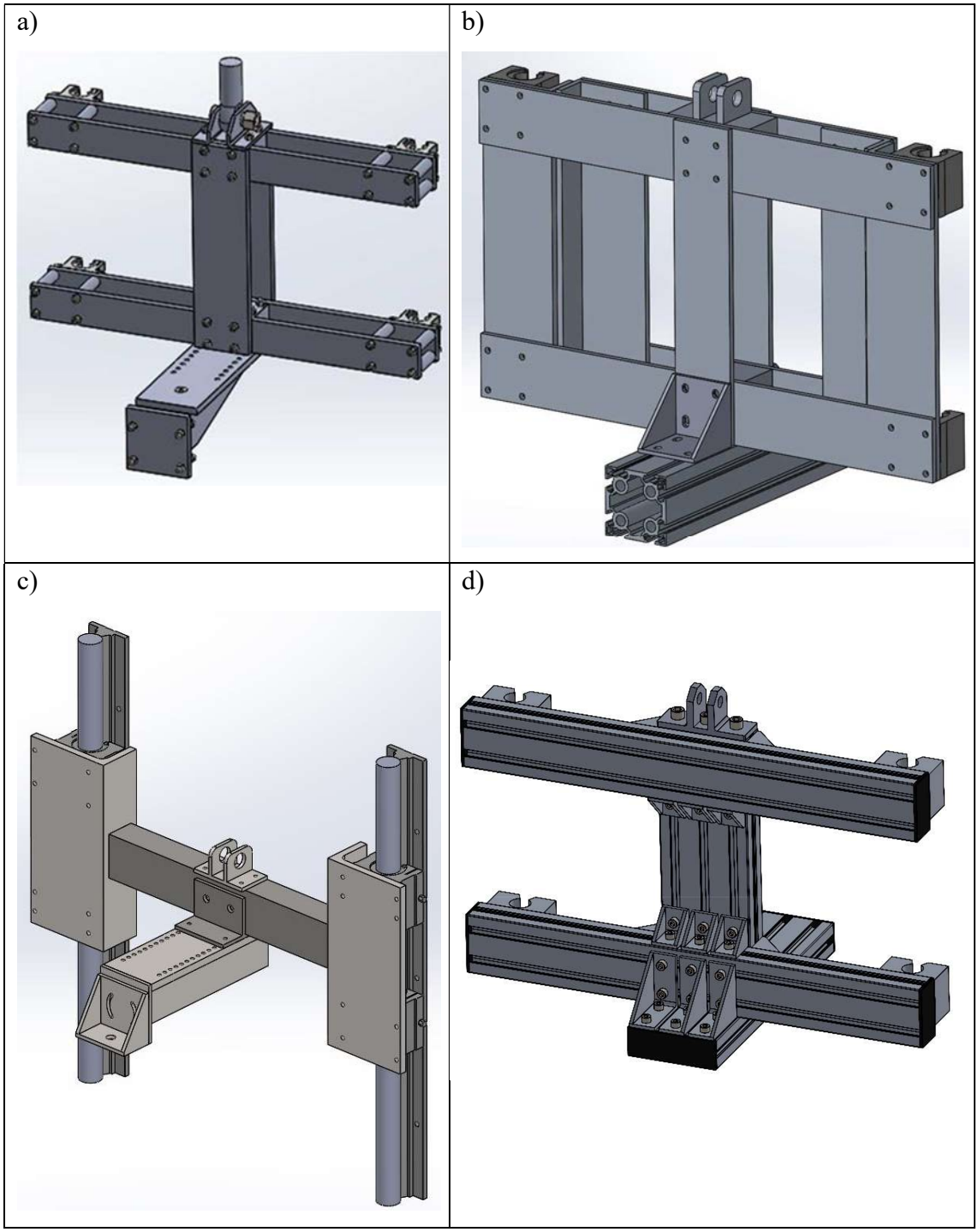

Figure 4.3.2 | Vertical slide versions. a),b),c) Previous versions of the sled, d) Definitive version

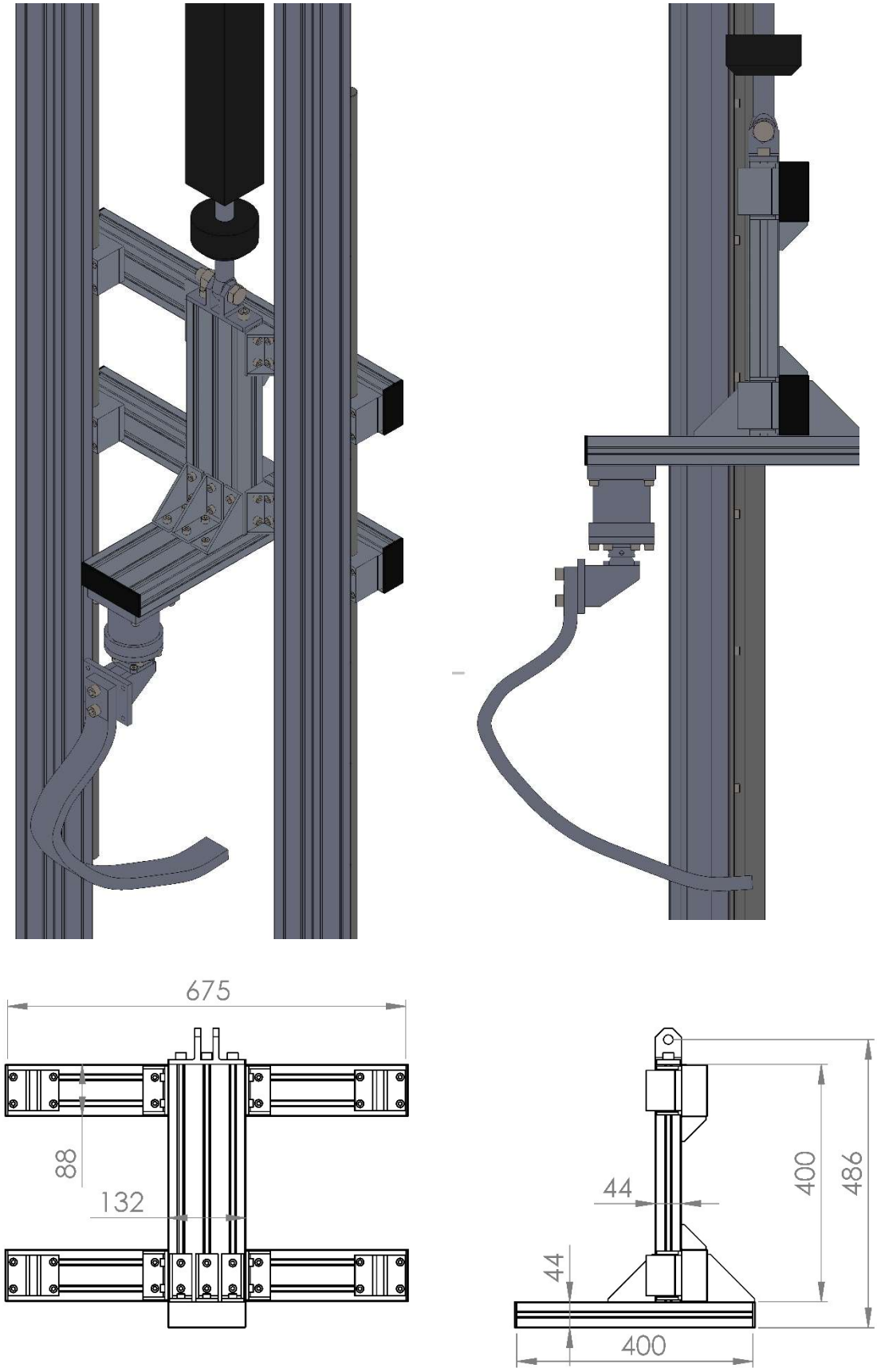

Figure 4.3.3 | Definitive vertical slide. Quotes are in mm.

3.5.1. Vertical slide verifications.

To dimension the bushings and the slide we determined the maximum loads that the sled would have to bear. The primary purpose of the sled is to absorb the moment generated by GRF. In fact, for a correct use of the hydraulic actuators on the stem must act exclusively a normal effort, otherwise there are oil leakages and asymmetric wear of the gaskets. From the preliminary study we understood that the pressure center (COP) moves along the prosthesis sole, and the sole of the prosthesis itself advances anteriorly during compression, so the GRFy certainly has a non-zero arm with respect to the sliding axis of the slide. Furthermore, GRFx is non-zero. In Figure it is shown how the moment M has been estimated that the prosthesis generates in the sagittal plane.

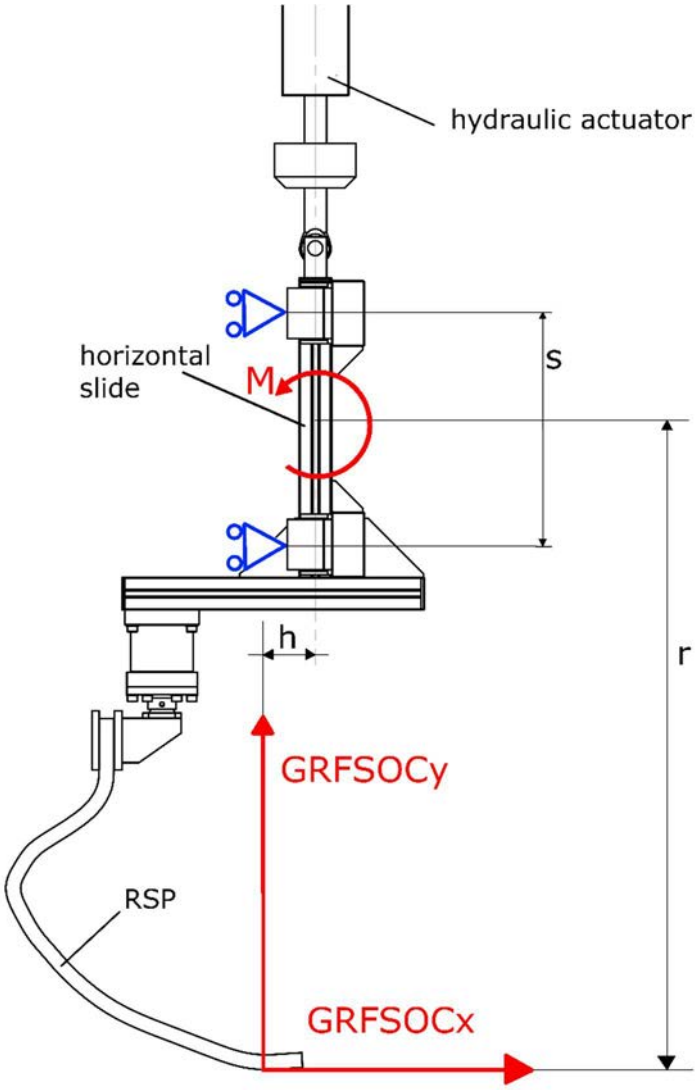

Figure 4.2.4 | Double portal designs with hydraulic actuator.

The acting moment on the sled is:

$$M = GRFSOCx * r - GRFSOCy * h$$

GRFSOCy is always positive (as shown in the Figure), while GRFSOCx can be both positive and negative. According to the data in the literature [16,22,23], the peak GRF reaches a maximum of 4 times the body weight of the athlete. Assuming an athlete of 120kg, multiplicative factor 4, the maximum force is:

$$GRF = 120 * 9.81 * 4 \ = \ 4709\ N \cong 5000N$$

The maximum value of h was estimated at 0.1m, while the maximum value of r was estimated at 1m. Moment M is mainly due to the GRFsocx component, as it has a lever arm 5 times that of the GRFSOCy. To estimate the maximum value of M we have therefore considered the case in which GRFSOCx is maximum. As reported (Beck, Taboga and Grabowski, 2016) [20] the angle that the peak GRF forms with the axis of the prosthesis (Fooy) is between 10 ° and 20 °. As a limit value we took a beta angle of 30 °. Ultimately the moment turns out to be

$$M = GRFpeak * \cos(30°) * r + GRFpeak * \sin(30°) * h$$

$$= 5000 * \cos(30°) * 0.1 + 5000 * \sin(30°) * 1$$

$$\cong 2940\ Nm$$

The moment M transmitted to the slide is the dimensioning parameter. Moment M is balanced by the radial forces on the bearings; the greater the height of the slide (see the dimension s in Figure) the greater the arm of the radial forces. To make the slide compact, it was decided that the dimension s should be no more than 0.3m. The radial force on each bearing is:

$$F = \frac{1}{4} * \frac{M}{s/2} = \frac{1}{4} * \frac{2940}{0.3/2} = 4900\ N$$

There are no axial forces, so dynamic equivalent radial load for single bearings, P, (ISO 281:2007 [43]) it's equal to F.

$$P = F = 4900\ N$$

We used the Niko®'s slide bush, in particular the linear ball bearing SO LME 30 UUOP AS. The company provides a formula for calculating the rated life L [45]:

$$L = \left(\frac{C}{P}\right)^3 * 50$$

The rated life L is the total travelled distance which 90% of a statistically significant number of apparently identical bearings would reach under the same operating conditions without the apparent appearance of metal fatigue.

L = rated life [km]

C = dynamic load ratings [N]

P = equivalent dynamic load [N]

The load ratings dynamic for the specific model selected is:

$$C = 1570\ N$$

The rated life is

$$L = \left(\frac{1570}{4900}\right)^3 * 50 = 1.65\ km = 1650\ m$$

Estimating that each load cycle of the prosthesis requires a slide run of 0.2m, if only halfway along the path the prosthesis is subjected to the maximum stress, there is a total number of load cycles equal to:

$$\frac{1650}{0.1} = 16500\ cycles$$

For the structural check on the slide I focused on the crosspiece on which the prosthesis is fixed as it is the most stressed part.

PMA 44X132 SN

COD. 40010006

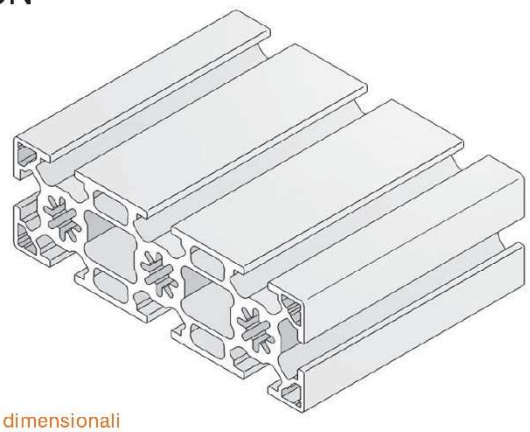

Caratteristiche tecniche e dimensionali

DIMENSIONI (mm) 44X132	LUNGHEZZA STANDARD (mm) 6000/7000
AREA (mm²) 2.208,96	PESO (Kg/m) 5,988
MOMENTI D'INERZIA Ix (mm⁴) 396.019	MOMENTI D'INERZIA Iy (mm⁴) 3.301.686
MODULO RESISTENTE Wx (mm³) 18.001	MODULO RESISTENTE Wy (mm³) 50.029
MATERIALE Lega Alluminio EN AW-6060 T66	TRATTAMENTO SUPERFICIALE anodizzazione naturale spessore 10 µm

Figure 4.2.5 | Supporting profile PMA 44X132 SN. [44]

The beam is considered jammed, with a cantilever length of L=0.3m and a load applied at the tip of F=5000N

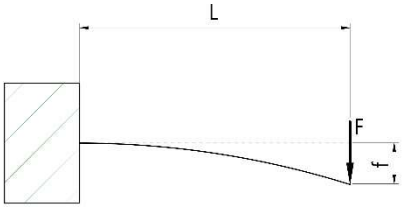

$$f = \frac{F \cdot L^3}{3 \cdot E \cdot I} \qquad \sigma = \frac{F \cdot L}{W} \leq \sigma_{max}$$

Figure 4.2.6 | Beam trapped [44]

Conditions of static security:

$$\sigma = \frac{F * L}{W} = \frac{5000 * 300}{8 * 18000} = 10.4\ MPa\ <\ \sigma_{max} = 107\ MPa$$

is verified.

The maximum displacement is:

$$f = \frac{F * L^3}{3 * E * I} = \frac{5000 * 300^3}{3 * 70000 * 396019} = 1.6\ mm$$

However small this displacement, it will be necessary to take this into account when measuring the rigidity of the prosthesis.

3.5.2. Force acquisition system on the vertical slide

To measure the forces and moments that the prosthesis transmits to the socket we used a 6-axis cell, which can measure the three components of force and the three moments. The cell we used is the K6D68 10kN/500Nm/CG produced by ME (Germany). The cell has been fixed on the vertical slide by means of specially made aluminium plates. The prosthetic foot is instead fixed to the cell by means of a custom-made angular aluminium bracket. (Figure 3.6.1)

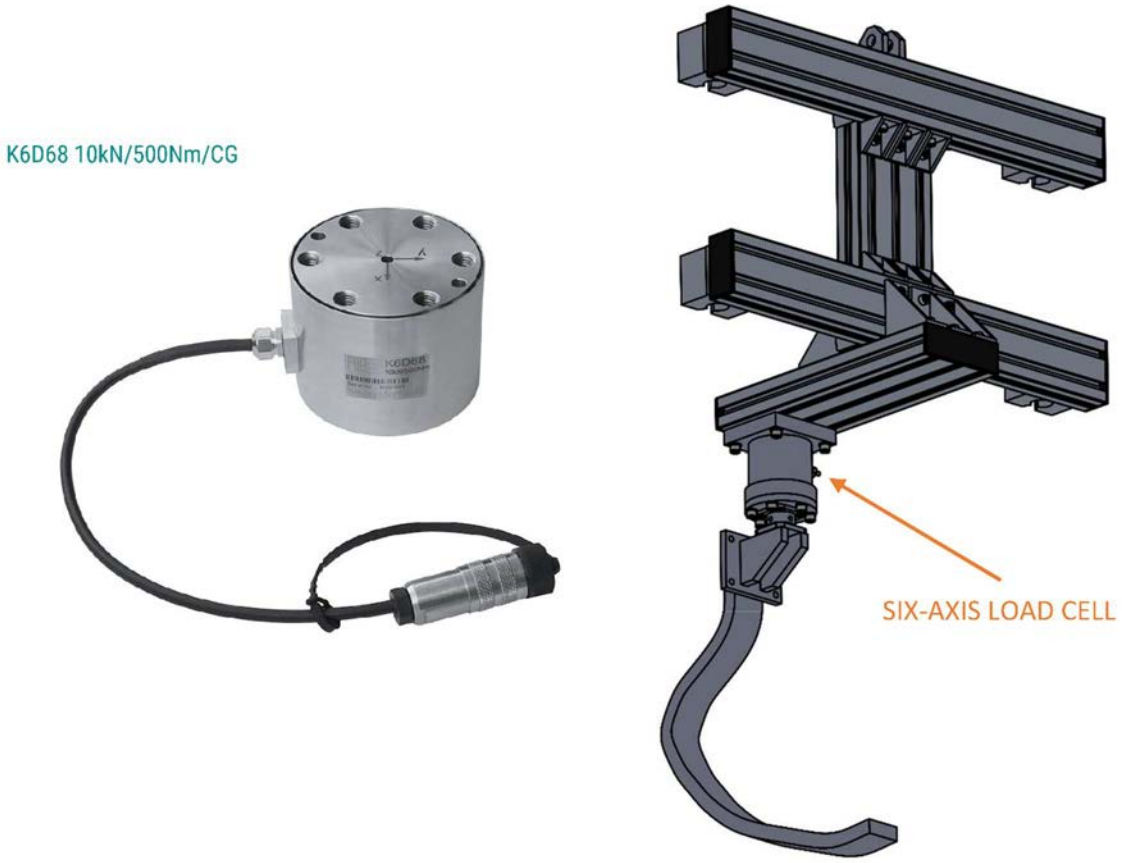

Figure 3.6.1 | Left: six-axis load cell. On the right: cell fixing.

Below the six-cell we have connected an Ottobock pyramid receiver so that we can connect all the prostheses equipped with pyramid adapter. For J prosthetics, we have found that in the agonistic field, custom sockets are always created, on which the prosthesis is connected by means of two screws. We therefore created a corner bracket that would allow this connection. Not only that, the plate is prepared for fixing j-shaped prostheses for clamping (Figure 3.6.2)

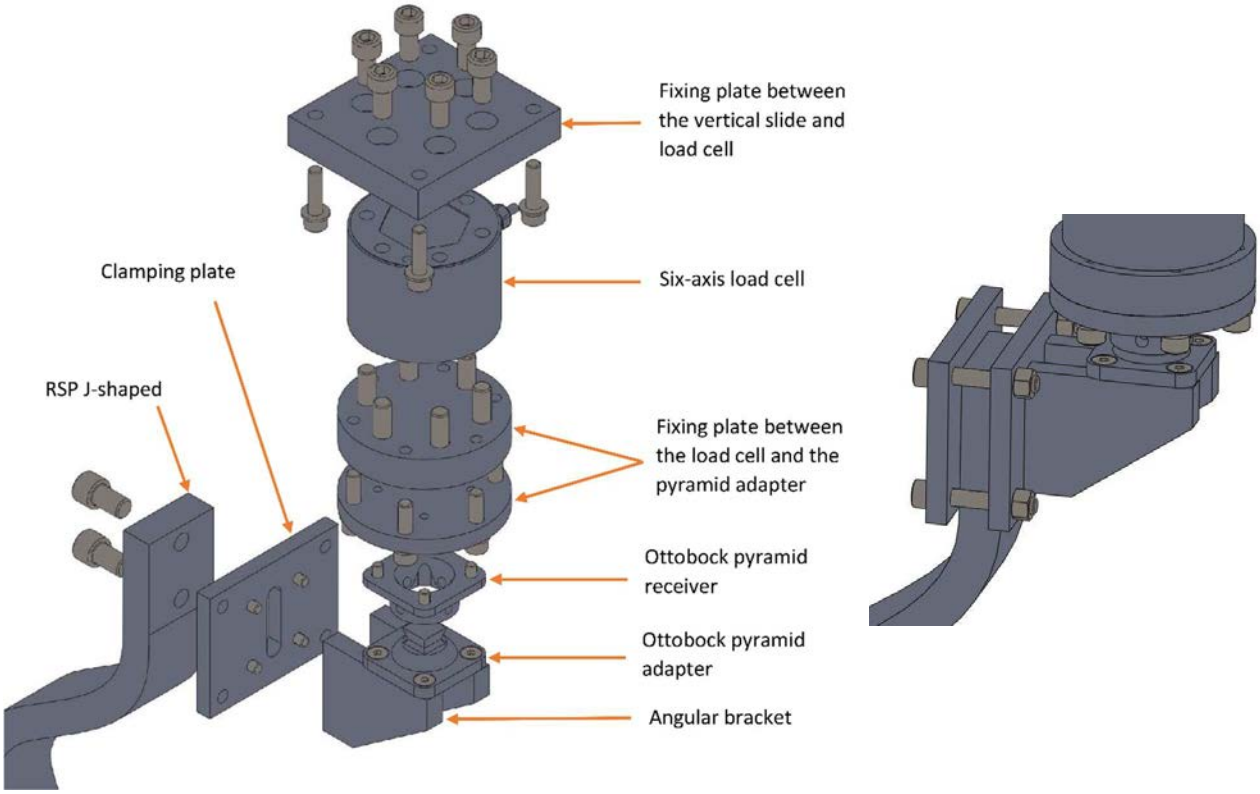

Figure 3.6.2 | To the left: Exploded view of the RSP-load cell-vertical slide connections. To the right: clamp fixing.

The figure shows the six stress components measured by the six-axis cell. The cell is aligned with the reference system of the prosthetic foot.

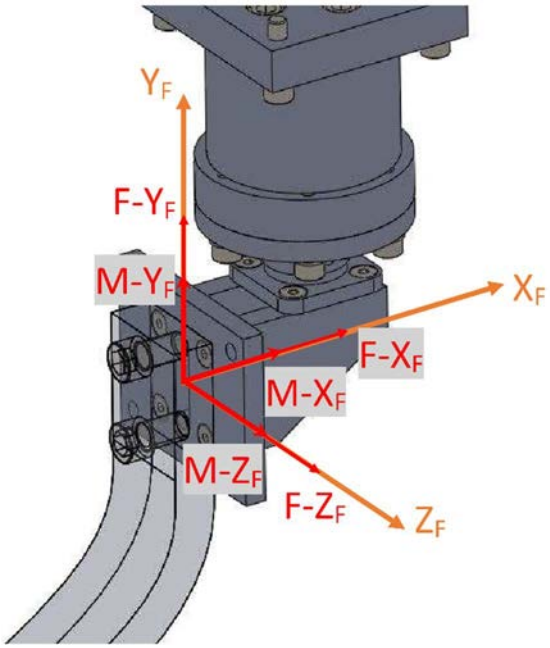

Figure 3.6.3 | Components measured by the six-axis cell.

3.5.3. 5-axis cell calibration

During the test bench setup, we realized that one of the six-axis cell channels was out of order. Before sending assistance, we took the opportunity to try a calibration of a load cell, transforming it into a 5-axis cell. The cell manufacturer does not provide the diagram of the strain gauge bridges and the geometry of the deforming element, furthermore the cell is inaccessible inside. Generally, the direct load cells are constructed in such a way that each channel is mainly sensitive to a single stress, so it is obtained that the calibration matrix has components much greater in the diagonal than the other positions. In our case, however, the calibration matrix was not diagonal at all, indicating that all the channels felt, albeit differently, all the components. Having a channel out of order, we had to choose which solicitation to give up. Since there is no preferential request for the out-of-use channel, we decided not to consider the solicitation of lesser interest, in our case the MZ.

The calibration process involves measuring the coefficients of the sensitivity matrix. The sensitivity is defined as the ratio between the bridge imbalance (expressed in mV / V) and the load (expressed in N or in Nm).

$$(ch) = [S](L)$$

$$\begin{pmatrix} ch1 \\ ch2 \\ ch3 \\ ch4 \\ ch5 \end{pmatrix} = \begin{bmatrix} S11 & S12 & S13 & S14 & S15 \\ S21 & S22 & S23 & S24 & S25 \\ S31 & S32 & S33 & S34 & S35 \\ S41 & S42 & S43 & S44 & S45 \\ S51 & S52 & S53 & S54 & S55 \end{bmatrix} \begin{pmatrix} F-XF \\ F-YF \\ F-ZF \\ M-XF \\ M-YF \end{pmatrix}$$

$$ch_i = S_{i2} * FY_F + S_{i4} * MX_F$$

(ch) : channel vector

[S] : sensitivity matrix

(L) : load vector

Renaming the components of the load vector

$$\begin{pmatrix} F-XF \\ F-YF \\ F-ZF \\ M-XF \\ M-YF \end{pmatrix} = \begin{pmatrix} F1 \\ F2 \\ F3 \\ F4 \\ F5 \end{pmatrix}$$

The components of the sensitivity matrix are therefore defined as

$$Sij = \frac{ch_i}{F_j}$$

To obtain the element of the matrix [S] of position ij we must:

1) apply only the F_j force

2) measure ch_i

Usually to check the linearity a step load curve is applied and with more points the sensitivity is obtained as a slope of the curve ch-F. Figure 3.6.4

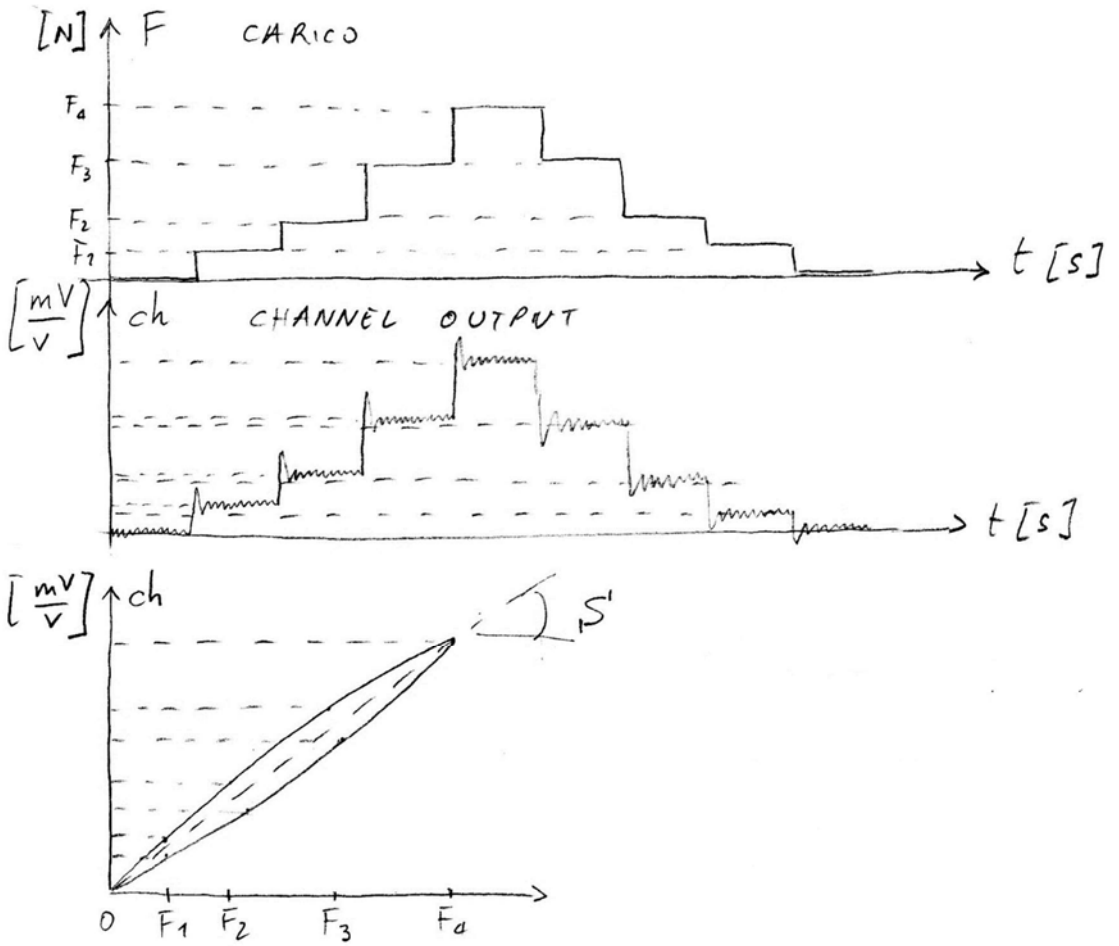

Figure 3.6.4 | Step load curve.

Our procedure was to first apply the three forces, F-X_F, F-Y_F, F-Z_F, with a step loading and unloading curve. In this way we have obtained the value of the elements of the first three columns of the sensitivity matrix.

To obtain the coefficients of the fourth and fifth columns it was necessary to apply pure moments. Not having the necessary equipment, we applied forces with a lever arm to produce the desired moment. In determining the coefficients, however, consideration must also be given to the presence of a cutting load.

For example, to apply an M-XF we applied an F-YF with a long lever arm b. Consequently, we have for example that:

$$ch_i = S_{i2} * FY_F + S_{i4} * MX_F$$

The sensitivity coefficient will in this case be given by:

$$S_{i4} = \frac{ch_i - S_{i2} * FY_F}{MX_F}$$

We have defined the point S, the center of the prosthetic foot reference system, as the center of the cell reference system.

$$\begin{pmatrix} F1 \\ F2 \\ F3 \\ F4 \\ F5 \end{pmatrix} = \begin{bmatrix} 114.79 & 72.66 & 13.50 & 36.98 & 91.75 \\ 2.41 & 50.43 & 51.41 & -51.76 & -51.46 \\ -167.27 & 26.75 & -148.25 & -184.09 & -11.09 \\ -0.40 & 8.43 & 8.88 & -2.47 & -2.67 \\ -12.75 & -6.69 & -2.97 & -2.01 & -12.45 \end{bmatrix} \begin{pmatrix} ch1 \\ ch2 \\ ch3 \\ ch4 \\ ch5 \end{pmatrix}$$

Figure 3.6.5 | Calibration matrix.

3.6. FIRT VERSION OF THE HORIZONTAL SLIDE

The final version of the horizontal slide envisages a tilting plane driven by an electric motor mounted on the slide itself. Before realizing the final version, we have created a first version in which the plane can be manually tilted to fixed θ_{TH} angles. We adapted a slide that had been used in another test bench: on it we mounted a hinge flange. To keep the fixed inclination, two aluminium plates were made, fixed on the upper part of the

flange, with a slotted hole. The friction between the aluminium plates and the lower part of the flange allows to keep the inclination of the flange fixed.

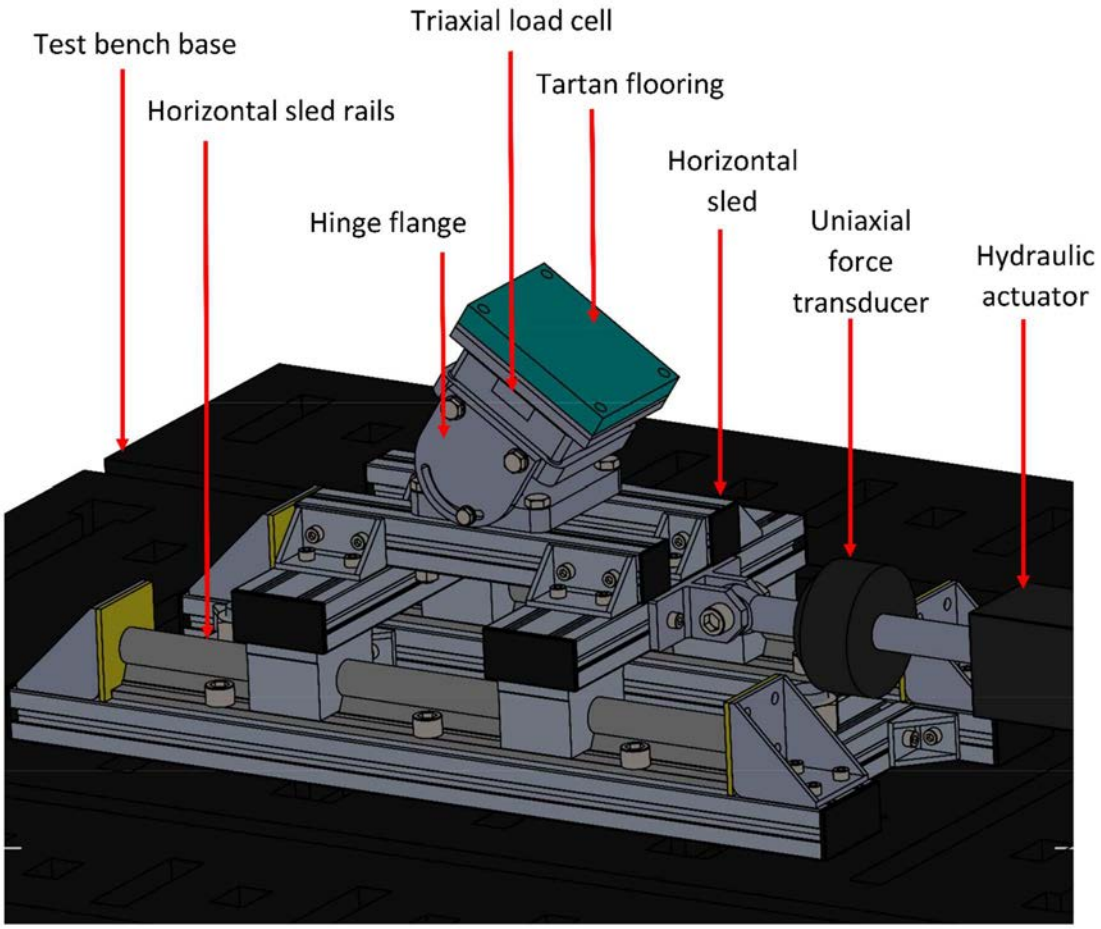

Figure 3.6.1 | First version of the horizontal slide.

To measure the GRFs we placed a triaxial cell above the ground, capable of measuring the three components of force. Specifically, we used the K3D120 ± 5kN / VA produced by ME (Germany). The 3-axis force sensor K3D120 is suitable for measuring force in three mutually perpendicular axes. It is ready for 50N to 5kN in all three axes and can optionally be manufactured in other measurement ranges (Figure 3.7.2)

Figure 3.6.2 | 3-axis force sensor K3D120.

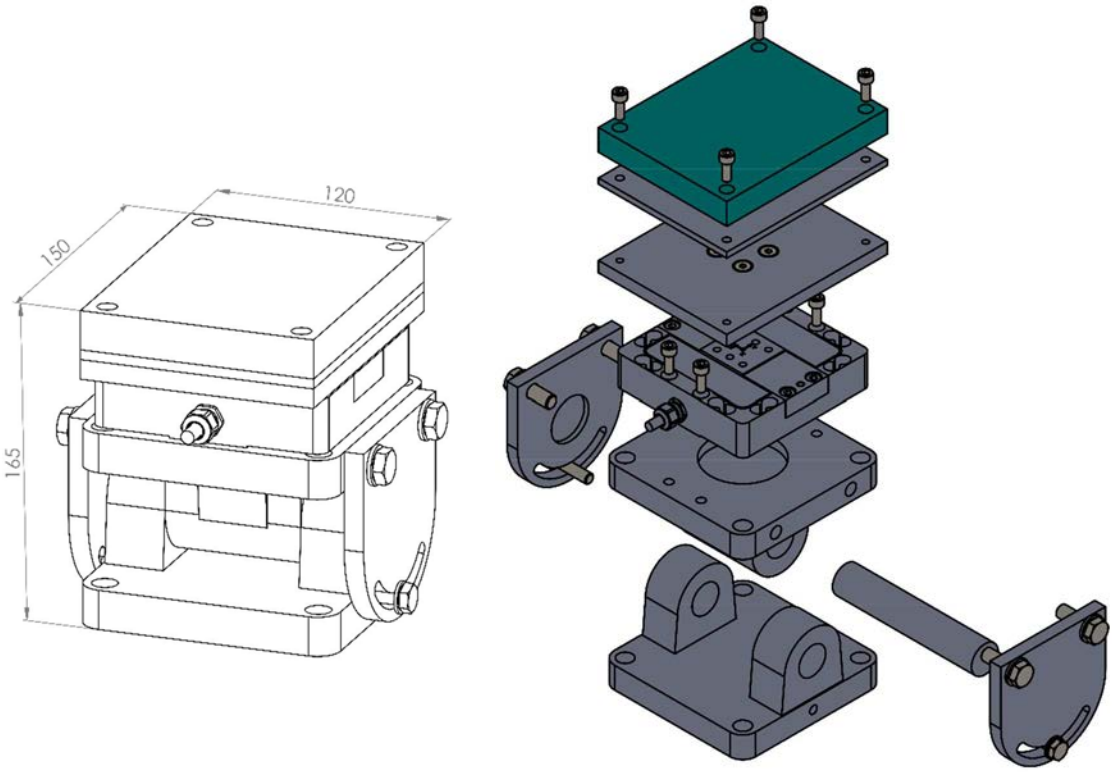

Figure 3.6.3 | System of ground inclination adjustment, dimensions and exploded view.

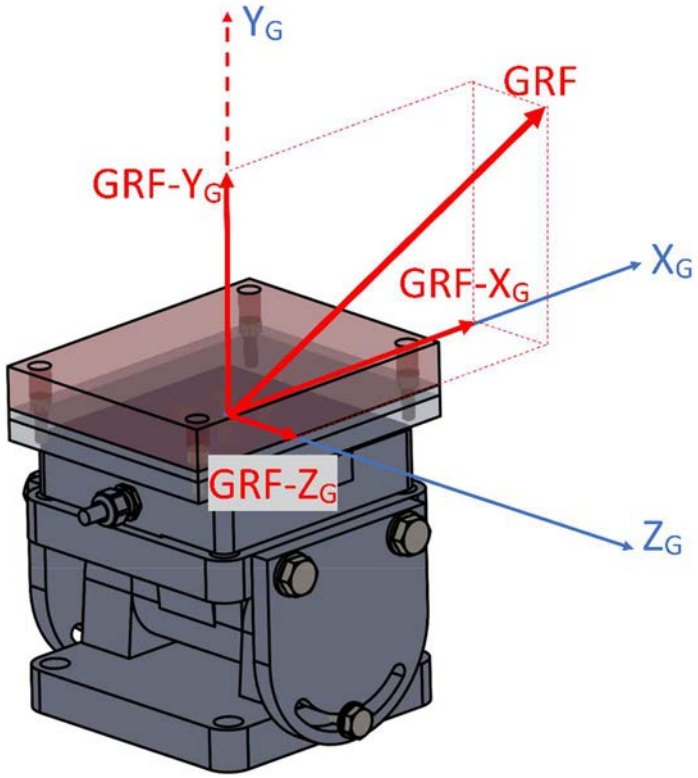

Figure 3.6.4 | Forces measured the triaxial cell.

3.7. TEST BENCH CONSTRUCTION

immagini a confronto tra il progetto e il banco realizzato

4. TEST IN VITRO INDOOR

To test the functionality of the test bench we performed pilot tests on the prosthetic foot in our possession (Össur's «Cheetah Xtreme», size 7). The main objective was to determine the mechanical stiffness of the prosthesis with quasistatic compression tests. In particular, we tried to determine the influence that the shear force produces on the rigidity of the prosthesis.

4.1. DATA ACQUISITION SYSTEM

Our data acquisition system consists of load cells mounted on slides and load cells mounted on hydraulic actuators. As shown in Figure 4.1.1 the data acquisition system consists of:

Uniaxial force transducer of vertical hydraulic actuator: measures the F1 force.

5-axis load cell mounted on the vertical slide: measures the F forces and the M moments. In the sagittal plane the 5-axis cell measures the F-Y_F, F-X_F and M-Z_F.

3-axis load cell mounted on the horizontal slide: measures the GRFs. In the sagittal plane it measures GRF-X_G and GRF-Y_G.

Uniaxial force transducer mounted on the horizontal actuator: measures the force F2.

For the balance of forces we have:

$$F1 = F - Y_F = GRF - Y_F$$

$$F2 = F - X_F = GRF - X_F$$

The displacement of the vertical slide is C1, while that of the horizontal slide is C2. For convenience, C1 and C2 are null at the moment of first contact between the prosthesis and the ground.

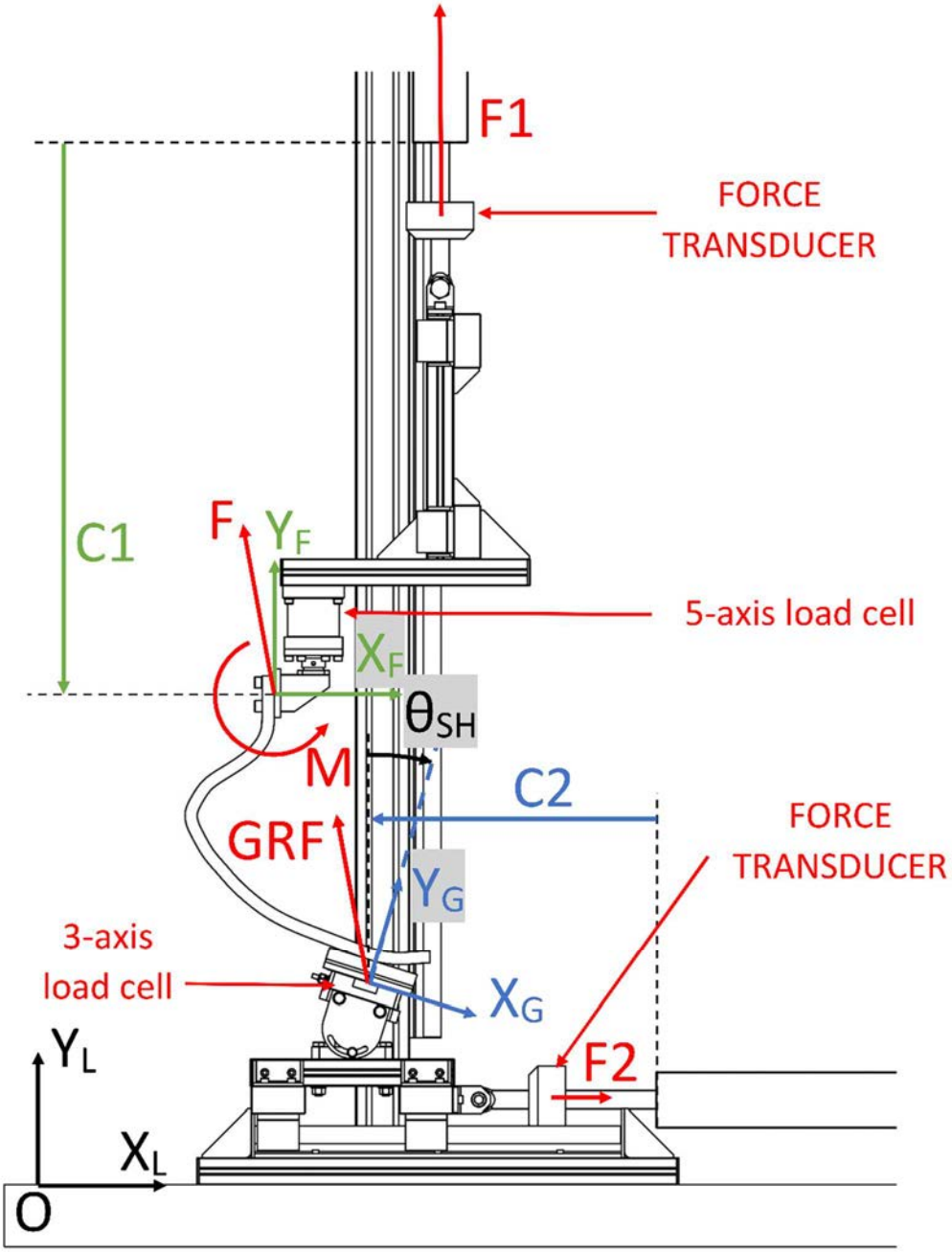

Figure 4.1.1 | Data acquisition system.

4.2. TRIAL PROGRAM

For these tests the angle of alignment in the sagittal plane, γ, it was equal to 0 °, while the angle of inclination of the leg with the ground, $\theta_{SH,}$ it was equal to 0°.

Inspired by the tests performed by Dyer, Sewell and Noroozi, 2014 [21], we have developed two different tests:

1) UDE test: Unfixed distal end. We have imposed that the GRF-YG was always nothing equindi that the sole could freely translate in direction of the Xf axis (command given to the hydraulic actuator that moves the horizontal slide: force control with F2 = 0)

2) set FDE: Fixed distal end. We have established that the prosthetic foot sole does not move in the direction of the XF axis

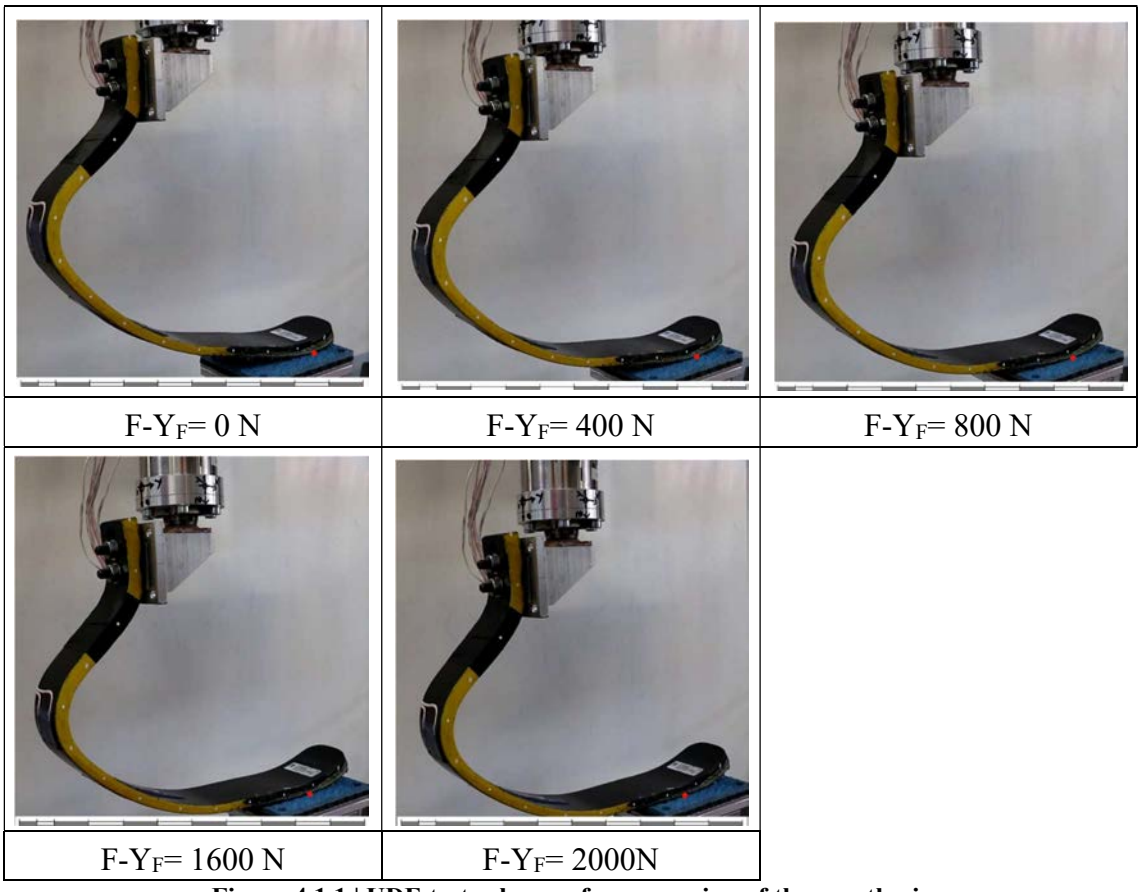

Figure 4.1.1 | UDE test: phases of compression of the prosthesis.

4.3. DATA ACQUIRED

1) UDE test

Figure 4.3.1 shows the GRF-YG recorded by the 3-axis cell (force platform), the 5-axis cell and the force transducer. The measures are compatible with each other.

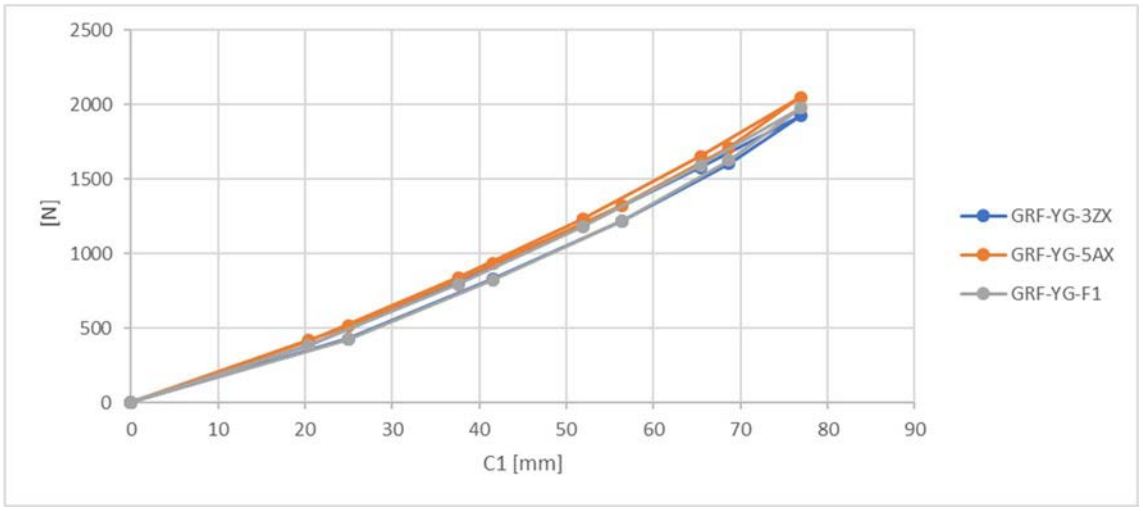

Figure 4.3.1 | UDE test: stiffness curve.

The equation is obtained by interpolating the curve with a straight line:

$$GRF\ Y_G\ =\ 25.931 * C1\ -\ 76.163 \quad R^2\ =\ 0.9899$$

The mechanical stiffness of the prosthesis in an UDE test is:

$$k_{leg} = \frac{GRF\ Y_G}{C1} = 25900\ N/m$$

Instead, using a second-degree curve, one has:

$$GRF\ Y_G\ =\ 0.1131 * C1^2\ +\ 17.601 * C1\ +\ 3.0914 \quad R^2\ =\ 0.9994$$

An interpolation with a second-degree curve is therefore more suitable to describe the straight line of the prosthesis, according to Beck, Taboga and Grabowski (2016) [20].

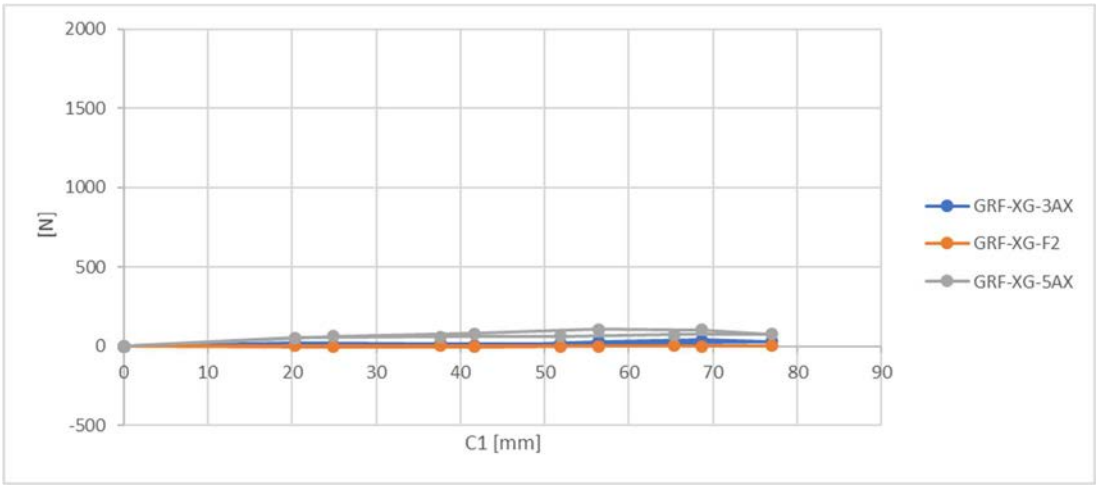

Figure 4.3.2 | UDE test: GRF-XG trend.

Figure 4.3.3 shows the trend of C2 as a function of C1. During the compression the distal end moves forward, whereby C2 passes from zero to negative values. The relationship between the two displacements that has been measured is:

$$\frac{C2}{C1} = -0.57$$

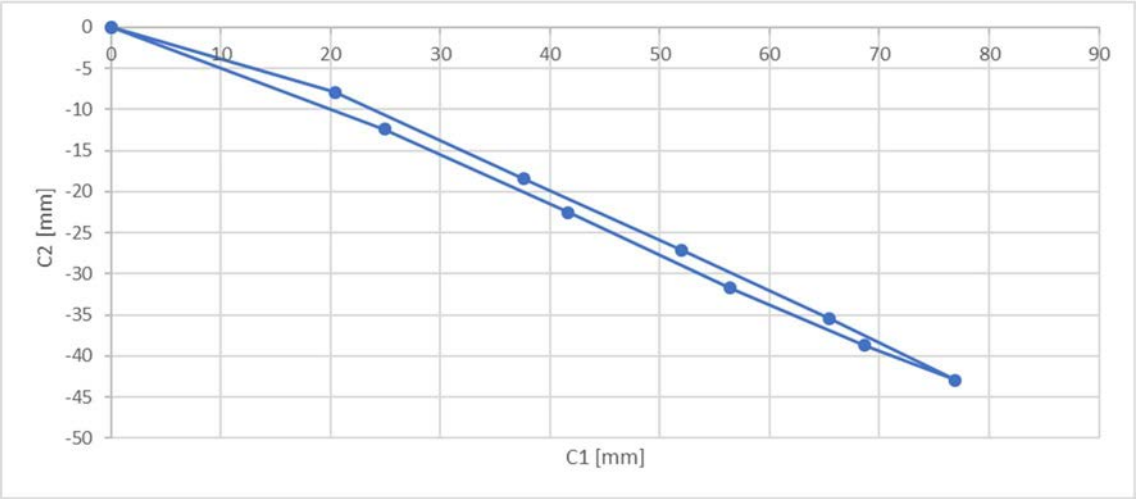

Figure 4.3.3 | UDE test: Trend of the C2 displacement.

Thanks to the 5-axis load cell we measured the ZF axis moment transmitted from the prosthesis to the slide, M-ZF. In Figure 4.3.4 it is shown its trend as a function of C1.

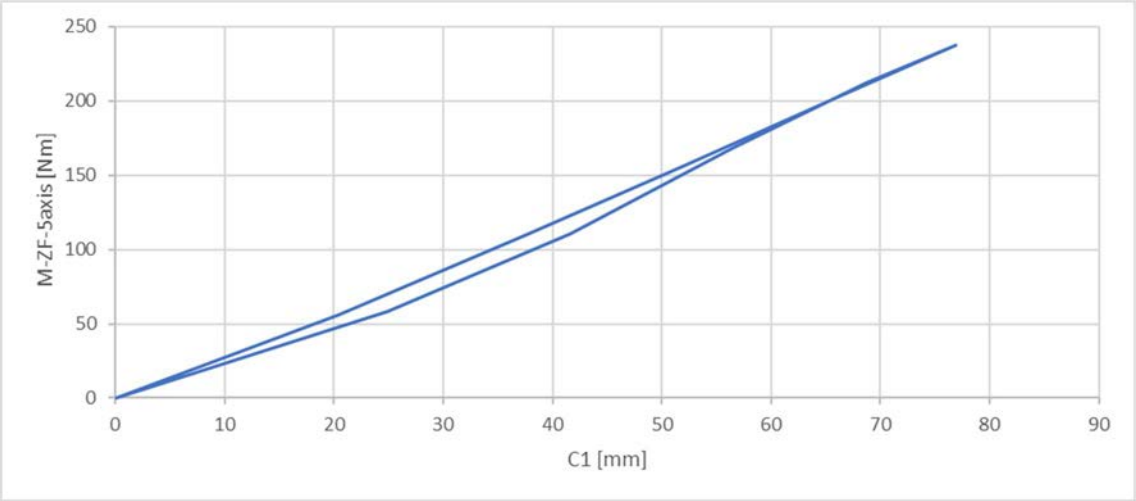

Figure 4.3.4 | UDE test: Trend of the M-ZF.

2) FDE test

The mechanical stiffness curve is shown in the Figure 4.3.5

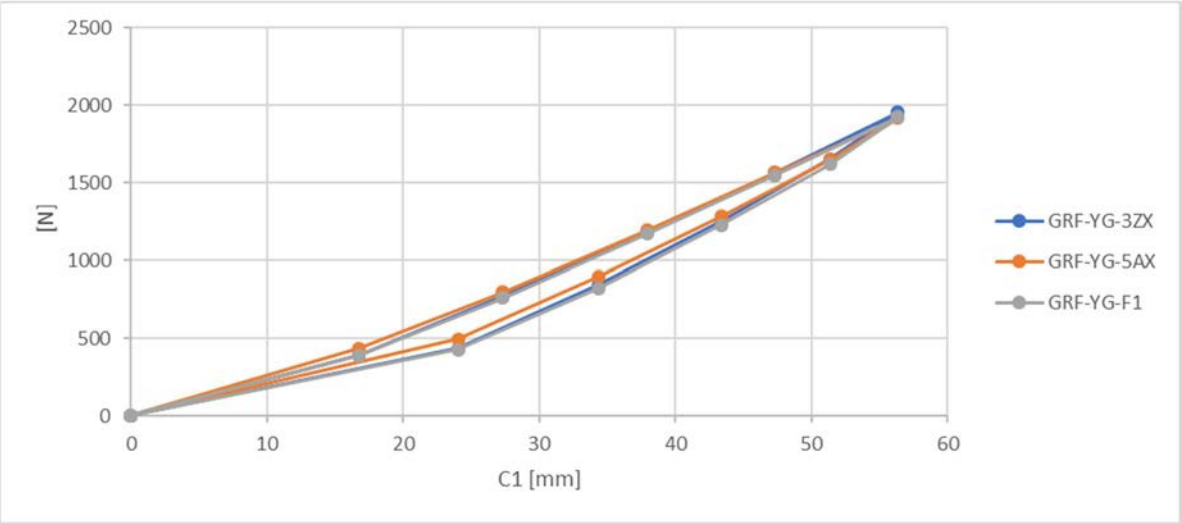

Figure 4.3.5 | FDE test: stiffness curve.

The equation is obtained by interpolating the curve with a straight line:

$$GRF\ Y_G = 35.238 * C1 - 113.54 \quad R^2 = 0.9867$$

The mechanical stiffness of the prosthesis in an UDE test is:

$$k_{leg} = \frac{GRF\ Y_G}{C1} = 35240\ N/m$$

Instead, using a second-degree curve, one has:

$$GRF\ Y_G = 0.2324 * C1^2 + 22.104 * C1 - 12.248 \quad R^2 = 0.9993$$

Also in this case an interpolation with a second degree curve is more accurate.

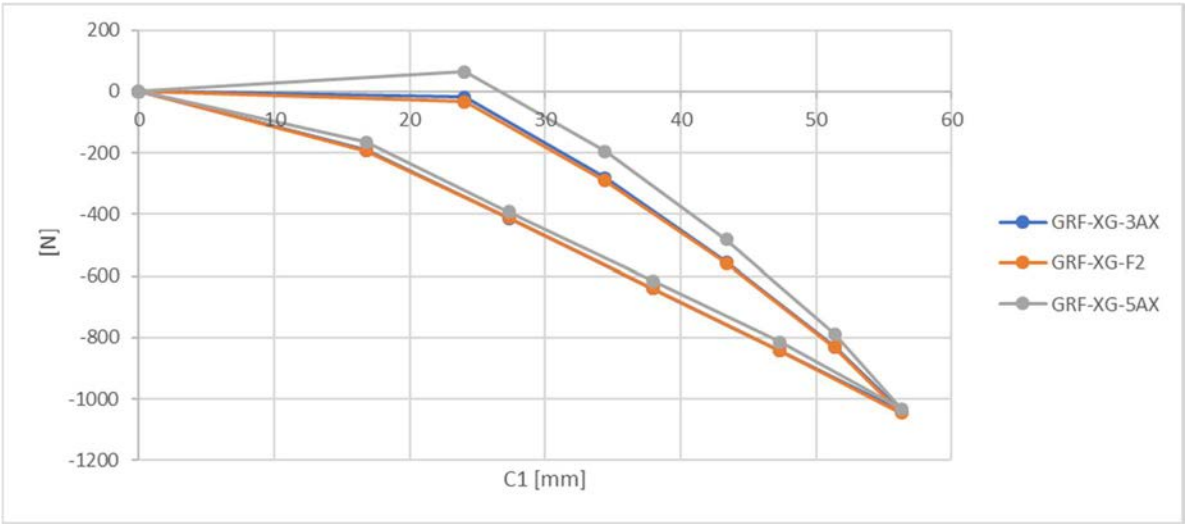

Figure 4.3.6 | FDE test: GRF-XG trend.

The deviation of the discharge curve from the loading curve is due to a slippage of the sole of the prosthesis on the ground. In fact, racing tachets tend to tear the tartan and this causes a decrease in grip. it is useful to represent the trend of GRF-XG according to GRF-YG. It is observed that there is a direct proportionality between the two forces. In fact the linear interpolating line is

$$GRF\ X_G\ =\ -0.5432 * GRF\ Y_G\ +\ 5.9581 \quad R^2\ =\ 0.9995$$

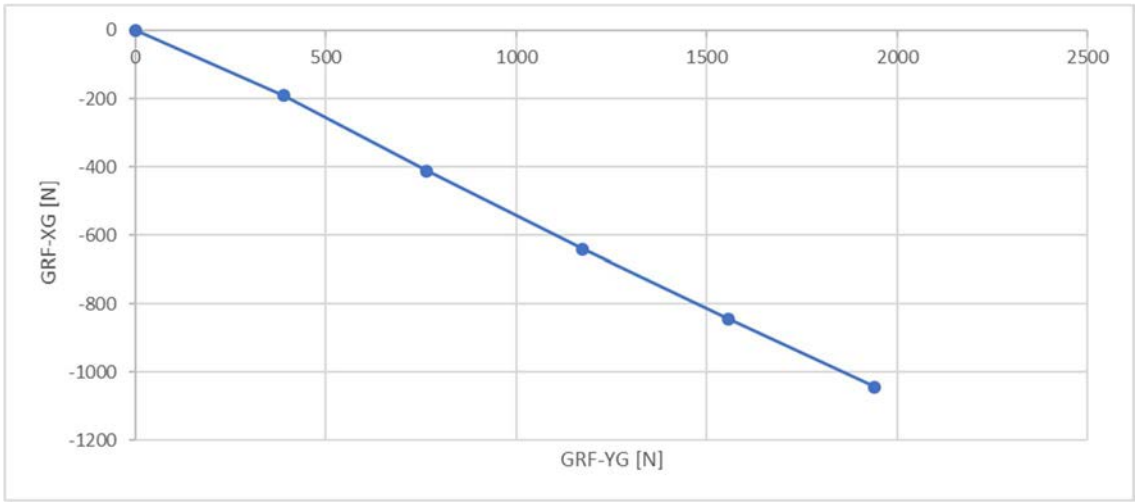

Figure 4.3.7 | FDE test: GRF-XG trend.

The relationship between the two forces therefore results:

$$\frac{GRF - X_G}{GRF - Y_G} = -0.54$$

Unlike the UDE test, there is a considerable GRF-XG cutting force in an FDE test. Being negative, it produces a negative M-ZF moment. The total moment is negative and therefore we infer that the GRF-XG component, although smaller than the GRF-YG, produces a greater M-Z moment because the lever arm is greater.

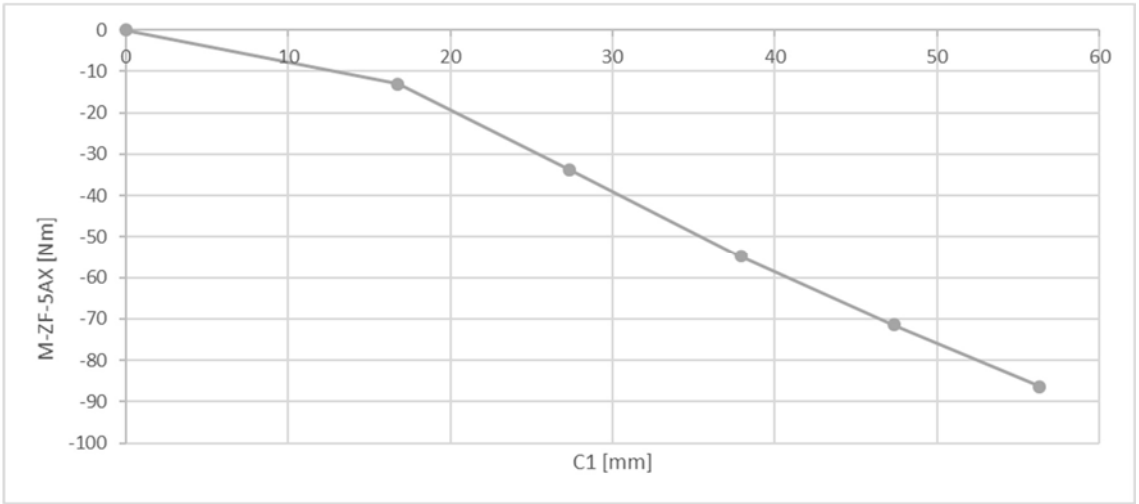

Figure 4.3.8 | UDE test: Trend of the M-ZF.

5. INSTRUMENTED RSP

Tests on sports or rehabilitative equipment are generally divided into two groups:

- in vivo tests: a person uses the device trying to reproduce a normal use
- in vitro tests: dummies / test benches are used to simulate the stress produced by a person.

The tests are also divided into:

- in-door tests: if they are performed in a laboratory
- field tests: if they are performed in the normal environment in which the equipment is used.

In our case, an in vivo field test requires the development of measuring equipment that can be easily carried by the athlete during the race, without weighing it down or limiting its movements. In particular, there are three methods that can be used:

- use force platforms along the way:

  it is certainly the strategy that guarantees an absence of the instrumental load on the measurements, it allows to use very precise equipment that are therefore often heavy. It can also be used by any athlete with any prosthesis. On the other hand a platform of strength is able to grasp the GRFs of a single stride for each passage, provided that the contact takes place entirely on the force platform.

- use load cells:

  in our case we could place a carious cell between the socket and the prosthetic foot. To prevent the cell from modifying the normal dimensions of the prosthesis, it will have to be compact and it will be necessary to obtain the space inside the socket. Since there are no such cells in the market, it is therefore necessary to design and build a customized product. In addition, the data acquisition system must be light, easily transportable by the athlete in a backpack. This solution allows to measure the stresses transmitted by the prosthesis to the socket, with the advantage of being able to compare different adjustments and different prostheses provided that the same socket is used. On the other hand, for every athlete it is necessary to create a socket capable of hosting the load cell. Unlike force platforms, it will be possible to acquire data for each stride.

- Place strain gauge bridges directly on the prosthetic foot:

This solution eliminates the problem of having to create a custom socket for housing the load cell. On the other hand, it will be necessary to use every prosthesis you want to test.

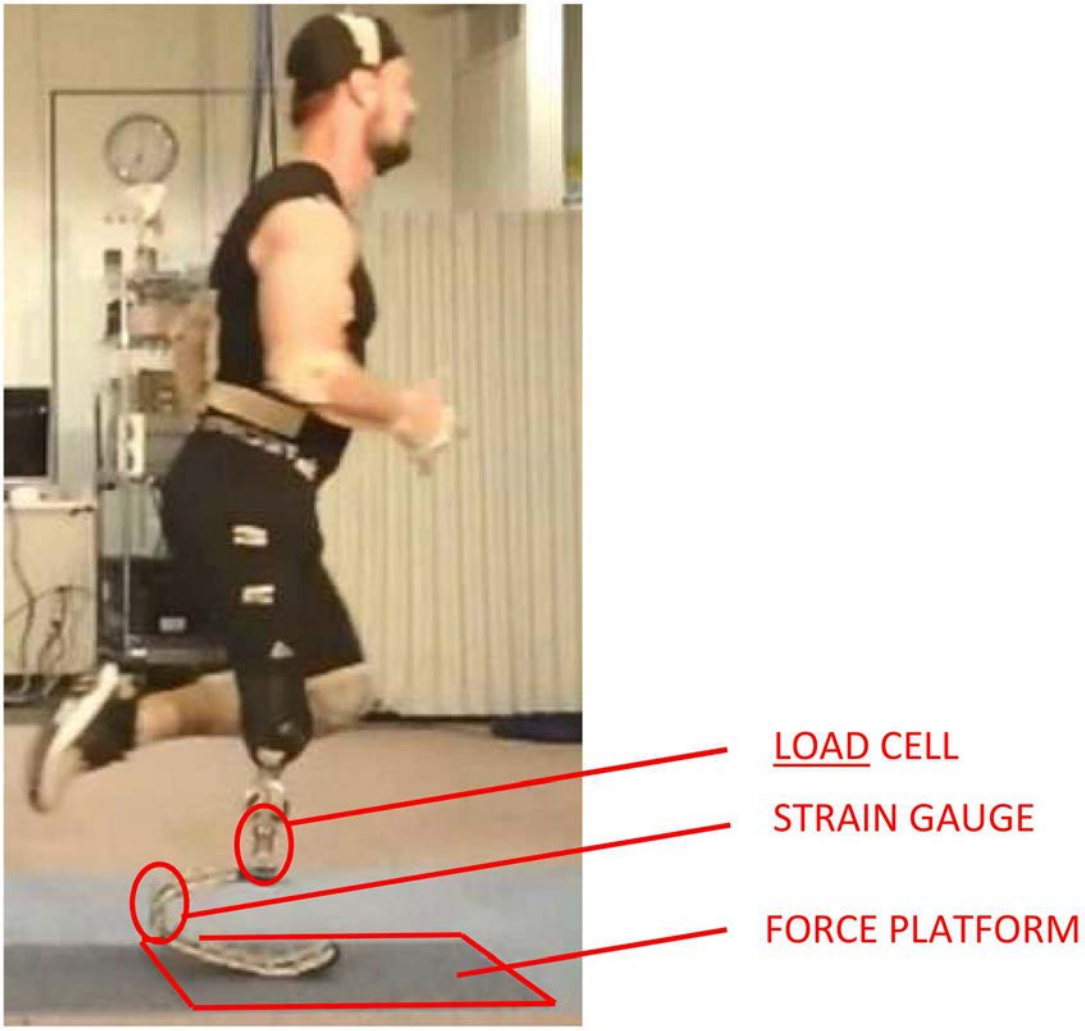

Figure 3.7.3 | Position of the three types of instrumentation.

In our case, we first opted for placing strain gauge bridges directly on the prosthesis.

5.1. STRAIN GAUGE BRIDGES

The application of strain gauge bridges requires an accurate study of which stresses one wants to make the measurement and how to arrange the bridges. We have opted for the construction of two strain gauge bridges: a bending moment sensitive bridge and a cutting force sensitive bridge.

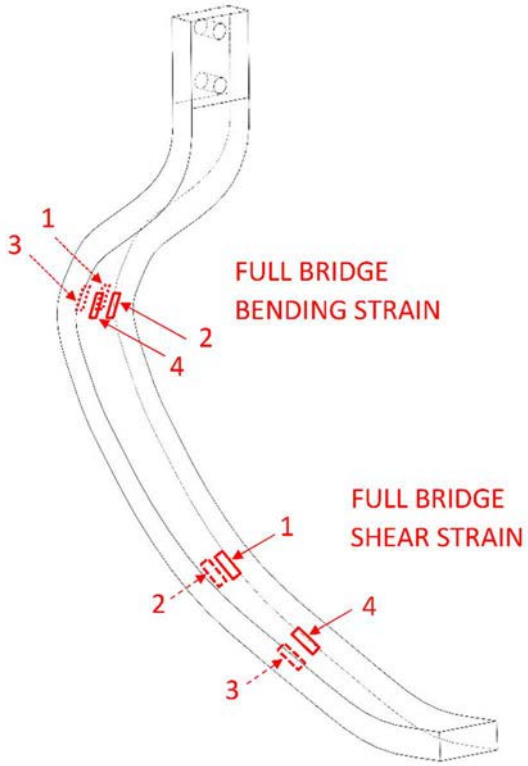
1
3
FULL BRIDGE
BENDING STRAIN
2
4
FULL BRIDGE
SHEAR STRAIN
1
2
4
3


ÖSSUR

5.2. CALIBRATION OF STRAIN GAUGE BRIDGES

5.2.1. Calibration of the bending bridge.

It has correlated the signal read by the moment strain with the moment transmitted by the GRF with respect to the moment axis itself.

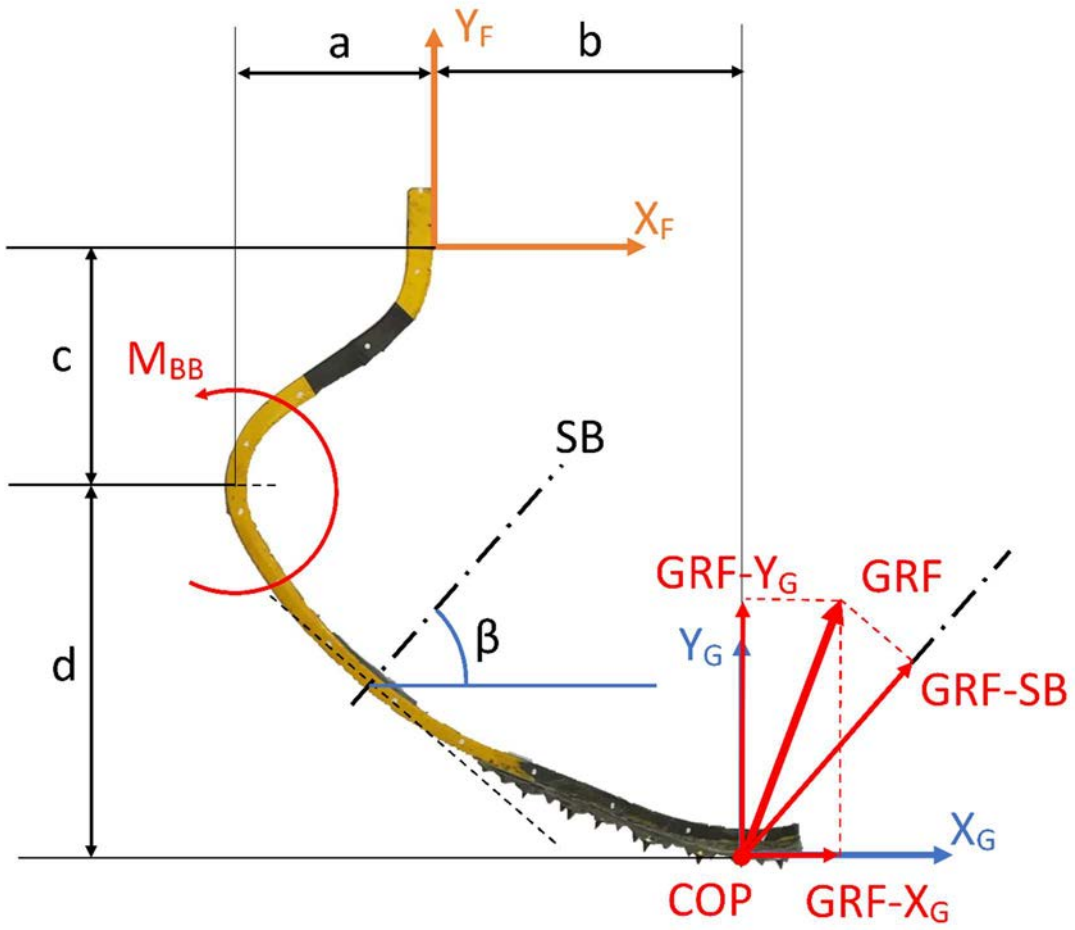

Figure 5.2.1.1 | Lever arms of the GRF and axis of the shear bridge.

The moment acting on the prosthesis in the section where it is installed in bending bridge, M_{BB}, is calculated as follows:

$$M_{BB} = GRF\ X_G * (c + d) + GRF\ Y_G * b$$

The dimensions a and c are assumed constant, in fact in the proximal tract the lamina has a much greater flexural rigidity than the distal tract. During the compression of the prosthesis, the lowering is entirely due to the decrease in the dimension called d. From the video analysis of the DFE test we observed that the contact point remains unchanged during the test. In fact, the forward movement of the toe is compensated by the spot on the back of the center of pressure.

Ultimately, we have:

$$a = 0.12\ m$$

$$b = 0.165\ m$$

$$c = 0.15\ m$$

$$d = 0.225 - C_1\ m$$

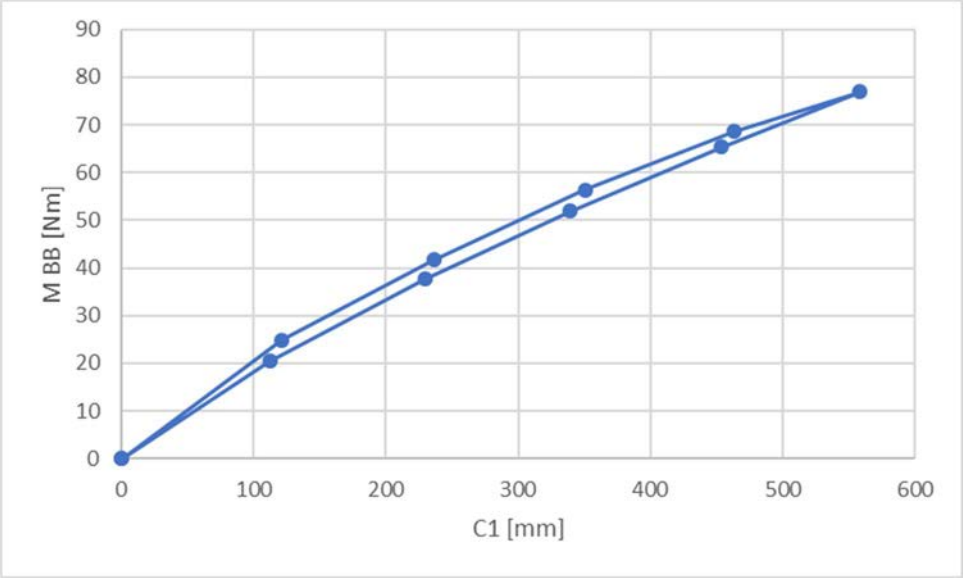

Figure 5.2.1.1 | Moment of bending bridge as a function of the displacement C1.

Diagramming the signal read from the bending bridge with respect to the MBB moment we have the graph of the Figure 5.2.1.1

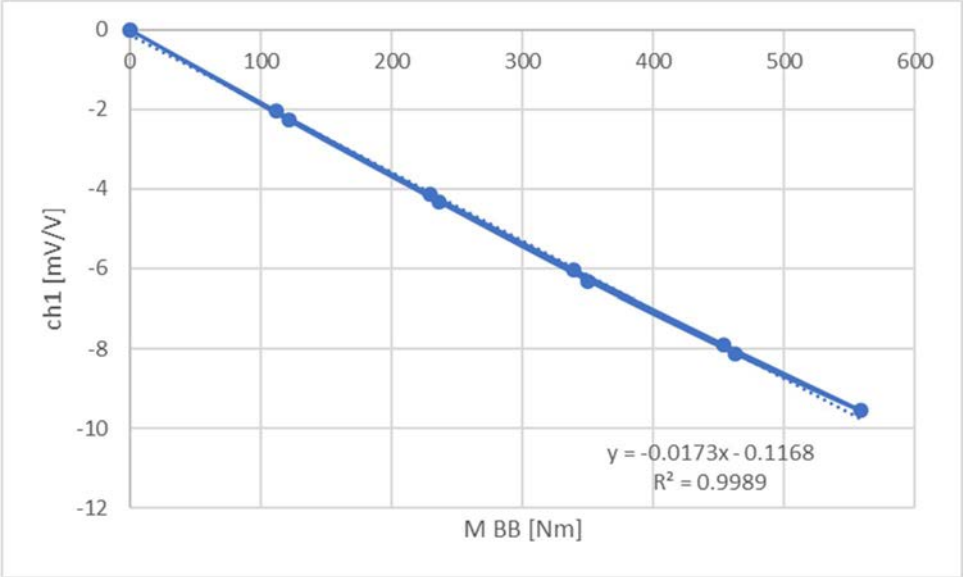

Figure 5.2.1.1 | Channel of bending bridge as a function of moment of bending .

The sensitivity constant S is then determined as the slope of the line:

$$S = \frac{chBB}{MBB} = -0.0173$$

5.2.2. Calibration of the shear bridge

The shear bridge is sensitive to the GRF component along the SB axis. During the deformation of the prosthesis the inclination of this axis changes, whose value we have estimated from the video analysis. beta gradually passes from 51 ° to 46 °.

$$GRF\ SB = GRF\ X_G * \cos(\beta) + GRF\ Y_G * \sin(\beta)$$

The trend of GRF-SB as a function of C1 is shown in the Figure 5.2.2.1

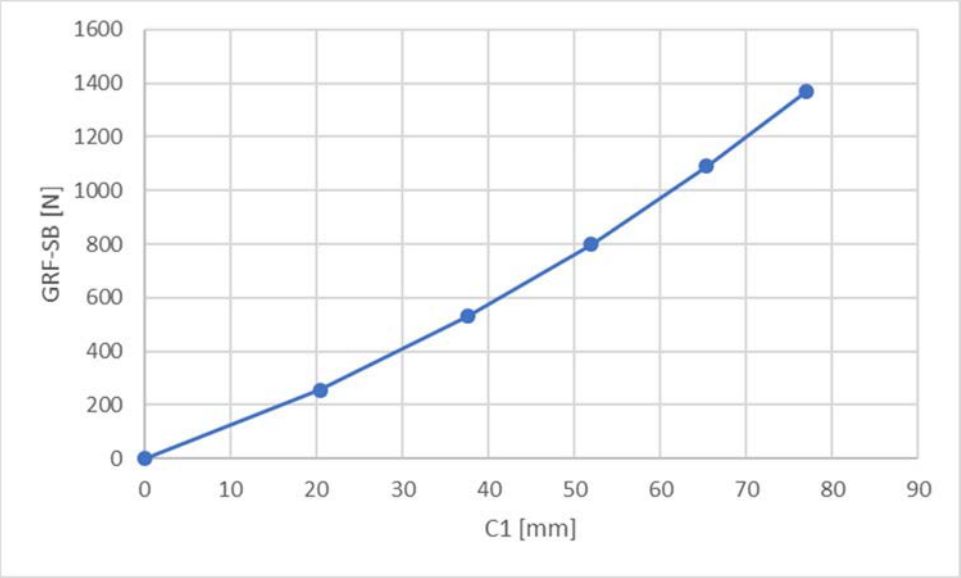

Figure 5.2.2.1 | GRF-SB

Diagramming the signal read from the shear bridge with respect to the GRF-SB force we have the graph of the Figure 5.2.2.2

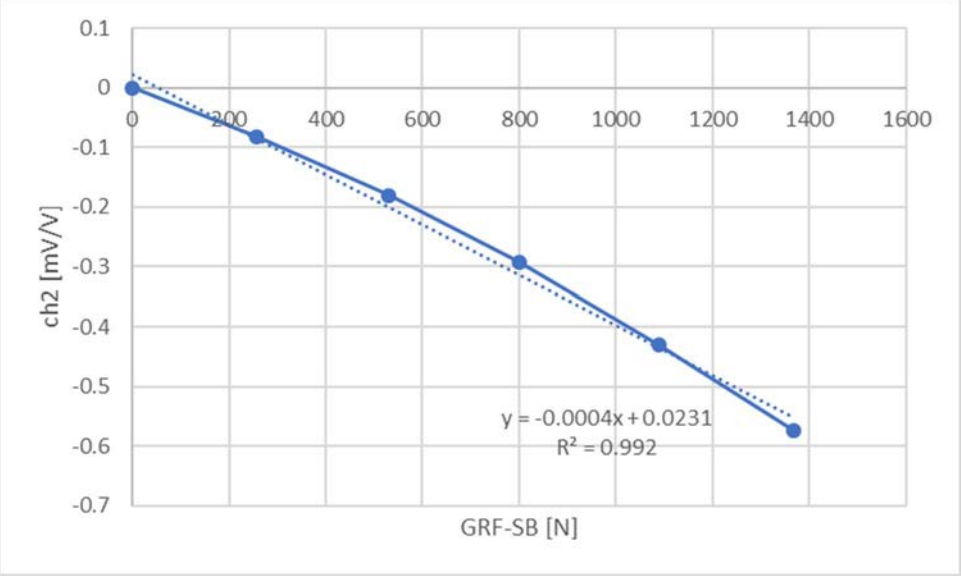

Figure 5.2.2.2 | GRF-SB

$$S = \frac{ch2}{GRF\ SB} = -0.0004$$

6. Appendix A: medical vocabulary [47]

abduction: Motion of a limb or body part away from the median plane of the body. The resulting effect can cause problems with proper gait and/or ambulation and may prolong the rehabilitation process, especially in cases of lower extremity limb loss—adduction is its opposite.

ablation: Removal of a body part and/or its function by way of surgery, morbid process or traumatic occurrence.

acquired amputation: The surgical removal of a limb(s) due to complications associated with disease or trauma.

adherent scar tissue: Usually formed during the healing process, the scar tissue sticks to underlying tissue such as muscle, fascia or bone and may cause pain or lessen the ability for a full range of motion; it also can limit proper fit of the socket. Massage techniques can be employed to combat irritation and/or inflammation, working to soften the hardened tissue.

AK (above-the-knee): A specific level of amputation—also known as **transfemoral**.

alignment: The position of the prosthetic socket in relation to the foot and knee.

ambulation: The action of walking or moving. For lower extremity amputees, rehabilitation is primarily concerned with helping the patient achieve proper gait and/or ambulation.

amelia: Medical term for the congenital absence or partial absence of one or more limbs at birth. Amelia can sometimes be caused by environmental or genetic factors.

amputation: The cutting off of a limb or part of a limb.

anterior: The front portion of a shoe or foot.

architectural barrier: Barriers such as stairs, ramps, curbs, etc. that could obstruct a person's ability to walk or mobilize in a wheelchair.

assistive/adaptive equipment: Devices that assist in activities or mobility (i.e., wheelchair ramps, hand bars/rails, car and home modifications, canes, crutches, walkers and other similar devices).

atrophy: A wasting away of a body part, or the decrease in size of a normally developed extremity or organ, due to a decrease in function and/or use.

bilateral amputee: A person who is missing or has had amputated both arms or both legs. For example, a person that is missing both legs below-the knee is considered a bilateral BK.

biomechanics: Applying mechanical principles to the study of human movement; or the science concerned with the action of forces on the living body.

BK (below-the-knee): A specific level of amputation—also known as transtibial.

body image: The awareness and perception of one's own body in relation to both appearance and function.

bumper: Rubber like, polymer based devices that are available in varying degrees of density, depending on an amputee's desired level of stiffness in a prosthetic knee or heel. As with other prosthetic componentry, basic maintenance or replacement may be required as a result of wear and tear.

C-Leg: The Otto Bock C-Leg features a swing and stance phase control system that senses weight bearing and positioning to provide the knee's microprocessor information about the amputee's gait, thus promoting smoother ambulation. The outer shell houses a hydraulic cylinder, microchip, and rechargeable battery.

causalgia: A persistent, often severe burning pain usually resulting from injury to a peripheral nerve.

check or test socket: A temporary socket, often transparent, made over the plaster model to aid in obtaining proper fit and function of the prosthesis.

congenital anomaly: A birth malformation such as an absent or poorly developed limb. (see amelia and phocomelia)

contracture: The tightening of muscles around a joint, restricting the range of motion and suppressing muscular balance.

contralateral: Originating in or affecting the opposite side of the body.

cosmesis: Used to describe the outer, aesthetic covering of a prosthesis.

definitive, or **permanent prosthesis**: The definitive prosthetic replacement for the missing limb or part of a limb, meeting standards for comfort, fit, alignment, function, appearance and durability.

disarticulation: An amputation of a limb through the joint, without cutting any bone—performed at the hip, knee, ankle, shoulder, elbow and wrist levels.

distal: (1) The end of the residual limb. (2) The end that is farthest from the central portion of the body. Distal is the opposite of **proximal**.

distal muscle stabilization: During an amputation, it is important to retain the maximum amount of functioning muscle to ensure strength, shape and circulation. To achieve this, the remaining muscles at the site of amputation must be secured and stabilized.Myodesis andmyoplasty are the most common techniques for achieving this stabilization.

donning and doffing: Putting on and taking off a prosthesis, respectively.

dorsiflexion: An upward movement or extension of the foot/toes or the hand/fingers.

edema: A type of localized swelling that is characterized by an excess of fluid in body tissues. Many amputees experience inflammatory edema (red, tender, and/or warm skin) at the residual level.

functional prosthesis: Designed with the primary goal of controlling an individual's anatomical function, such as providing support or stability or assisting ambulation.

gait: A manner of walking that is specific to each individual.

gait training: Part of ambulatory rehabilitation, or learning how to walk with your prosthesis or prostheses.

Ischial containment socket: In some amputation cases, usually those of the HP or HD, this socket is used to support the ischium.

ischium: The lower portion of the hipbone, which sometimes protrudes from the pelvis and may get sore while sitting on a hard surface for extended periods of time.

kinesiology: The study of muscles and human movement.

lateral: To the side, away from the median plane of the body.

LEA: Acronym for a lower extremity amputation or amputee.

Liner (roll-on liner): Suspension systems used to hold the prosthesis to the residual limb and to provide additional comfort and protection for the residual limb. Roll-on liners can also accommodate volumetric changes in the residual limb. These liners may be made of silicon, pelite, or gel substances.

medial: Motion of a body part toward the median plane of the body.

microprocessor-controlled knee: These devices are equipped with a sensor that detects full extension of the knee and automatically adjusts the swing phase of ambulation, allowing for a more natural gait.

modular prosthesis: An artificial limb assembled from components or modules usually of the endoskeletal type, where the supporting member (pylon) may have a cosmetic covering (cosmesis) shaped and finished to resemble the natural limb.

neuroma: When a nerve is severed during amputation, the nerve endings form a mass (neuroma) reminiscent of a cauliflower shape. Neuromas can be troublesome, especially when they are in places that are subject to pressure from the socket. They can also cause an amputee to experience sensory phenomena in or around the residual limb, which can be aggravating and/or painful.

neuropathy: An abnormal and usually degenerative state of the nervous system or nerve that can lead to loss of feeling in the feet or other extremities, especially in the diabetic patient.

nylon sheath: A sock interface worn close to the skin on the residual limb to add comfort and deter perspiration.

Occupational Therapy: The teaching of how to perform activities of daily living as independently as possible, or how to maximize independence in the case of disability.

orthosis: A device that is used to protect, support or improve function of parts of the body that move, i.e., braces, splints, slings, etc. Orthoses is plural.

orthotics: The profession of providing devices to support and straighten the body.

orthotist: A skilled professional who fabricates orthotic devices that are prescribed by a physician.

partial suction: Usually refers to the socket of an AK prosthesis that has been modified to allow the wearing of prosthetic socks.

phantom pain: Painful sensations, usually moderate, that originate in the amputated portion of the limb.

phantom sensation: This is the feeling that the missing body part is still there. It may involve uncomfortable but not necessarily painful sensations such as burning, tingling and/or itching.

physiatrist: A doctor of rehabilitation medicine who specializes in the comprehensive management of patients with impairments and disabilities arising from neuromuscular, musculoskeletal, and vascular disorders.

Physical Therapy: A rehabilitative therapy that is concerned with a patient's gross motor activities such as transfers, gait training, and how to function/mobilize with or without a prosthesis.

pistoning: Refers to the residual limb slipping up and down inside the prosthetic socket while walking.

plantar: The bottom section or sole of the foot.

plantarflexion: When the toe/foot is pointing down, away from the median plane of the body.

ply: In this context, it refers to the thickness of stump sock material. The higher the ply number, the thicker the sock.

pneumatic/hydraulic resistance: Used in reference to knee joints that provide controlled changes in the speed of walking, or that provide the necessary resistance for the swing and stance phase of ambulation, helping the amputee achieve a more natural gait.

posterior: The back side of the body or part in question, i.e., posterior knee or patellar region.

preparatory prosthesis: An unfinished, functional replacement for an amputated limb, fitted and aligned to accelerate the rehabilitation process, control edema, and prepare the residual limb for the external forces associated with wearing a prosthesis on a day to day basis.

prosthesis: An artificial limb, usually an arm or a leg, that provides a replacement for the amputated or missing limb. Prostheses is plural.

prosthetics: The profession of providing those with limb loss or with a limb difference (congenital anomaly) a functional and/or cosmetic restoration of missing or underdeveloped human parts.

prosthetist: A person involved in the science and art of prosthetics; one who designs and fits artificial limbs.

proximal: Nearer to the central portion of the body. Proximal is the opposite of distal.

pylon: A rigid member, usually tubular, between the socket or knee unit and the foot that provides a weight bearing, shock-absorbing support shaft for the prosthesis.

quad socket: A socket designed for an AK amputee that has four distinctive sides. The design allows the muscles to function as much as possible as it works to improve the AK amputee's ability to control knee function. The distal end of the socket should match the

shape and size of the residual limb and should provide secure contact, alleviating edema and other skin problems.

range of motion: The amount of movement a limb has in a specific direction.

rehabilitation: The process of restoring a person who has been debilitated by a disease or injury to a normal, functional life.

residual limb: The portion of the arm or leg remaining after an amputation, sometimes referred to as a stump or residuum.

revision: Surgical modification of the residual limb.

SACH foot (Solid-Ankle Cushion Heel): The foot is made of wood with a flexible rubber shell that surrounds the wooden core. The SACH foot is usually prescribed to moderately active or less active amputees, but can be prescribed to amputees of all activity levels. SACH feet are also used in the design of foreshortened prostheses, or stubbies.

shrinker: A prosthetic device made of elastic material and designed to help control swelling of the residual limb or to shrink it in preparation for a prosthetic fitting.

shuttle lock: A mechanism that has a locking pin attached to the distal end of the liner, which locks or suspends the residual limb into the socket.

socket: The portion of the prosthesis that fits around and envelopes the residual limb and to which the prosthetic components are attached.

stance control knee: These prosthetic knee joints typically offer a weight-activating friction brake that locks the knee into place during pivotal points of ambulation, offering stability and balance where needed.

stubbies (Foreshortened Prostheses): Stubbies are used during and sometimes after initial ambulatory rehabilitation. They are customized to each individual and are usually made up of standard sockets, no articulated knee joints or shank, with modified rocker bottoms or SACH feet turned backward for balance and stability.

stump: A word commonly used to refer to the residual limb.

stump shrinker: An elastic wrap or compression sock worn on the residual limb to reduce swelling and to help properly shape the residual limb.

suction socket: Mainly for use by AK level amputees, this socket is designed to provide suspension by means of negative pressure vacuuming. This is achieved by forcing air out of the socket through a one-way valve when donning and using the prosthesis. In order for this type of socket to work properly, the soft tissues of the residual limb must precisely

fit the contours of the socket. Suction sockets work very well for those whose residual limbs maintain a constant shape and size.

suspension system(s): One of many suspension systems must be used in order to keep the prosthesis attached to the residual limb. Most of these systems are integral parts of the socket and prosthesis.

swing phase: This is when the prosthesis moves from full flexion to full extension. The term is usually used in reference to prosthetic knee units.

switch control: A control switch for an electronically-controlled prosthesis (see myoelectrics) that is used to regulate current from the battery to the operator.

Symes amputation: An amputation through the ankle joint that retains the fatty heel pad portion and is intended to provide end weight bearing.

temporary prosthesis: A prosthesis that is made soon after an amputation as an inexpensive way to help retrain a person to walk and balance while shrinking the residual limb (see IPOP).

TES belt: A neoprene or Lycra suspension system for an AK prosthesis, which has a ring that the prosthesis slides into. The neoprene belt attaches around your waist by Velcro/hook and loop fastener. It is used to provide added suspension and/or control rotation.

transmetatarsal amputation: An amputation through the metatarsal section of the foot bone. (see partial foot amputation)

traumatic amputation: An amputation that is the result of an injury.

unilateral: An amputation that affects only one side of the body (opposite of bilateral).

variable-volume socket: A lightweight and custom-made socket. The two-piece design makes it possible to don and doff the prosthesis without subjecting the limb to unnecessary shear. The patient can adjust the socket itself as well as vary the sock ply to maintain proper fit. Socket adjustability eliminates the need to replace the preparatory socket several times before stabilization occurs.

7. BIBLIOGRAPHY

[1] BLICKHAN, Reinhard. The spring-mass model for running and hopping. *Journal of biomechanics*, 1989, 22.11-12: 1217-1227.

[2] FULL, R. J.; BLICKHAN, R. Generality of spring-mass model in predicting the dynamics of many-legged, terrestrial locomotion. *Physiologist*, 1992, 35: 185.

[3] CAVAGNA, G. A., et al. The determinants of the step frequency in running, trotting and hopping in man and other vertebrates. *The Journal of Physiology*, 1988, 399.1: 81-92.

[4] HE, J. P.; KRAM, Rodger; MCMAHON, Thomas A. Mechanics of running under simulated low gravity. *Journal of Applied Physiology*, 1991, 71.3: 863-870.

[5] MCGEER, Tad. Passive bipedal running. *Proc. R. Soc. Lond. B*, 1990, 240.1297: 107-134.

[6] MCMAHON, Thomas A.; GREENE, Peter R. The influence of track compliance on running. *Journal of biomechanics*, 1979, 12.12: 893-904.

[7] THOMPSON, Clay M.; RAIBERT, Marc H. Passive dynamic running. In: *Experimental Robotics I*. Springer, Berlin, Heidelberg, 1990. p. 74-83.

[8] FARLEY, Claire T.; GLASHEEN, James; MCMAHON, Thomas A. Running springs: speed and animal size. *Journal of experimental Biology*, 1993, 185.1: 71-86.

[9] MCMAHON, Thomas A.; CHENG, George C. The mechanics of running: how does stiffness couple with speed?. *Journal of biomechanics*, 1990, 23: 65-78.

[10] ALEXANDER, R. McNeil. Energy-saving mechanisms in walking and running. *Journal of Experimental Biology*, 1991, 160.1: 55-69.

[11] SAIBENE, F. P.; MARGARIA, R. Mechanical work in running. *J. appl. Physiol*, 1964, 19: 249-256.

[12] [19] FARLEY, Claire T.; GONZALEZ, Octavio. Leg stiffness and stride frequency in human running. *Journal of biomechanics*, 1996, 29.2: 181-186.

[13] [20] KUITUNEN, Sami; KOMI, Paavo V.; KYRÖLÄINEN, Heikki. Knee and ankle joint stiffness in sprint running. *Medicine and science in sports and exercise*, 2002, 34.1: 166-173.

[14] [21] ARAMPATZIS, Adamantios; BRÜGGEMANN, Gert-Peter; METZLER, Verena. The effect of speed on leg stiffness and joint kinetics in human running. *Journal of biomechanics*, 1999, 32.12: 1349-1353.

[15] VENTURA, Jonathan; SHVO, Galit. Yellow as "Non-Black": Prosthetics, Semiotics, Hermeneutics, Freedom and Function. *The Design Journal*, 2017, 20.sup1: S4652-S4670.

[16] STAROS, Anthony. The SACH (solid-ankle cushion-heel) foot. *Ortho Pros Appl J*, 1957, 23-31.

[17] https://www.thecanadianencyclopedia.ca/en/article/terry-fox-and-the-development-of-running-prostheses/

[18] Aruin, A. S.: Sports after amputation, *Biomechanics in sport: performance enhancement and injury prevention*, 637-650, (2000).

[19] HOBARA, Hiroaki. Running-specific prostheses: The history, mechanics, and controversy. *Journal of the Society of Biomechanisms*, 2014, 38.2: 105-110.

[20] BECK, Owen N.; TABOGA, Paolo; GRABOWSKI, Alena M. Characterizing the mechanical properties of running-specific prostheses. *PloS one*, 2016, 11.12: e0168298.

[21] DYER, Bryce TJ; SEWELL, Philip; NOROOZI, Siamak. An investigation into the measurement and prediction of mechanical stiffness of lower limb prostheses used for running. *Assistive Technology*, 2014, 26.3: 157-163.

[22] GROBLER, Lara. *Characterisation of running specific prostheses and its effect on sprinting performance*. 2015. PhD Thesis. Stellenbosch: Stellenbosch University.

[23] NISHIKAWA, Yasuhiro; HOBARA, Hiroaki. Mechanical stiffness of running-specific prostheses in consideration of clamped position. *Mechanical Engineering Letters*, 2018, 4: 17-00452-17-00452.

[24] DYER, Bryce TJ; SEWELL, Philip; NOROOZI, Siamak. How should we assess the mechanical properties of lower-limb prosthesis technology used in elite sport?: An initial investigation. *Journal of Biomedical Science and Engineering*, 2013, 6.2: 116-123.

[25] MCGOWAN, Craig P., et al. Leg stiffness of sprinters using running-specific prostheses. *Journal of The Royal Society Interface*, 2012, rsif20110877.

[26] STÅLBOM, Markus, et al. Reliability of kinematics and kinetics associated with Horizontal Single leg drop jump assessment. A brief report. *Journal of sports science & medicine*, 2007, 6.2: 261.

[27] BRUGHELLI, Matt; CRONIN, John. A review of research on the mechanical stiffness in running and jumping: methodology and implications. Scandinavian journal of medicine & science in sports, 2008, 18.4: 417-426.

[28] MERO, A.; KOMI, P. V.; GREGOR, R. J. Biomechanics of sprint running. *Sports medicine*, 1992, 13.6: 376-392.

[29] CZERNIECKI, Joseph M.; GITTER, Andrew; MUNRO, Carolyn. Joint moment and muscle power output characteristics of below knee amputees during running: the influence of energy storing prosthetic feet. *Journal of biomechanics*, 1991, 24.1: 67-75.

[30] NOLAN, Lee. Carbon fibre prostheses and running in amputees: a review. *Foot and ankle surgery*, 2008, 14.3: 125-129.

[31] BRÜGGEMANN, Gert-Peter, et al. Biomechanics of double transtibial amputee sprinting using dedicated sprinting prostheses. *Sports Technology*, 2008, 1.4-5: 220-227.

[32] ZATSIORSKY, Vladimir (ed.). *Biomechanics in sport: performance enhancement and injury prevention*. John Wiley & Sons, 2008.

[33] MORIN, Jean-Benoît, et al. A simple method for measuring stiffness during running. *Journal of applied biomechanics*, 2005, 21.2: 167-180.

[34] GRABOWSKI, Alena M., et al. Running-specific prostheses limit ground-force during sprinting. *Biology letters*, 2009, rsbl20090729.

[35] WEYAND, Peter G., et al. The fastest runner on artificial legs: different limbs, similar function?. *Journal of applied physiology*, 2009, 107.3: 903-911.

[36] HOBARA, Hiroaki, et al. Amputee locomotion: Spring-like leg behavior and stiffness regulation using running-specific prostheses. *Journal of biomechanics*, 2013, 46.14: 2483-2489.

[37] BECK, Owen N.; TABOGA, Paolo; GRABOWSKI, Alena M. How do prosthetic stiffness, height and running speed affect the biomechanics of athletes with bilateral transtibial amputations?. *Journal of The Royal Society Interface*, 2017, 14.131: 20170230.

[38] ARELLANO, Christopher J., et al. Effect of running speed and leg prostheses on mediolateral foot placement and its variability. *PloS one*, 2015, 10.1: e0115637.

[39] MAKIMOTO, Atsushi, et al. Ground reaction forces during sprinting in unilateral transfemoral amputees. *Journal of applied biomechanics*, 2017, 33.6: 406-409.

[40] DYER, Bryce TJ; SEWELL, Philip; NOROOZI, Siamak. How should we assess the mechanical properties of lower-limb prosthesis technology used in elite sport?: An initial investigation. *Journal of Biomedical Science and Engineering*, 2013, 6.2: 116-123.

[41] DICKINSON, A. S.; STEER, J. W.; WORSLEY, P. R. Finite element analysis of the amputated lower limb: a systematic review and recommendations. *Medical engineering & physics*, 2017, 43: 1-18.

[42] ISO, ISO. 10328: Prosthetics–Structural testing of lower-limb prostheses–Requirements and test methods. 2006.

[43] BS ISO 281 2007

[44] CATALOGO PROFILAT I : U M S - P 4 4 - 0 1 N 0 5 - I T

[45] NIKO® http://nipponkodobearings.com

[46] FANTI, Giulio. Appunti di misure meccaniche e termiche. Libreria Progetto, 2010.

[47] https://www.amputee-coalition.org/resources/limb-loss-definitions/.